

STEREOCHEMICAL INVESTIGATIONS ON 2-ARYLIMINO-3-ARYL-
THIAZOLIDINE-4-ONE DERIVATIVES

by

Şule Erol

B.S. in Chem., İstanbul University, 2001

Submitted to the Institute for Graduate Studies in
Science and Engineering in partial fulfillment of
the requirements for the degree of
Master of Science

Graduate Program in Chemistry

Boğaziçi University

2006

ACKNOWLEDGEMENTS

I would like to express my sincere gratitude to my thesis supervisor, Prof. Dr. İlknur Doğan for her support, guidance, advice and patience in every stage of this project. It was a great pleasure for me to work with her.

I also wish to thank the Prof. Dr. Hadi Özbal and Assoc. Prof. Dr. Safiye Erdem, for their advice and comments on the final manuscript.

My sincere thanks to my group friends, Esra Müjde Yılmaz and Öznur Demir Ordu, for being very helpful and their sincerity. I also would like to express my thanks to Elif Olgun, who helped me in the early stage of the experiments.

I owe great thanks to Selda Erkoç for her endless support and friendship. I also wish to thank all my friends, especially to Elçin Sayınsöz, Gökhan Çaylı, Sinan Şen, Aylin Albayrak, Barış Yağcı, Kevser Topal.

I would like to express my thanks to Ayla Türkekul and Burcu Selen for patiently recording the NMR spectra.

I am grateful to the all the members of the chemistry department. I wish to thank especially to Hülya Metiner, always willing to help and share the problems.

I owe great thanks to my family, especially to my grandmother, for her encouragement, support and endless love throughout my life.

This project has been supported by Boğaziçi University Scientific Research Fund with the project number 05B501.

ABSTRACT

STEREOCHEMICAL INVESTIGATIONS ON 2-ARYLIMINO-3-ARYL-THIAZOLIDINE-4-ONE DERIVATIVES

In this study, stereostructures of 2-arylimino-3-aryl-thiazolidine-4-ones have been investigated. The compounds to be studied have been synthesized by the reaction of the corresponding N,N'-diarylthioureas with α -bromoacetic acid.

In these compounds the N₃-aryl bond rotation is hindered and except for 2-phenylimino-3-phenyl-thiazolidine-4-one the restricted rotation around this bond gives rise to **M** and **P** stereoisomers. Therefore, the protons on C-5 of the heterocyclic ring are diastereotopic and give AB type splitting in the ¹H NMR spectrum. In addition, as far as C=N double bond is concerned, this bond may have **E** and **Z** configurations.

In this project, ¹H NMR spectra of the compounds were examined in various solvents and the spectra were found to show a strong solvent dependence. For 2-phenylimino-3-phenyl-thiazolidine-4-one and 2-(*o*-tolyl)imino-3-(*o*-tolyl)-thiazolidine-4-one both **E** and **Z** isomers were found to be present in aromatic solvents revealed by the splittings of the signals for the protons present at C-5 of the heterocyclic ring. For the other compounds studied, 2-(α -naphthyl)imino-3-(α -naphthyl)-thiazolidine-4-one, 2-(*o*-chlorophenyl)imino-3-(*o*-chlorophenyl)-thiazolidine-4-one, 2-(*o*-methoxyphenyl)imino-3-(*o*-methoxyphenyl)-thiazolidine-4-one and in the other solvents studied, DMF-d₇, methanol-d₄ and CDCl₃, only one isomer was observed which was assigned to the **Z** isomer by comparison of the energy barriers determined with the barriers of the previously studied structurally related compounds. The 2D-NOESY experiments which were used in order to prove the presence of the **E** isomer did not show any crosspeaks due to through space interactions.

¹H NMR spectra of the compounds taken at various temperatures in order to find out whether the **E** and **Z** isomers were thermally interconvertible, did not show any coalescence up to 100°C.

The stereoisomers were separated using enantioselective HPLC and barriers to rotation about N₃-aryl bond of the compounds have been determined by thermal racemization of the resolved enantiomers.

ÖZET

2-ARİLİMİNO-3-ARİL-TİYOAZOLİDİN-4-ON TÜREVLERİNİN STEREOKİMYASAL İNCELENMESİ

Bu çalışmada 2-arilimino-3-aril-tiyozolidin-4-on türevlerinin stereoyapıları incelenmiştir. Çalışılan bileşikler uygun N,N'-diariltiyüerelerin α -bromoasetikasid ile tepkimesinden sentezlenmiştir.

Bu bileşiklerde N₃-aril bağındaki dönme engellidir ve 2-fenilimino-3-fenil-tiyozolidin-4-on dışındaki bileşiklerde bu bağ etrafındaki dönme M ve P stereoisomerlerini verir. Bu yüzden heterosiklik halkanın 5. carbonunda bulunan protonlar diastereotopiktirler ve ¹H NMR spektrumunda AB tipinde yarıma verirler. Ayrıca C=N bağı düşünüldüğünde bu bağ E ve Z konfigürasyonlarını alabilir.

Bu projede bileşiklerin ¹H NMR spektrumları değişik çözücülerde incelenmiştir ve spektrumlar güçlü çözücü bağımlılığı göstermiştir. Aromatik solventlerde alınan ¹H NMR spektrumlarında E ve Z izomerlerinin varlığı 2-fenilimino-3-fenil-tiyozolidin-4-on ve 2-(*o*-tolil)imino-3-(*o*-tolil)-tiyozolidin-4-on bileşikleri için heterosiklik halkanın 5. carbonundaki protonların sinyallerinin yarımasıyla açıklanmıştır. Diğer çalışılan bileşiklerde, 2-(α -naftil)imino-3-(α -naftil)-tiyozolidin-4-on, 2-(*o*-klorofenil)imino-(*o*-klorofenil)- tiyozolidin-4-on ve 2-(*o*-metoksifenil)imino-3-(*o*-metoksiphenyl)-tiyozolidin-4-on, ve diğer çalışılan çözücülerde, DMF-d₇, metanol-d₄, ve CDCl₃, önceden çalışılan yapısal olarak ilişkili bileşiklerin enerji bariyerlerinin karşılaştırılmasıyla Z olarak belirlenen bir izomer gözlemlendi. E isomerin varlığını kanıtlamak için kullanılan 2D-NOESY deneyleri halkalar arasında bir etkileşim olmadığını gösterdi.

E ve Z izomerlerin sıcaklıkla birbirine dönüşüp dönüşmediğini anlamak için değişik sıcaklıklarda alınan ¹H NMR spektrumları 100 °C ye kadar hiçbir birleşme göstermedi.

Stereoizomerler enantioseçimli HPLC kullanılarak ayrıldı ve N₃-aril bağı etrafındaki dönme bariyeri ayrılmış olan enantiyomerlerin termal rasemizasyonu ile belirlendi.

TABLE OF CONTENTS

ACKNOWLEDGEMENTS.....	iii
ABSTRACT.....	iv
ÖZET.....	vi
LIST OF FIGURES.....	xi
LIST OF TABLES.....	xx
LIST OF SYMBOLS/ABBREVIATIONS.....	xxi
1. INTRODUCTION.....	1
2. THEORY.....	7
2.1. Chirality.....	7
2.2. Atropisomerism (Axial Chirality) and Hindered Rotation in 2-arylimino- 3-aryl-thiazolidine-4-ones.....	8
2.3. The E-Z Isomerization of Imines.....	9
2.3.1. Rotation about the C=N Double bond.....	10
2.3.2. Inversion of Nitrogen (Lateral Shift Mechanism).....	11
2.4. Factors Affecting C=N Double Bond Isomerization.....	11
2.4.1. Solvent Effects.....	12
2.4.2. Electronic Effects.....	12
2.4.3. Steric Effects.....	13
2.5. Assignment of the Stereochemistry of the Imino bond in 2-arylimino- 3-aryl-thiazolidine-4-ones.....	13
2.5.1. 2D-NOESY Spectroscopy.....	14
2.5.2. Comparison of the Energy Barriers of Structurally Related Compounds...	14
2.6. Determination of the Barriers to Rotation by Thermal Racemization.....	15
2.6.1. A Review of High Performans Liquid Chromatography.....	15
2.6.2. Separation of Stereoisomers by Chiral HPLC.....	16
2.6.3. Determination of the Kinetic and Thermodynamic Constants of the Internal Rotation process for 2-arylimino-3-aryl-thiazolidine-4-one.....	17
3. ORGANIC SYNTHESIS.....	20
3.1. Synthesis of N,N'-Diarylthioureas.....	20

3.1.1. General Procedure.....	20
3.1.1.1. N,N'-Diphenylthiourea.....	20
3.1.1.2. N,N'-Di-(<i>o</i> -tolyl)thiourea.....	21
3.1.1.3. N,N'-Di-(α -naphthyl)thiourea.....	21
3.1.1.4. N,N'-Di-(<i>o</i> -chlorophenyl)thiourea.....	22
3.1.1.5. N,N'-Di-(<i>o</i> -methoxyphenyl)thiourea.....	23
3.2. Synthesis of 2-arylimino-3-aryl-thiazolidine-4-ones.....	23
3.2.1. General Procedure.....	23
3.2.1.1. 2-phenylimino-3-phenyl-thiazolidine-4-one.....	24
3.2.1.2. 2-(<i>o</i> -tolyl)imino-3-(<i>o</i> -tolyl)-thiazolidine-4-one.....	25
3.2.1.3. 2-(α -naphthyl)imino-3-(α -naphthyl)-thiazolidine-4-one.....	26
3.2.1.4. 2-(<i>o</i> -chlorophenyl)imino-3-(<i>o</i> -chlorophenyl)-thiazolidine-4-one..	27
3.2.1.5. 2-(<i>o</i> -methoxyphenyl)imino-3-(<i>o</i> -methoxyphenyl)-thiazolidine- 4-one.....	28
3.3. Apparatus.....	29
3.4. List of Chemicals.....	30
4. RESULTS AND DISCUSSIONS.....	31
4.1. 2-phenylimino-3-phenyl-thiazolidine-4-one.....	31
4.1.1. ^1H NMR Spectra of 2-phenylimino-3-phenyl-thiazolidine-4-one.....	31
4.1.2. ^{13}C NMR Spectra of 2-phenylimino-3-phenyl-thiazolidine-4-one.....	45
4.1.3. 2D-NOESY and 2D-COSY Spectra of 2-phenylimino- 3-phenyl-thiazolidine-4-one in Benzene- d_6 and DMF- d_7	45
4.2. 2-(<i>o</i> -tolyl)imino-3-(<i>o</i> -tolyl)-thiazolidine-4-one.....	50
4.2.1. ^1H NMR Spectra of 2-(<i>o</i> -tolyl)imino-3-(<i>o</i> -tolyl)-thiazolidine-4-one.....	50
4.2.2. ^{13}C NMR Spectra of 2-(<i>o</i> -tolyl)imino-3-(<i>o</i> -tolyl)-thiazolidine-4-one.....	59
4.2.3. 2D-NOESY and 2D-COSY Spectra of 2-(<i>o</i> -tolyl)imino- 3-(<i>o</i> -tolyl)-thiazolidine-4-one in CDCl_3 and Toluene- d_8	59
4.2.4. Barrier to Rotation about N_3 -Aryl Bond of 2-(<i>o</i> -tolyl)imino- 3-(<i>o</i> -tolyl)-thiazolidine-4-one.....	62
4.2.5. Comparison of the Energy Barrier of 2-(<i>o</i> -tolyl)imino- 3-(<i>o</i> -tolyl)-thiazolidine-4-one with Structurally Related Compound.....	64
4.3. 2-(α -naphthyl)imino-3-(α -naphthyl)-thiazolidine-4-one.....	66

4.3.1.	¹ H NMR Spectra of 2-(α -naphthyl)imino-3-(α -naphthyl)-thiazolidine-4-one.....	66
4.3.2.	¹³ C NMR Spectra of 2-(α -naphthyl)imino-3-(α -naphthyl)-thiazolidine-4-one.....	67
4.3.3.	2D-NOESY and 2D-COSY Spectra of 2-(α -naphthyl)imino-3-(α -naphthyl)-thiazolidine-4-one.....	76
4.3.4.	Barrier to Rotation about N ₃ -Aryl Bond of 2-(α -naphthyl)imino-3-(α -naphthyl)-thiazolidine-4-one.....	77
4.3.5.	Comparison of the Energy Barrier of 2-(α -naphthyl)imino-3-(α -naphthyl)-thiazolidine-4-one.....	79
4.4.	2-(<i>o</i> -chlorophenyl)imino-3-(<i>o</i> -chlorophenyl)-thiazolidine-4-one.....	81
4.4.1.	¹ H NMR Spectra of 2-(<i>o</i> -chlorophenyl)imino-3-(<i>o</i> -chlorophenyl)-thiazolidine-4-one.....	81
4.4.2.	¹³ C NMR Spectra of 2-(<i>o</i> -chlorophenyl)imino-3-(<i>o</i> -chlorophenyl)-thiazolidine-4-one.....	91
4.4.3.	2D-NOESY and 2D-COSY Spectra of 2-(<i>o</i> -chlorophenyl)imino-3-(<i>o</i> -chlorophenyl)-thiazolidine-4-one.....	91
4.4.4.	Barrier to Rotation about N ₃ -Aryl Bond of 2-(<i>o</i> -chlorophenyl)imino-3-(<i>o</i> -chlorophenyl)-thiazolidine-4-one.....	92
4.5.	2-(<i>o</i> -methoxyphenyl)imino-3-(<i>o</i> -methoxyphenyl)-thiazolidine-4-one.....	94
4.5.1.	¹ H NMR Spectra of 2-(<i>o</i> -methoxyphenyl)imino-3-(<i>o</i> -methoxyphenyl)-thiazolidine-4-one.....	94
4.5.2.	¹³ C NMR Spectra of 2-(<i>o</i> -methoxyphenyl)imino-3-(<i>o</i> -methoxyphenyl)-thiazolidine-4-one.....	95
4.5.3.	2D-NOESY and 2D-COSY Spectra of 2-(<i>o</i> -methoxyphenyl)imino-3-(<i>o</i> -methoxyphenyl)-thiazolidine-4-one.....	104
4.5.4.	Barrier to Rotation about N ₃ -Aryl Bond of 2-(<i>o</i> -methoxyphenyl)imino-3-(<i>o</i> -methoxyphenyl)-thiazolidine-4-one.....	105
4.6.	Barriers to Rotations About N ₃ -Aryl Bond of the Compounds Studied.....	107
5.	CONCLUSIONS.....	108
	REFERENCES.....	110

LIST OF FIGURES

Figure 1.1. The structure of 6,6'- dinitro- 2,2'- diphenic acid.....	1
Figure 1.2. The generalstructure of N-phenylpyroles.....	1
Figure 1.3. The structure of N-(<i>o</i> -aryl) and N-(<i>o</i> - aryl)- 2- thioxo-4-oxazolidinones and thiazolidinones.....	1
Figure 1.4. The 5,5-dimethyl-1-(<i>o</i> -aryl)barbituric and 2-thiobarbituric acid derivatives	3
Figure 1.5. The structure of 5,5-dimethyl-3-(<i>o</i> -aryl)-2,4-oxazolidinediones.....	3
Figure 1.6. The structure of the compounds studied in this project.....	4
Figure 1.7. The stucture of N-isopropylideneanilines.....	5
Figure 1.8. The stucture of N,N,N',N'tetramethyl-N''-arylguanidines.....	6
Figure 2.1. Enantiomeric chiral biphenyls.....	8
Figure 2.2. Descriptors for the axially chiral 2-arylimino-3-aryl-thiazolidine-4-one derivatives.....	9
Figure 2.3. E and Z configuration of 2-arylimino-3-aryl-thiazolidine-4-ones.....	10
Figure 2.4. Mechanism of Rotation about the C=N double bond.....	10
Figure 2.5. The rotation about C=N double bond of 2-arylimino-3-aryl-thiazolidine-4-ones	11
Figure 2.6. Mechanism of inversion of nitrogen.....	11

Figure 2.7. Transition state for rotation.....	12
Figure 2.8. Electronic effects on the isomerization of imines.....	12
Figure 2.9. Steric effect on the isomerization of N-aryl imines.....	13
Figure 2.10. E and Z configuration of 2-arylimino-3-aryl-thiazolidine-4-ones.....	13
Figure 2.11. The structure of 2,4-thiazolidinediones and rhodanines.....	15
Figure 2.12. Internal rotation between two rotamers.....	18
Figure 3.1. The synthesis of N,N'-diarylthioureas.....	20
Figure 3.2. Synthesis of 2-arylimino-3-aryl-thiazolidine-4-ones.....	23
Figure 4.1. The structure of 2-phenylimino-3-phenyl-thiazolidine-4-one.....	32
Figure 4.2. The Z to E isomerization of 2-phenylimino-3-phenyl-thiazolidine-4-one.....	33
Figure 4.3. The methylene peak of 2-phenylimino-3-phenyl-thiazolidine-4-one in various solvents at 25 °C.....	34
Figure 4.4. ¹ H NMR signals of methylene protons on C-5 of 2-phenylimino-3-phenyl-thiazolidine-4-one at various temperatures in DMF-d ₇	35
Figure 4.5. ¹ H NMR signals of methylene protons on C-5 of 2-phenylimino-3-phenyl-thiazolidine-4-one at various temperatures in toluene-d ₈	36
Figure 4.6. ¹ H NMR signals of methylene protons on C-5 of 2-phenylimino-3-phenyl-thiazolidine-4-one at various temperatures in benzene-d ₆	37

Figure 4.7. The 400 MHz ^1H NMR spectrum of 2-phenylimino-3-phenyl-thiazolidine-4-one in DMF- d_7	38
Figure 4.8. The 400 MHz ^1H NMR spectrum of 2-phenylimino-3-phenyl-thiazolidine-4-one in CDCl_3	39
Figure 4.9. The 400 MHz ^1H NMR spectrum of 2-phenylimino-3-phenyl-thiazolidine-4-one in methanol- d_4	40
Figure 4.10. The 400 MHz ^1H NMR spectrum of 2-phenylimino-3-phenyl-thiazolidine-4-one in toluene- d_8	41
Figure 4.11. The 400 MHz ^1H NMR spectrum of 2-phenylimino-3-phenyl-thiazolidine-4-one in benzene- d_6	42
Figure 4.12. The ^{13}C NMR spectrum of 2-phenylimino-3-phenyl-thiazolidine-4-one in CDCl_3	43
Figure 4.13. The ^{13}C NMR spectrum of 2-(<i>o</i> -tolyl)imino-3-(<i>o</i> -tolyl)-thiazolidine-4-one in benzene- d_6	44
Figure 4.14. The 3D structure of 2-phenylimino-3-phenyl-thiazolidine-4-one.....	46
Figure 4.15. The resonance structure of 2-phenylimino-3-phenyl-thiazolidine-4-one.....	47
Figure 4.16. Aromatic region of the 2D-NOESY spectrum of 2-phenylimino-3-phenyl-4-thiazolidinone in DMF- d_7	48
Figure 4.17. Aromatic region of 2D-COSY spectrum of 2-phenylimino-3-phenyl-thiazolidine-4-one in benzene- d_6	49
Figure 4.18. Aromatic region of 2D-NOESY spectrum of 2-phenylimino-3-phenyl-thiazolidine-4-one in benzene- d_6	49

Figure 4.19. The structure of 2-(<i>o</i> -tolyl)imino-3-(<i>o</i> -tolyl)-thiazolidine-4-one.....	50
Figure 4.20. The AB spectra of diastereotopic methylene protons on the C-5 of 2-(<i>o</i> -tolyl)imino-3-(<i>o</i> -tolyl)-thiazolidine-4-one in various solvents at 25 °C...	51
Figure 4.21 ¹ H NMR signals for diastereotopic methylene protons on C-5 of 2-(<i>o</i> -tolyl)imino-3-(<i>o</i> -tolyl)-thiazolidine-4-one at various temperatures in toluene- <i>d</i> ₈	52
Figure 4.22. The 400 MHz ¹ H NMR spectrum of 2-(<i>o</i> -tolyl)imino-3-(<i>o</i> -tolyl)-thiazolidine-4-one in DMF- <i>d</i> ₇	53
Figure 4.23. The 400 MHz ¹ H NMR spectrum of 2-(<i>o</i> -tolyl)imino-3-(<i>o</i> -tolyl)-thiazolidine-4-one in CDCl ₃	54
Figure 4.24. The 400 MHz ¹ H NMR spectrum of 2-(<i>o</i> -tolyl)imino-3-(<i>o</i> -tolyl)-thiazolidine-4-one in methanol- <i>d</i> ₄	55
Figure 4.25. The 400 MHz ¹ H NMR spectrum of 2-(<i>o</i> -tolyl)imino-3-(<i>o</i> -tolyl)-thiazolidine-4-one in toluene- <i>d</i> ₈	56
Figure 4.26. The ¹³ C NMR spectrum of 2-(<i>o</i> -tolyl)imino-3-(<i>o</i> -tolyl)-thiazolidine-4-one in CDCl ₃	57
Figure 4.27. The ¹³ C NMR spectrum of 2-(<i>o</i> -tolyl)imino-3-(<i>o</i> -tolyl)-thiazolidine-4-one in toluene- <i>d</i> ₈	58
Figure 4.28. Aromatic part of 2D-NOESY spectrum of 2-(<i>o</i> -tolyl)imino-3-(<i>o</i> -tolyl)-thiazolidine-4-one in CDCl ₃	60
Figure 4.29. Aromatic part of 2D-COSY spectrum of 2-(<i>o</i> -tolyl)imino-3-(<i>o</i> -tolyl)-thiazolidine-4-one in CDCl ₃	60

- Figure 4.30. Aromatic part of 2D-NOESY spectrum of 2-(*o*-tolyl)imino-3-(*o*-tolyl)-thiazolidine-4-one in toluene- d_861
- Figure 4.31. Aromatic part of 2D-COSY spectrum of 2-(*o*-tolyl)imino-3-(*o*-tolyl)-thiazolidine-4-one in toluene- d_861
- Figure 4.32. The chromatograms taken to follow thermal racemization process of 2-(*o*-tolyl)imino-3-(*o*-tolyl)-thiazolidine-4-one.....63
- Figure 4.33. The plot of $\ln\left(\frac{[M]_0 - [M]_{eq}}{[M] - [M]_{eq}}\right)$ versus time at 333 K for 2-(*o*-tolyl)imino-3-(*o*-tolyl)-thiazolidine-4-one.....64
- Figure 4.34. The energy barriers and the structures of 2-(*o*-tolyl)imino-3-(*o*-tolyl)-thiazolidine-4-one and 3-(*o*-tolyl)rhodanine.....65
- Figure 4.35. 3D structures of 2-(*o*-tolyl)imino-3-(*o*-tolyl)-thiazolidine-4-one and 3-(*o*-tolyl)rhodanine.....65
- Figure 4.36. The structure of 2-(α -naphthyl)imino-3-(α -naphthyl)-thiazolidine-4-one.....66
- Figure 4.37. The AB spectra of diastereotopic methylene protons on the C-5 of 2-(α -naphthyl)imino-3-(α -naphthyl)-thiazolidine-4-one in various solvents at 25 °C.....67
- Figure 4.38. ^1H NMR signals for diastereotopic methylene protons on C-5 of 2-(α -naphthyl)imino-3-(α -naphthyl)-thiazolidine-4-one at various temperatures in DMF- d_768
- Figure 4.39. ^1H NMR signals for diastereotopic methylene protons on C-5 of 2-(α -naphthyl)imino-3-(α -naphthyl)-thiazolidine-4-one at various temperatures in toluene- d_869

- Figure 4.40. The 400 MHz ^1H NMR spectrum of 2-(α -naphthyl)imino-3-(α -naphthyl)-thiazolidine-4-one in DMF-d_770
- Figure 4.41. The 400 MHz ^1H NMR spectrum of 2-(α -naphthyl)imino-3-(α -naphthyl)-thiazolidine-4-one in methanol- d_471
- Figure 4.42. The 400 MHz ^1H NMR spectrum of 2-(α -naphthyl)imino-3-(α -naphthyl)-thiazolidine-4-one in CDCl_372
- Figure 4.43. The 400 MHz ^1H NMR spectrum of 2-(α -naphthyl)imino-3-(α -naphthyl)-thiazolidine-4-one in toluene- d_873
- Figure 4.44. The ^{13}C NMR spectrum of 2-(α -naphthyl)imino-3-(α -naphthyl)-thiazolidine-4-one in CDCl_374
- Figure 4.45. The ^{13}C NMR spectrum of 2-(α -naphthyl)imino-3-(α -naphthyl)-thiazolidine-4-one in toluene- d_875
- Figure 4.46. Aromatic region of 2D-NOESY spectrum of 2-(α -naphthyl)imino-3-(α -naphthyl)-thiazolidine-4-one in CDCl_376
- Figure 4.47. Aromatic region of 2D-COSY spectrum of 2-(α -naphthyl)imino-3-(α -naphthyl)-thiazolidine-4-one in CDCl_377
- Figure 4.48. The chromatograms taken to follow thermal racemization process of 2-(α -naphthyl)imino-3-(α -naphthyl)-thiazolidine-4-one.....78
- Figure 4.49. The plot of $\ln\left(\frac{[\text{M}]_0 - [\text{M}]_{\text{eq}}}{[\text{M}] - [\text{M}]_{\text{eq}}}\right)$ versus time at 333 K for 2-(α -naphthyl)imino-3-(α -naphthyl)-thiazolidine-4-one.....79

- Figure 4.50. The energy barriers and the structures of 2-(α -naphthyl)imino-3-(α -naphthyl)-thiazolidine-4-one, 3-(α -naphthyl)-2,4 thioazolidinedione, 3-(α -naphthyl)rhodanine.....80
- Figure 4.51. 3D structures of 2-(α -naphthyl)imino-3-(α -naphthyl)-thiazolidine-4-one, 3-(α -naphthyl)-2,4 thioazolidinedione and 3-(α -naphthyl)rhodanine.....80
- Figure 4.52. The general structure of 2-(*o*-chlorophenyl)imino-3-(*o*-chlorophenyl)-thiazolidine-4-one.....81
- Figure 4.53. The AB spectra of diastereotopic methylene protons on the C-5 of 2-(*o*-chlorophenyl)imino-3-(*o*-chlorophenyl)-thiazolidine-4-one in various solvents at 25 °C.....82
- Figure 4.54. ^1H NMR signals for diastereotopic methylene protons on the C-5 of 2-(*o*-chlorophenyl)imino-3-(*o*-chlorophenyl)-thiazolidine-4-one at various temperatures in toluene- d_883
- Figure 4.55. The 400 MHz ^1H NMR spectrum of 2-(*o*-chlorophenyl)imino-3-(*o*-chlorophenyl)-thiazolidine-4-one in DMF- d_784
- Figure 4.56. The 400 MHz ^1H NMR spectrum of 2-(*o*-chlorophenyl)imino-3-(*o*-chlorophenyl)-thiazolidine-4-one in CDCl_385
- Figure 4.57. The 400 MHz ^1H NMR spectrum of 2-(*o*-chlorophenyl)imino-3-(*o*-chlorophenyl)-thiazolidine-4-one in methanol- d_486
- Figure 4.58. The 400 MHz ^1H NMR spectrum of 2-(*o*-chlorophenyl)imino-3-(*o*-chlorophenyl)-thiazolidine-4-one in toluene- d_887
- Figure 4.59. The 400 MHz ^1H NMR spectrum of 2-(*o*-chlorophenyl)imino-3-(*o*-chlorophenyl)-thiazolidine-4-one in benzene- d_688

- Figure 4.60. The ^{13}C NMR spectrum of 2-(*o*-chlorophenyl)imino-3-(*o*-chlorophenyl)-thiazolidine-4-one in CDCl_389
- Figure 4.61. The ^{13}C NMR spectrum of 2-(*o*-chlorophenyl)imino-3-(*o*-chlorophenyl)-thiazolidine-4-one in toluene- d_890
- Figure 4.62. Aromatic region of the 2D-COSY spectrum of 2-(*o*-chlorophenyl)imino-3-(*o*-chlorophenyl)-thiazolidine-4-one in benzene- d_691
- Figure 4.63. Aromatic region of the 2D-NOESY spectrum of 2-(*o*-chlorophenyl)imino-3-(*o*-chlorophenyl)-thiazolidine-4-one in benzene- d_692
- Figure 4.64. The plot of $\ln\left(\frac{[\text{M}]_0 - [\text{M}]_{\text{eq}}}{[\text{M}] - [\text{M}]_{\text{eq}}}\right)$ versus time at 343 K for 2-(*o*-chlorophenyl)imino-3-(*o*-chlorophenyl)-thiazolidine-4-one.....93
- Figure 4.65. The chromatograms taken to follow thermal racemization process of 2-(*o*-chlorophenyl)imino-3-(*o*-chlorophenyl)-thiazolidine-4-one.....93
- Figure 4.66. The general structure of 2-(*o*-methoxyphenyl)imino-3-(*o*-methoxyphenyl)-thiazolidine-4-one.....94
- Figure 4.67. The AB spectra of diastereotopic methylene protons on the C-5 of 2-(*o*-methoxyphenyl)imino-3-(*o*-methoxyphenyl)-thiazolidine-4-one in various solvents at 25 °C.....95
- Figure 4.68. ^1H NMR signals diastereotopic methylene protons on the C-5 of 2-(*o*-methoxyphenyl)imino-3-(*o*-methoxyphenyl)-thiazolidine-4-one at various temperatures in toluene- d_896
- Figure 4.69. The 400 MHz ^1H NMR spectrum of 2-(*o*-methoxyphenyl)imino-3-(*o*-methoxyphenyl)-thiazolidine-4-one in DMF- d_797

- Figure 4.70. The 400 MHz ^1H NMR spectrum of 2-(*o*-methoxyphenyl)imino-3-(*o*-methoxyphenyl)-thiazolidine-4-one in CDCl_398
- Figure 4.71. The 400 MHz ^1H NMR spectrum of 2-(*o*-methoxyphenyl)imino-3-(*o*-methoxyphenyl)-thiazolidine-4-one in methanol- d_499
- Figure 4.72. The 400 MHz ^1H NMR spectrum of 2-(*o*-methoxyphenyl)imino-3-(*o*-methoxyphenyl)-thiazolidine-4-one in toluene- d_8100
- Figure 4.73. The 400 MHz ^1H NMR spectrum of 2-(*o*-methoxyphenyl)imino-3-(*o*-methoxyphenyl)-thiazolidine-4-one in benzene- d_6101
- Figure 4.74. The ^{13}C NMR spectrum of 2-(*o*-methoxyphenyl)imino-3-(*o*-methoxyphenyl)-thiazolidine-4-one in CDCl_3102
- Figure 4.75. The ^{13}C NMR spectrum of 2-(*o*-methoxyphenyl)imino-3-(*o*-methoxyphenyl)-thiazolidine-4-one in benzene- d_6103
- Figure 4.76. Aromatic region of the 2D-COSY spectrum of 2-(*o*-methoxyphenyl)imino-3-(*o*-methoxyphenyl)-thiazolidine-4-one in benzene- d_6104
- Figure 4.77. Aromatic region of the 2D-NOESY spectrum of 2-(*o*-methoxyphenyl)imino-3-(*o*-methoxyphenyl)-thiazolidine-4-one in benzene- d_6105
- Figure 4.78. The plot of $\ln\left(\frac{[\text{M}]_0 - [\text{M}]_{\text{eq}}}{[\text{M}] - [\text{M}]_{\text{eq}}}\right)$ versus time at 308K for 2-(*o*-methoxyphenyl)imino-3-(*o*-methoxyphenyl)-thiazolidine-4-one.....106
- Figure 4.79. The chromatograms taken to follow thermal racemization process of 2-(*o*-methoxyphenyl)imino-3-(*o*-methoxyphenyl)-thiazolidine-4-one.....106

LIST OF TABLES

Table 3.1. Chemical used in this study.....	30
Table 4.1. 400 MHz spectral data for 2-phenylimino-3-phenyl-thiazolidine-4-one in different solvents.....	32
Table 4.2. 400 MHz spectral data for 2-(<i>o</i> -tolyl)imino-3-(<i>o</i> -tolyl)-thiazolidine-4-one in various solvents	50
Table 4.3. 400 MHz spectral data for 2-(α -naphthyl)imino-3-(α -naphthyl)-thiazolidine-4-one in various solvents	66
Table 4.4. 400 MHz spectral data for 2-(<i>o</i> -chlorophenyl)imino-3-(<i>o</i> -chlorophenyl)-thiazolidine-4-one in various solvents.....	81
Table 4.5. 400MHz spectral data for 2-(<i>o</i> -methoxyphenyl)imino-3-(<i>o</i> -methoxyphenyl)-thiazolidine-4-one in various solvents.....	94
Table4.6. The Rate Constants and Energy Barriers of the compounds studied.....	107

LIST OF SYMBOL/ABBREVIATIONS

A_m	Amount of the compound in the mobile phase
A_s	Amount of the compound in the stationary phase
C_m	Concentration of the compound in the mobile phase
C_s	Concentration of the compound in the stationary phase
F	Flow rate
h	Planck's constant
Hz	Hertz
J	Joule
K	Equilibrium constant
k'	Capacity factor
k_b	Boltzman constant
k_f	Rate constant for forward reaction
k_r	Rate constant for reverse reaction
s	Second
t	Time
T	Temperature
t_R	Retention time
V_0	Dead volume
V_n	Net retention volume
V_R	Retention volume
α	Separation factor
δ	Chemical shift
ΔG^\ddagger	Free energy of activation
$CDCl_3$	Deuterated chloroform
Chiralcel OD-H	Cellulose tris-(3,5-dimethyl)phenylcarbamate
Chiralpak AD-H	Amylose tris-(3,5-dimethyl)phenylcarbamate
CSP	Chiral stationary phase
DMSO- d_6	Hexadeuterated dimethylsulfoxide
HPLC	High pressure liquid chromatography

1. INTRODUCTION

Atropisomerism, the phenomenon of chirality due to restricted rotation about a single bond, has been a widely applicable area of stereochemistry from the first resolution of a chiral atropisomeric biaryl by Chistie and Kenner in 1922. They resolved 6,6'-dinitro-2,2'-diphenic acid (Figure 1.1) into optically active forms. The resolvability of this biphenyl derivative was attributed to steric interaction between bulky *ortho* substituents on each ring, and thus two nonplanar, axially chiral enantiomers exist [1].

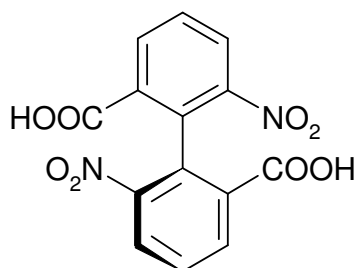


Figure 1.1. The structure of 6,6'- dinitro- 2,2'- diphenic acid

After investigations of restricted rotation about the C-C single bond of biphenyl derivatives, Adams *et al.*, in 1931, examined hindered rotations about the C-N bond of N-phenylpyroles (Figure 1.2), which are heterocyclic analogous of biphenyls [2-4].

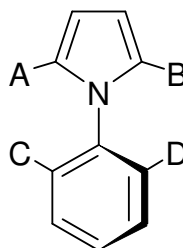


Figure 1.2. The general structure of N-phenylpyroles

In 1970, Colebrook *et al.* reported high barriers to rotation about C-N bond in aryl substituted heterocyclic compounds. The equilibration of rotational isomers was followed

by integration of their NMR signals and their activation parameters for hindered rotation about C-N bond was determined [5].

Determination of rotational barriers about C-N bond in some aryl substituted heterocyclic compounds lacking bulky *ortho* substituents by dynamic NMR was presented, again by Colebrook *et al.*, in 1972 [6].

In 1985, Mannschreck *et al.* investigated enantiomers of sterically hindered N-aryl-4-pyridones. The enrichment of the enantiomers was achieved by liquid chromatograph on triacetylcellulose. The barriers to rotation were determined by thermal racemization [7].

In 1992, Mintas *et al.* worked with N-aryl and N-heteroarylpyroles. They achieved the enrichment of the related rotomers by liquid chromatography on triacetylcellulose and estimated the barriers to rotation by thermal racemization [8].

In 1992, Doğan *et al.* synthesized the sterically hindered N-(*o*-tolyl) and N-(*o*-chlorophenyl)- 2- thioxo-4-oxazolidinones and thiazolidinones (Figure 1.3). Chirality of the compounds was proven by the presence of diastereotopic protons detected by ^1H NMR. In the presence of (S)-(+)-1-(9-anthryl)-2,2,2-trifluoroethanol as an chiral auxiliary the enantiomers showed ^1H NMR shift differences [9].

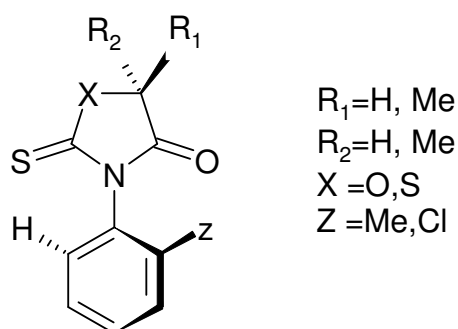


Figure 1.3. The structure of N-(*o*-aryl) and N-(*o*- aryl)- 2- thioxo-4-oxazolidinones and thiazolidinones

In 1993, Doğan and Mannschreck investigated the enantiomers of N-aryl-2-thioxo-4-oxazolidinones and N-arylrhodanines for the first time analytically and enriched semi-preparatively by liquid chromatography on triacetyl and tribenzoylcellulose [10].

In 2003, Oğuz and Doğan separated the enantiomers of 5,5-dimethyl-1-(*o*-aryl)barbituric and 2-thiobarbituric acid derivatives (Figure 1.4) by micropreparative liquid chromatography. The activation barriers for the conversion of one enantiomer to its counterpart have been determined upon thermal racemization of separated enantiomers [11].

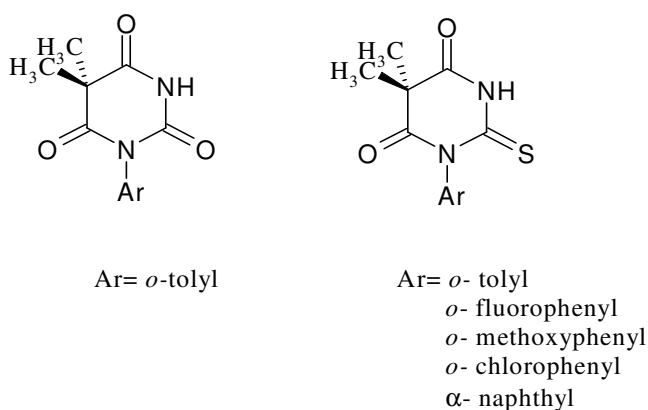


Figure 1.4. The 5,5-dimethyl-1-(*o*-aryl)barbituric and 2-thiobarbituric acid derivatives

Recently, Demir Ordu and Doğan calculated the activation barriers for the interconversion between the enantiomers of 5,5-dimethyl-3-(*o*-aryl)-2,4-oxazolidinediones (Figure 1.5) by temperature dependent NMR and by thermal racemization. They found that the activation barriers increase linearly with the size of the van der Waals radii of the *ortho*-halogen substituents [12].

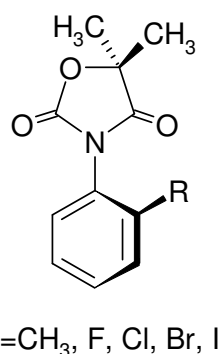
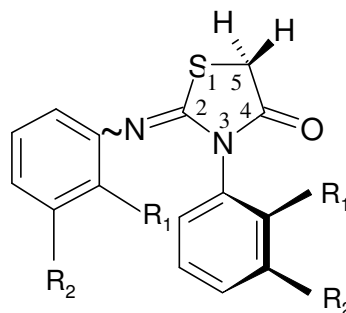


Figure 1.5. The structure of 5,5-dimethyl-3-(*o*-aryl)-2,4-oxazolidinediones

In the present project, the stereostructures of 2-arylimino-3-aryl-thiazolidine-4-ones (Figure 1.6) have been investigated. In this new set of compounds with the introduction of N_{imino} -aryl bond additional stereochemical features come into question.



1. $R_1 = R_2 = H$
2. $R_1 = CH_3$ $R_2 = H$
3. $R_1 = R_2 = \text{Benzo}$
4. $R_1 = Cl$ $R_2 = H$
5. $R_1 = OCH_3$ $R_2 = H$

Figure 1.6. The structure of the compounds studied in this project

It is known that N_3 -aryl bond rotation is hindered and gives rise to **M** and **P** stereoisomers. Now as far as the $C=N_{\text{imino}}$ is concerned, this bond may have an **E** and **Z** configuration. In addition, the N_{imino} -aryl bond may be hindered due to the presence of the other aryl ring and/or the lone pair of electrons on sulfur.

Previously, in 1983, 2-arylimino-5-methyl-3-aryl-thiazolidine-4-one derivatives were synthesized by Doğan *et al.* and the presence of diastereomeric isomers were shown by 60 MHz 1H and ^{13}C NMR. [13].

In recent years Roussel *et al.* published a paper reporting on determination of the barriers to rotation in some N,N' -diaryl-2-imino thiazoline derivatives, but they did not take into account the configuration of $C=N_{\text{imino}}$ bond [14].

The mechanism of $C=N$ double bond isomerization has been subject of debate, and considered in terms of either rotation about $C=N$ double bond or inversion of nitrogen

(lateral shift mechanism). In some cases, a mechanism between these two extremes may be possible [15,16]

In chemical literature there are several reports concerning the factors influencing the **E** and **Z** isomerization in imines.

Kessler and Leibfritz reported that protic solvents retard the syn-anti isomerization by protonation or by hydrogen bonding to the nitrogen lone pair which is needed for inversion. In addition, highly polar nature of the transition state of the rotation makes this mechanism favorable in polar solvents [15].

Mannschreck *et al.* reported that the magnitude of the barriers to isomerization in N-isopropylideneanilines (Figure 1.7) is not enhanced by the presence of bulky (**R**) substituents. These results argue against the rotation mechanism because the severe interactions between the *ortho* substituent and the methyl group in the isopropylene moiety are expected in the transition state for rotation. Therefore, they concluded that inversion mechanism would be preferred [15, 16].

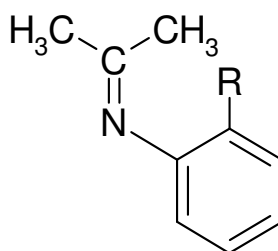
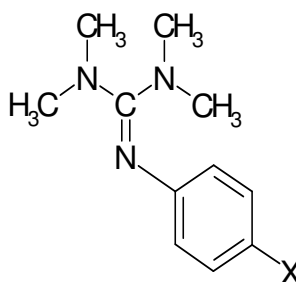


Figure 1.7. The structure of N-isopropylideneanilines

Kessler and Leibfritz examined the electronic effects on the syn-anti isomerization barrier in tetramethyl-N''-arylguanidines (Figure 1.8). They observed that electron-withdrawing substituents reduce the magnitude of the barrier which was interpreted in terms of the inversion mechanism [16].



X= NO₂, COCH₃, COOCH₃, Br, Cl, F, H, CH₃, OCH₃, N(CH₃)₂

Figure 1.8. The structure of N,N,N',N'-tetramethyl-N''-arylguanidines

The aims of this project are the followings:

- To synthesize 2-arylimino-3-aryl-thiazolidine-4-one derivatives.
- To investigate hindered rotations about the N₃-aryl bond and, if it exists, about N_{imino}-aryl bond using NMR techniques and enantioselective HPLC.
- To determine the rotational barriers by thermal racemization.
- To identify the configuration of C=N double bond by using 2D-NOESY experiments and by comparing the energy barriers of structurally related compounds.

2. THEORY

2.1. Chirality

The concept of 'chirality' has been known in chemistry since the 1870's although it would be nearly a hundred years chemists began using this term. The term chiral is derived from cheiro meaning 'hand' and apparently was coined by Lord Kelvin in 1904, in his *Baltimore Lectures on Molecular Dynamics and Wave Theory of Light* in which he stated "*I call any geometrical figure, or group of points, chiral and say it has chirality, if its image in a plane mirror, ideally realized, cannot be brought to coincide with itself*".

In extremely simple terms, chirality is 'handedness', that is the property of an object being non-superimposable on its mirror image. A chiral molecule and its non-superimposable mirror image are described as 'enantiomers' of each other. In absence of an external chiral influence enantiomers have identical physical and chemical properties. Diastereomers are basically stereoisomers that are not enantiomers of each other and exhibit different physical and chemical properties.

There are four main types of chirality. These are central chirality, axial chirality, planar chirality, and helical chirality.

Central chirality arises when a tetrahedral atom has four different groups attached to it. Such an atom is called a 'stereocenter' and the most common example is a carbon atom having four different groups attached to it. Besides carbon, tetrahedral nitrogen, sulfur, and phosphorus would be a stereocenter.

Axial chirality results from the non-planar arrangement of four groups about a chiral axis. This type chirality will be discussed in detail later because the compounds studied in this project are axially chiral.

Planar chirality results from the arrangement of out-of-plane groups with respect to a plane (chirality plane).

A helical molecule can adopt either a right- or left-handed twist giving rise to helical chirality.

2.2. Atropisomerism (Axial Chirality) and Hindered Rotation in 2-arylimino-3-aryl-thiazolidine-4-ones

Atropisomers are stereoisomers resulting from hindered rotation about a single bond. Atropisomers also display axial chirality. Classical examples of such molecules are the biphenyls (Figure 2.1). The steric interaction between the *ortho* substituents is to make the planar conformation an energy maximum, two nonplanar, axially chiral enantiomers exist. If the interconversion through the planar conformation is slow enough they may, under suitable circumstances, be resolved.

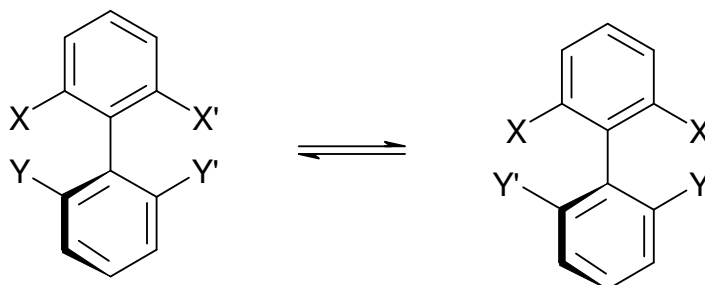


Figure 2.1. Enantiomeric chiral biphenyls

Rotation about the N_3 -aryl bond in 2-(*o*-aryl)imino-3-(*o*-aryl)-4-thiazolidinones is hindered due to the steric interaction between the *ortho* substituent on the N_3 -aryl and the exocyclic oxygen and imino nitrogen. In addition, there is a possibility that the N_{imino} -aryl bond rotation is hindered due to the presence of the N_3 -aryl ring and the lone pair electron on sulfur. Therefore, compounds investigated in this project are axially chiral.

According to Cahn-Ingol-Prelog rules [17] stereochemical descriptors **M** and **P** are used to specify the absolute configuration of axially chiral molecules (Figure 2.2). In this system, first an axis is drawn through the single bond around which conformation is

defined and the smallest torsion angle formed between the carbon atoms bearing the groups of the highest priority is used to define helix. A resulting clockwise rotation is denoted as '**P**' (plus) and the counter clockwise rotation is denoted as '**M**' (minus).

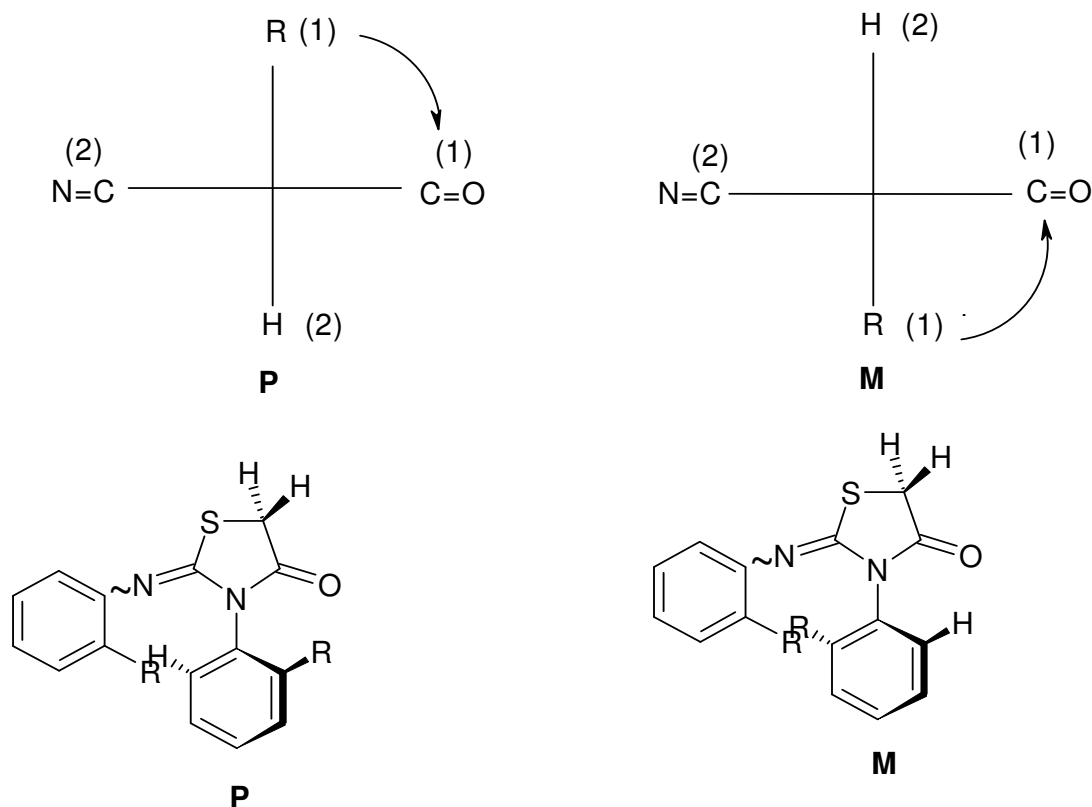


Figure 2.2. Descriptors for the axially chiral 2-arylimino-3-aryl-thiazolidine-4-one derivatives

2.3. The E-Z Isomerisation of Imines

Since 2-arylimino-3-aryl-thiazolidine-4-ones have the imino functional group, isomerization of C=N double bond should be taken into account (Figure 2.3).

Actually there are two mechanisms by which the imines interconvert between E and Z isomers.

- Rotation about the C=N double bond
- Inversion of nitrogen (Lateral shift mechanism)

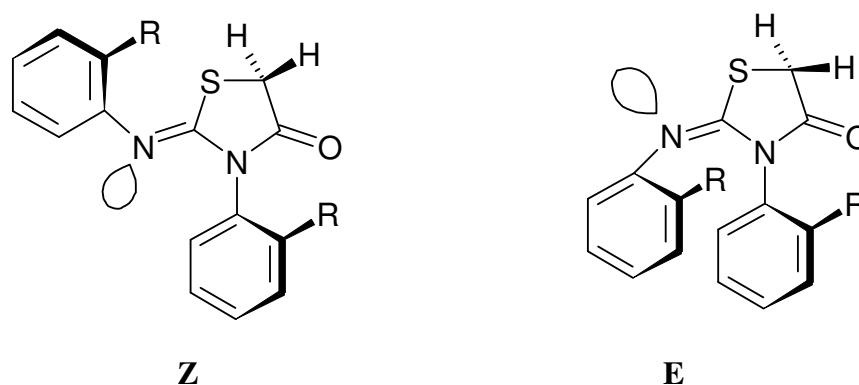


Figure 2.3. E and Z configuration of 2-arylimino-3-aryl-thiazolidine-4-ones

2.3.1. Rotation about the C=N Double Bond

Rotation mechanism is made possible by polarization [15]. Partial negative charge accumulates on nitrogen, which makes rotation possible. Transition state for this mechanism is out of plane (Figure 2.4).

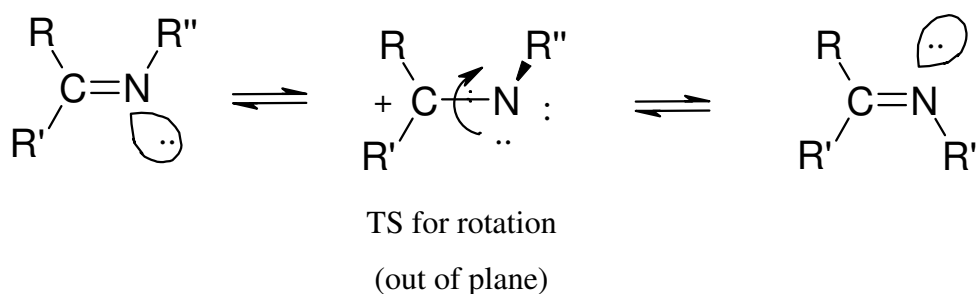


Figure 2.4. Mechanism of Rotation about the C=N double bond

Lone pair orbital lobe of nitrogen (N_3) of 2-arylimino-3-aryl-thiazolidine-4-ones is perpendicular to the p orbitals of N_3 -aryl ring, thus it does not participate in electron delocalization. But this lone pair can in principle go into conjugation with the imino bond. As a result, double bond character of the imino bond may be reduced so that the rotation can occur (Figure 2.5).

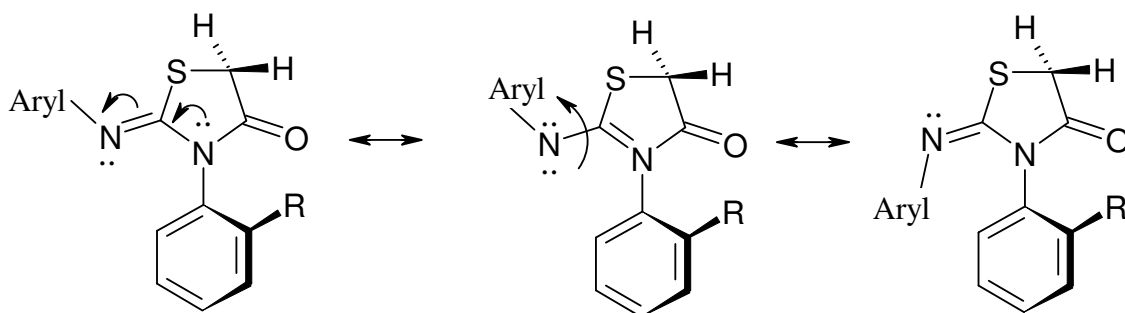


Figure 2.5. The rotation about C=N double bond of 2-arylimino-3-aryl-thiazolidine-4-ones

2.3.2. Inversion of Nitrogen (Lateral Shift Mechanism)

Inversion of nitrogen involves a change of hybridization of the nitrogen from sp^2 to sp orbital where the lone pair move from sp^2 to p orbital [15]. In contrast to transition state for rotation mechanism, transition state for this mechanism is in plane (Figure 2.6).

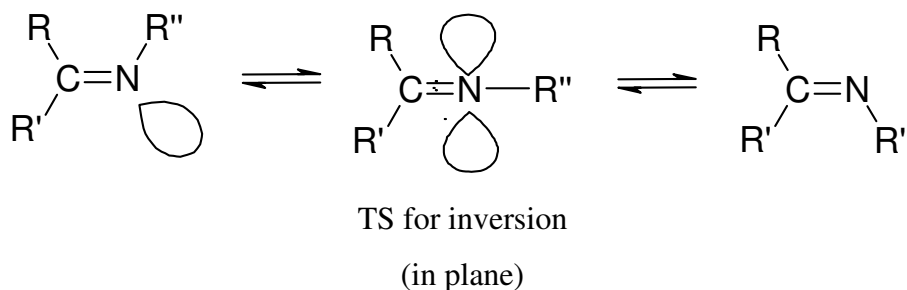


Figure 2.6. Mechanism of inversion of nitrogen

Whether imines isomerize via rotation or via inversion of imino nitrogen has been subject of debate. In some cases, both mechanisms may be responsible for isomerization [15,16]

2.4. Factors Affecting C=N Double Bond Isomerization

The mechanism of isomerization can be speculated about by examining which factors influence the isomerization process.

The factors influencing the rate of isomerization are the followings:

- Solvent effects
- Electronic effects
- Steric effects

2.4.1. Solvent Effects

Rotation about the C=N double bond is facilitated by polar solvents because the transition state for this mechanism is highly polar (Figure 2.7).

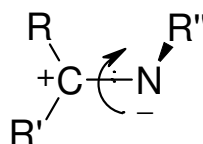


Figure 2.7. Transition state for rotation

In addition, inversion mechanism is retarded in protic solvents, which can be explained by protonation or by a hydrogen bond to the lone pair which is needed for inversion.

2.4.2. Electronic Effects

When worked with N-aryl imines it was observed that the presence of electron withdrawing substituents on N-aryl ring stabilize TS for nitrogen inversion via delocalization (Figure 2.8).

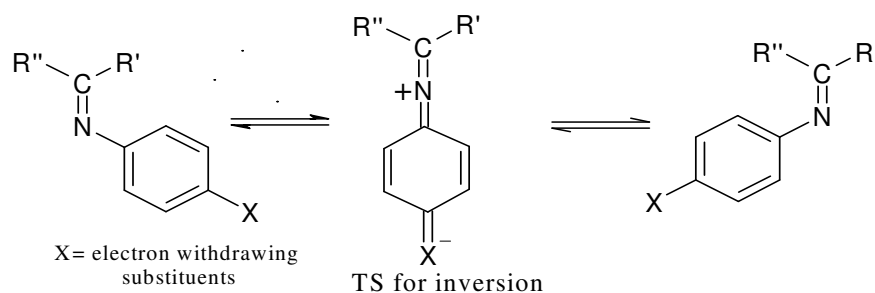


Figure 2.8. Electronic effects on the isomerization of imines

2.4.3. Steric Effects

In N-aryl imines containing an *ortho* substituent it has been found that if the bulkiness of the *ortho* substituent is increased, nitrogen inversion is preferred because severe interactions between the *ortho* substituents and the substituents on the carbon atom are expected in TS for rotation (Figure 2.9) [15,16]

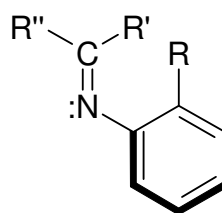


Figure 2.9. Steric effect on the isomerization of N-aryl imines

2.5. Assignment of the Stereochemistry of the Imino Bond in 2-arylimino-3-aryl-thiazolidine-4-ones

The assignment of the configuration of imino bond of 2-arylimino-3-aryl-thiazolidine-4-ones is made depending on whether the substituents having higher priority are on the same side or on the opposite side of the C=N double bond. Sulfur atom has higher priority than nitrogen, and also aryl ring has higher priority than the lone pair of nitrogen. If the substituents having higher priority are oriented toward the same side, then the descriptor **Z** is employed. In the contrary case **E** is used (Figure 2.10).

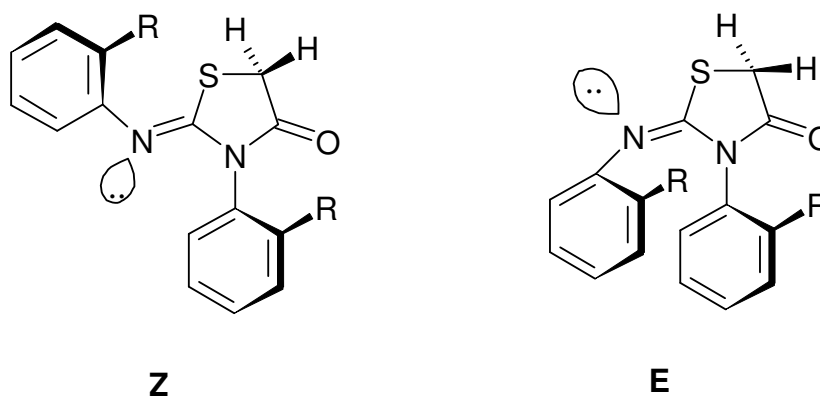


Figure 2.10. E and Z configuration of 2-arylimino-3-aryl-thiazolidine-4-ones

For compounds investigated in this study it can be thought that **Z** configuration may be predominant because of the steric hinderence brought by the other aryl ring. But it must be taken into account that π - π interaction between two rings in **E** configuration may also be a favorable interaction.

2.5.1. 2D-NOESY Spectroscopy

2D-NOESY experiments may be used to find out the stereochemistry of the C=N double bond of 2-arylimino-3-aryl-thiazolidine-4-one derivatives. This technique indicates which protons are close enough in space. If the through space distance is smaller than 4 Å, the crosspeaks will be observed in the spectrum.

If there is an **E** configuration of 2-arylimino-3-aryl-thiazolidine-4-ones (Figure 2.10), the crosspeaks can be observed for the protons of the two rings.

2.5.2. Comparison of the Energy Barriers of Structurally Related Compounds

Comparison of the energy barriers of 2-arylimino-3-aryl-thiazolidine-4-one derivatives with structurally related compounds, 2,4-thiazolidinediones and rhodanines, (Figure 2.11) is expected to give an idea about the stereochemistry of the C=N double bond of imino bond.

It is thought that there may be no big difference in the energy barriers between compounds studied in this project and structurally related compounds if 2-arylimino-3-aryl-thiazolidine-4-ones have **Z** configuration because the imino nitrogen would not hinder the rotation about N₃-aryl more than the oxygen and the sulfur.

In the case of **E** configuration, the other aryl group results in more hinderence, and thus the barriers to rotation is expected to be higher than that of 2,4-thiazolidinediones and that of rhodanines (Figure 2.11).

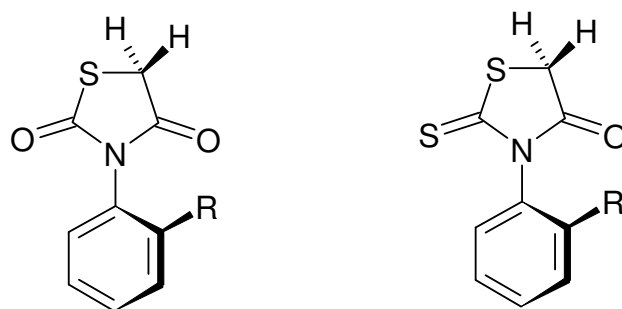


Figure 2.11. The structure of 2,4-thiazolidinediones and rhodanines

2.6. Determination of the Barriers to Rotation by Thermal Racemization

2.6.1. A Review of High Performans Liquid Chromatography

The concept of chromatography depends on the differential distribution of solute between the mobile and stationary phases, one of which is moving respect to the other. There are many types of chromatography, which are distinguished from one another depending on the nature of the mobile and the stationary phases.

High performance or high pressure liquid chromatography (HPLC) is an advanced liquid chromatographic technique used for chromatographic separation, and identification of compounds. HPLC instruments consist of a reservoir of mobile phase, a pump, an injector, a column, and a detector. The column contains a special solid packing material, which serves as the stationary phase. Compounds are separated by injecting the sample mixture onto column. The different components in the mixture are retained to different extents by solid packing material. The components that are strongly retained by the stationary phases move slowly with the flow of the mobile phases. On the other hand, components that are weakly held by the stationary phase travel rapidly.

The retention of a compound on a column can be expressed by its retention time (t_R), retention volume ($V_R = t_R F$, where F is the flow rate) or the capacity ratio (k'), which is directly related to its equilibrium distribution constant (K) in the stationary –mobile phase system. The capacity ratio is defined by:

$$k' = A_s/A_m \quad (2.1)$$

where A_s and A_m denote the amount of the compound in the stationary and the mobile phase, respectively. Let V_s and V_m be the volumes of the respective phases; then

$$k' = C_s V_s / C_m V_m = K V_s / V_m \quad (2.2)$$

V_m is commonly written as V_0 and represents the dead volume in the column, which does not contribute to the separation. Consequently, the net retention volume, V_n , can be written as $V_n = V_R - V_0$, since $K = V_n / V_s$, combination with equation (2.2) gives:

$$k' = (V_R - V_0) / V_0 \quad (2.3)$$

This expressions permits the determination of the capacity factor from the chromatogram. The chromatographic separation of two components (1 and 2) depends on the separation factor (α) of a column. It can be written as $k_2' / k_1' = K_2 / K_1 = \alpha$. From Equation (2.3), α can be formulated as:

$$\alpha = (V_{R2} - V_0) / (V_{R1} - V_0) \quad (2.4)$$

Thus the separation factor is simply the ratio of the net retention volumes of the two components. If the dead volume V_0 , has been determined, the separation factor is easily calculated from Equation (2.4).

2.6.2. Separation of Stereoisomers by Chiral HPLC

Enantiomers are known to behave chemically and physically in an identical manner. Therefore, it would be impossible to separate enantiomers by ordinary HPLC as they would be retained by the stationary phases to the same extent. However, the separation can be directly achieved by using chiral HPLC columns packed with chiral stationary phases (CSPs).

In chiral HPLC, resolution relies on the formation of transient diastereomeric complexes between the analyte and the chiral discriminating agent. The compounds which forms the most stable diastereoisomer will be most retained, where as the opposite enantiomer will form a less stable diastereoisomer and will elute first. To achieve discrimination between enantiomers there needs to be a minimum three points of interaction to achive chiral recognition.

The forces that lead to this interaction are very weak and require careful optimisation by adjustment of the mobile phase and temperature to maximize selectivity. The separation in chiral HPLC is a result of the sum of a large number of interactions. Typically a free energy of interaction difference of only 0.03 kJ/mol between the enantiomers and chiral stationary phase will lead to resolution.

The intermolecular forces involved in chiral recognition are polar/ionic interactions, pi-pi interactions, hydrophobic effects, and hydrogen bonding. These can be augmented by the formation of inclusion complexes and binding to specific sites. The analyst may manipulate these intermolecular forces by choosing suitable mobile phases. In addition, the effect of temperature is important in chiral HPLC. Lower temperature will increase chiral recognition.

Many different types of chiral stationary phases present in the market are cellulose type, pirkle type (brush), ligand-exchange type, and protein type.

In this study, resolution of the stereoisomers was attempted on Chiralcel OD-H and Chiralpak AD-H columns, packed with cellulose tris-3,5-dimethylphenyl carbamate and amylose tris-3,5-dimethylphenyl carbamate as chiral stationary phases, respectively.

2.6.3. Determination of the Kinetic and Thermodynamic Constants of the Internal Rotation Process for 2-arylimino-3-aryl-thiazolidine-4-ones

If one of the stereoisomers of 2-arylimino-3-aryl-thiazolidine-4-ones is separated or enriched from the other one by enantioselective HPLC, it thermally interconverts to the other one with time through the rotation about the N₃-aryl bond and finally reaches the

equilibrium (Figure 2.12). The process follows reversible first-order kinetics, the theory of which is given below:

The reversible reaction $M \rightleftharpoons P$ is first order in both the forward (f) and the reverse direction (r), so that $r_f = k_f [M]$ and $r_r = k_r [P]$. If $(d[M]/dt)_f$ denotes the rate of change of $[M]$ due to forward reaction, then $-(d[M]/dt)_f = r_f = k_f[M]$. The rate of formation of $[M]$ by reverse reaction is $(d[M]/dt)_r = r_r = k_r[P]$. Then,

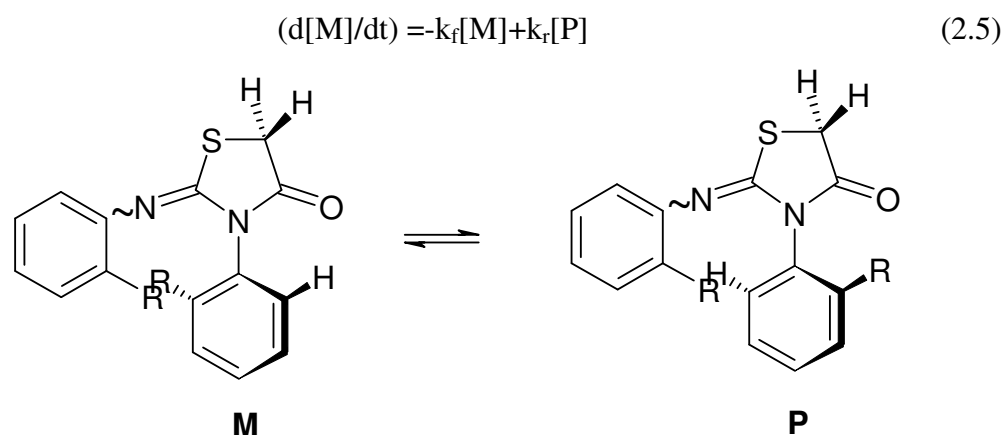


Figure 2.12. Internal rotation between two rotamers

We have $\Delta[P] = -\Delta[M]$, so $[P] - [P]_0 = -([M] - [M]_0)$. Substitution of $[P] = [P]_0 + [M]_0 - [M]$ into Equation (2.5) gives

$$d[M]/dt = k_r[P]_0 + k_r[M]_0 - (k_f + k_r)[M] \quad (2.6)$$

At equilibrium, the rates of the forward and reverse reactions become equal, the concentration of each species being constant, thus $d[M]/dt$ is 0. Let $[M]_{eq}$ be the equilibrium concentration of M. Setting $d[M]/dt = 0$ and $[M] = [M]_{eq}$ in Equation (2.6), we get

$$k_r[P]_0 + k_r[M]_0 = (k_f + k_r)[M]_{eq} \quad (2.7)$$

The use of Equation (2.7) in Equation (2.6) gives $d[M]/dt = (k_f + k_r) ([M]_{eq} - [M])$. Using the identity $\int (x + s)^{-1} dx = \ln(x + s)$ to integrate this equation, we get,

$$\ln ([M]-[M]_{eq}/[M]_0-[M]_{eq})= -(k_f+k_r)t \quad (2.8)$$

Since $k_f=k_r$ for the racemization of enantiomers, Equation (2.8) could be written as Equation (2.9) for the racemization of enantiomers

$$\ln ([M]-[M]_{eq}/[M]_0-[M]_{eq})=-2kt \quad (2.9)$$

By using Equation (2.9), a plot of $\ln ([M]-[M]_{eq}/[M]_0-[M]_{eq})$ versus time gives a straight line, the slope being equal to $-2k$. Having determined k , the free energy of activation can be calculated using the Eyring Equation (2.10),

$$\Delta G^\ddagger = RT \ln(k_b \cdot T / k \cdot h) \quad (2.10)$$

where $R=8.3143 \text{ J/mol.K}$, $T=\text{temperatue(Kelvin)}$ at which the interconversion takes place, $k_b(\text{Boltzmann constant})=1.3805 \cdot 10^{-23} \text{ J/K}$, $h (\text{Planck constant})=6.6256 \cdot 10^{-34} \text{ J.s}$, $k=\text{the rate constant for the racemization reaction}$.

3. ORGANIC SYNTHESIS

3.1. Synthesis of N,N'-Diarylthioureas

3.1.1. General Procedure

The N,N'-Diarylthioureas, which were used as starting material to synthesize 2-arylimino-3-aryl-thiazolidine-4-ones, were synthesized by the reaction of corresponding anilines with carbon disulfide (Figure 3.1)

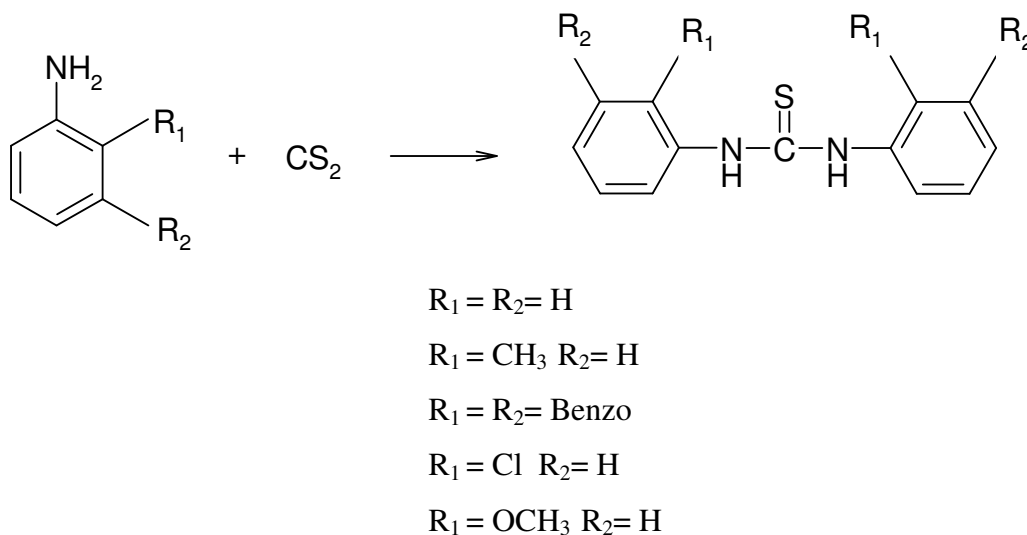


Figure 3.1. The synthesis of N,N'-diarylthioureas

The appropriate aniline was refluxed on a water bath for 3 hours with carbon disulfide, 40 per cent potassium hydroxide solution and ethanol. The crude N,N'-Diarylthiourea was purified by recrystallization from ethanol.

3.1.1.1. N,N'-Diphenylthiourea. The compound was synthesized according to the general procedure.

Starting materials:

Aniline: 8.37 g (0.09 mole)

Carbon disulfide: 9.12 g (0.12 mole)

40 % KOH solution: 14 ml

Ethanol: 10 ml

Yield: 1.64 g (8.0%)

Melting point: 154-155 °C

¹H NMR (400 MHz) data (ppm):

Solvent: DMSO-d₆

Aromatic protons: 7.08-7.46 (m)

-NH proton: 9.78 (s)

3.1.1.2. N,N'-Di-(*o*-tolyl)thiourea. The compound was synthesized according to the general procedure.

Starting materials:

o-toluidine: 9.63 g (0.09 mole)

Carbon disulfide: 9.12 g (0.12 mole)

40 % KOH solution: 14 ml

Ethanol: 10 ml

Yield: 2.30 g (10%)

Melting point: 165-166 °C

¹H-NMR (400 MHz) data (ppm):

Solvent: DMSO-d₆

Aromatic protons: 7.14-7.21 (m)

o-methyl protons: 2.22 (s)

-NH proton: 9.15 (s)

3.1.1.3. N,N'-Di-(α -naphthyl)thiourea. The compound was synthesized according to the general procedure.

Starting materials:

Solvent: DMSO-d₆

α -naphthylamine: 12.88 g (0.09 mole)

Carbon disulfide: 9.12 g (0.12 mole)

40 % KOH solution: 14 ml

Ethanol: 10 ml

Yield: 3.50 g (19%)

Melting point: 207-208 °C

¹H NMR (400 MHz) data (ppm):

Solvent: DMSO-d₆

Aromatic protons: 7.32-8.01 (m)

-NH proton: 9.80 (s)

3.1.1.4. N,N'-Di-(*o*-chlorophenyl)thiourea. The compound was synthesized according to the general procedure.

Starting materials:

o-chloroaniline: 11.43 g (0.09 mole)

Carbon disulfide: 9.12 g (0.12 mole)

40% KOH solution: 14 ml

Ethanol: 10 ml

Yield: 2.52 g (9.4%)

Melting point: 134-136 °C

¹H NMR (400 MHz) data (ppm):

Solvent: DMSO-d₆

Aromatic protons: 7.23-7.63 (m)

-NH proton: 9.62 (s)

3.1.1.5. N,N'-Di-(*o*-methoxyphenyl)thiourea. The compound was synthesized according to the general procedure.

Starting materials:

o-anisidine: 11.07 g (0.09 mole)

Carbon disulfide: 9.12 g (0.12 mole)

40 % KOH solution: 14 ml

Ethanol: 10 ml

Yield: 2.65 g (10.2%)

Melting point: 138-139 °C

¹H NMR (400 MHz) data (ppm):

Solvent: DMSO-d₆

Aromatic protons: 7.02-7.93 (m)

o-methoxy protons: 3.80 (s)

-NH proton: 9.36 (s)

3.2. Synthesis of 2-arylimino-3-aryl-thiazolidine-4-ones

3.2.1. General Procedure

The 2-arylimino-3-aryl-thiazolidine-4-ones were synthesized by the reaction of the corresponding N,N'-diarylthioureas and α -bromoacetic acid (Figure 3.2).

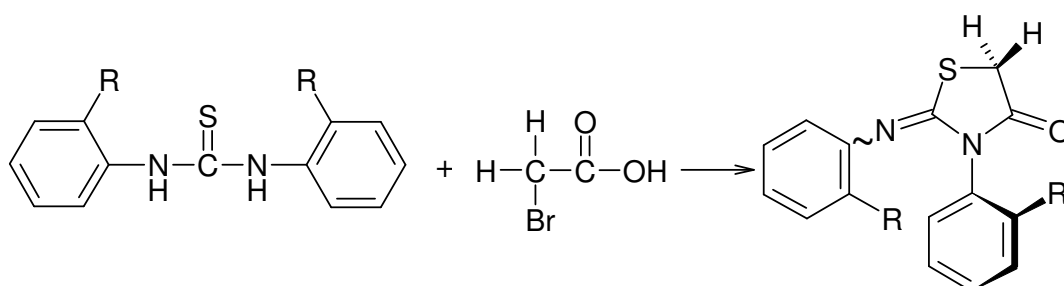


Figure 3.2. Synthesis of 2-arylimino-3-aryl-thiazolidine-4-ones

The appropriate N,N'-diarylthiourea and α -bromoacetic acid were refluxed for 6 hours in absolute ethanol in the presence of sodium acetate. At the end of this period, the crude product was purified by recrystallization from ethanol.

3.2.1.1. 2-phenylimino-3-phenyl-thiazolidine-4-one. This compound was synthesized according to the general procedure. After recrystallization from ethanol, 2-phenylimino-3-phenyl-thiazolidine-4-one was obtained as bright white crystals

Starting materials:

N,N'-diphenylthiourea: 1.14g (0.005 mole)

α -bromoacetic acid: 0.84 g (0.006 mole)

Sodium acetate: 0.49 g (0.006 mole)

Ethanol: 50 ml

Yield: 0.60 g (44.8 %)

Melting point :175-176 °C

¹H NMR (400 MHz) data (ppm):

Solvent :CDCl₃

Methylene protons at C-5: 3.99 (s)

Aromatic protons: 6.90-7.54 (m)

¹³C NMR (400MHz) data (ppm):

Solvent: CDCl₃

C-2 carbon of the heterocyclic ring: 155.14

C-4 carbon of the heterocyclic ring: 171.67

C-5 carbon of the heterocyclic ring: 33.15

Aromatic carbons: 121.10-148.27

Elemental analysis data:

Found: C, 66.78%; H, 4.29%; N, 9.66%; S, 12.12%

Calculated for C₁₅H₁₂ON₂S: C, 67.16%; H, 4.48%; N, 10.45%; S, 11.94%

IR data: $\nu_{\text{C=O}}$: 1724 cm^{-1} , C=O stretching $\nu_{\text{C=N}}$: 1630 cm^{-1} , C=N stretching

3.2.1.2. 2-(*o*-tolyl)imino-3-(*o*-tolyl)-thiazolidine-4-one. This compound was synthesized according to the general procedure. After recrystallization from ethanol, 2-(*o*-tolyl)imino-3-(*o*-tolyl)-thiazolidine-4-one was obtained as white crystals.

Starting materials:N,N'-di-(*o*-tolyl)thiourea: 0.64 g (0.0025 mole) α -bromoacetic acid: 0.42 g (0.003 mole)

Sodium acetate: 0.25 g (0.003 mole)

Ethanol: 50 ml

Yield: 0.41 g (55.4%)

Melting point: 154-155 °C

 ^1H NMR (400 MHz) data (ppm):Solvent: DMF- d_7 Diastereotopic methylene protons at C-5: δ_{A} = 4.51 and δ_{B} = 4.42*o*-methyl protons: 2.25(s) and 2.46(s)

Aromatic protons: 6.96-7.58 (m)

 ^{13}C NMR (400MHz) data (ppm):Solvent: CDCl_3

C-2 carbon of the heterocyclic ring: 154.13

C-4 carbon of the heterocyclic ring: 171.42

C-5 carbon of the heterocyclic ring: 33.26

o-methyl carbons: 17.97 and 17.86

Aromatic carbons: 120.0-146.98

Elemental analysis data:

Found: C, 67.51%; H, 4.97%; N, 8.51%; S, 11.09%

Calculated for C₁₇H₁₆ON₂S: C, 68.92%; H, 5.41%; N, 9.46%; S, 10.81%

IR data:

$\nu_{\text{C=O}}$: 1716 cm⁻¹, C=O stretching

$\nu_{\text{C=N}}$: 1631 cm⁻¹, C=N stretching

3.2.1.3. 2-(α -naphthyl)imino-3-(α -naphthyl)-thiazolidine-4-one. This compound was synthesized according to the general procedure. After recrystallization from ethanol, 2-(α -naphthyl)imino-3-(α -naphthyl)-thiazolidine-4-one was obtained as light pink colored and very thin crystals.

Starting materials:

N,N'-Di-(α -naphthyl)thiourea: 1.64 g (0.005 mole)

α -bromoacetic acid: 0.84 g (0.006 mole)

Sodium acetate: 0.49 g (0.006 mole)

Ethanol: 50 ml

Yield: 0.46 g (25.0 %)

Melting point: 180-181 °C

¹H NMR (400 MHz) data (ppm):

Solvent: CDCl₃

Diastereotopic methylene protons at C-5: $\delta_{\text{A}} = 4.09$ $\delta_{\text{B}} = 4.05$

Aromatic protons: 6.93-7.92 (m)

¹³C NMR (400MHz) data (ppm):

Solvent: CDCl₃

C-2 carbon of the heterocyclic ring: 166.38

C-4 carbon of the heterocyclic ring: 171.89

C-5 carbon of the heterocyclic ring: 33.40

Aromatic carbons: 115.23-144.50

Elemental analysis data:

Found: C, 73.26%; H, 4.05%; N, 7.04%; S, 8.79%

Calculated for C₂₃H₁₆ON₂S: C, 75.0%; H, 4.35%; N, 7.61%; S, 8.69%

IR data:

$\nu_{\text{C=O}}$: 1724 cm⁻¹, C=O stretching

$\nu_{\text{C=N}}$: 1630 cm⁻¹, C=N stretching

3.2.1.4. 2-(*o*-chlorophenyl)imino-3-(*o*-chlorophenyl)-thiazolidine-4-one. This compound was synthesized according to the general procedure. After recrystallization from ethanol, 2-(*o*-chlorophenyl)imino-3-(*o*-chlorophenyl)-thiazolidine-4-one was obtained as white crystals.

Starting material:

N,N'-Di-(*o*-chlorophenyl)thiourea: 1.48 g (0.005 mole)

α -bromoacetic acid: 0.84 g (0.006 mole)

Sodium acetate: 0.49 g (0.006 mole)

Ethanol: 50 ml

Yield: 0.20 g (11.9 %)

Melting point: 166-167 °C

¹H NMR (400 MHz) data (ppm):

Solvent: CDCl₃

Diastereotopic methylene protons at C-5: δ_{A} = 4.11 δ_{B} = 4.04

Aromatic protons: 6.93-7.06 (m)

¹³C NMR (400MHz) data (ppm):

Solvent: CDCl₃

C-2 carbon of the heterocyclic ring: 155.87

C-4 carbon of the heterocyclic ring: 170.71

C-5 carbon of the heterocyclic ring: 33.40

Aromatic carbons: 122.11-145.20

Elemental analysis data:

Found: C, 53.03%; H, 2.80%; N, 7.75%; S, 9.39%

Calculated for C₁₅H₁₀ON₂SCl₂: C, 53.57%; H, 2.98%; N, 8.33%; S, 9.52%

IR data:

$\nu_{\text{C=O}}$: 1732 cm⁻¹, C=O stretching

$\nu_{\text{C=N}}$: 1641 cm⁻¹, C=N stretching

3.2.1.5. 2 - (*o*-methoxyphenyl)imino - 3 -(*o*-methoxyphenyl) - thiazolidine - 4-one. The compound was synthesized according to the general procedure. After recrystallization from ethanol, 2-(*o*-methoxyphenyl)imino-3-(*o*-methoxyphenyl)-thiazolidine-4-one was obtained as thin white crystals.

Starting materials.

N,N'-Di-(*o*-methoxyphenyl)thiourea: 2.16 g (0.0075 mole)

α -bromoacetic acid: 1.25 g (0.009 mole)

Sodium acetate: 0.75 g (0.009 mole)

Ethanol: 50 ml

Yield: 0.30 g (12.2 %)

Melting point: 194-195 °C

¹H NMR (400 MHz) data (ppm):

Solvent: CDCl₃

Diastereotopic methylene protons at C-5: δ_{A} = 4.01 δ_{B} = 3.96

o-methoxy protons: 3.89(s) and 3.78(s)

Aromatic protons: 6.93-7.06 (m)

¹³C NMR (400 MHz) data (ppm):

Solvent: CDCl₃

C-2 carbon of the heterocyclic ring: 155.61

C-4 carbon of the heterocyclic ring: 171.62

C-5 carbon of the heterocyclic ring: 33.30

o-methoxy carbons: 56.14 and 56.35

Aromatic carbons: 112.46-155.16

Elemental analysis data:

Found: C, 61.52%; H, 4.62%; N, 7.87%; S, 9.11%

Calculated for C₁₇H₁₆O₃N₂S: C, 62.19%; H, 4.88%; N, 8.54%; S, 9.76%

IR data:

$\nu_{\text{C=O}}$: 1716 cm⁻¹, C=O stretching

$\nu_{\text{C=N}}$: 1631 cm⁻¹, C=N stretching

3.3. Apparatus

¹H NMR and ¹³C NMR spectra were recorded on the Varian-Mercury VX-400 MHz-BB.

Melting points were recorded using a Bibby Stuart Scientific melting point apparatus.

The IR analyses were performed on a Perkin Elmer 1600 FTIR using KBr windows.

Liquid chromatography analyses were performed using Chiralcel OD-H column (Daicel Ltd., particle size: 5µm, column size:250×4.6 mm) or Chiralpak AD column (Daicel Ltd., particle size: 5µm, column size:250×4.6 mm), Lab Alliance Series III pump and Water Assoc. UV absorbance detector.

Carlo Erba 1106 was used for elemental analysis of the compounds studied in this project.

3.4. List of Chemicals

Table 3.1. Chemical used in this study

Name	Formula	Supplier	% Purity
Aniline	C ₆ H ₇ N	Merck	
<i>o</i> -toluidine	C ₇ H ₉ N	Merck	>99
naphthylamine	C ₁₀ H ₉ N	Merck	>99
<i>o</i> -chloroaniline	C ₆ H ₆ ClN	Merck	>98
<i>o</i> -anisidine	C ₇ H ₉ NO	Merck	>99
carbendisulfide	CS ₂	Merck	99.5
Absolute ethanol	CH ₂ OH	Merck	99
α -bromoaceticacid	BrCH ₂ COOH	Fluka	99
Ethanol for HPLC	CH ₂ OH	J.T.Baker	99.5
Hexane for HPLC	CH ₃ (CH ₂) ₄ CH ₃	J:T:Baker	95
Potassium hydroxide	KOH	Labor Teknik	
sodiumacetate	CH ₃ COONa		

4. RESULTS AND DISCUSSION

Rotation about the N₃-aryl bond in 2-(*o*-aryl)imino-3-(*o*-aryl)-thiazolidine-4-ones is hindered due to the steric interaction between the *ortho* substituent on the N₃-aryl and the exocyclic oxygen and imino nitrogen. Therefore, the protons on C-5 of the heterocyclic ring are diastereotopically related and give AB type splitting in the ¹H NMR spectrum at room temperature. In addition, due to the possibility that the N_{imino}-aryl bond rotation may be hindered due to the presence of the N₃-aryl ring and the lone pair electron on sulfur, and the **E-Z** isomerization of the C=N double bond further AB splittings in the ¹H NMR spectrum may be observed.

In this study, ¹H NMR spectrum of the compounds were taken in various solvents in order to investigate the AB splittings. To assign the stereochemistry of the imino bond, 2D-NOESY experiments were used.

It could be thought the **Z** configuration of the compounds studied may be predominant because of the steric hindrance brought by the N₃-aryl ring. However, π - π interaction between two rings for **E** configuration may be a favorable interaction. Furthermore, the energy barriers of 2-(*o*-aryl)imino-3-(*o*-aryl)-thiazolidine-4-ones were determined by thermal racemization of the resolved enantiomers on a chiral column and compared with structurally related compounds, 2,4-thiazolidinediones and rhodanines, in order to get information about the stereochemistry of the C=N double bond.

4.1. 2-Phenylimino-3-phenyl-thiazolidine-4-one

4.1.1. ¹H NMR Spectra of 2-phenylimino-3-phenyl-thiazolidine-4-one

Since 2-phenylimino-3-phenyl-thiazolidine-4-one (Figure 4.1) lacks a chiral axis, there is only the possibility of the presence of **E** and **Z** isomers, which are diastereomers of each other. Therefore, two different NMR chemical shifts for protons on C-5 of the heterocyclic ring in the spectra were expected if two isomers coexist.

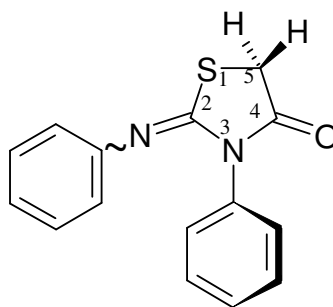


Figure 4.1. The structure of 2-phenylimino-3-phenyl-thiazolidine-4-one

The ^1H NMR spectral assignments in various solvents for the 2-phenylimino-3-phenyl-thiazolidine-4-one are given in Table 4.1 (Figures 4.7, 4.8, 4.9, 4.10, 4.11). The protons on the C-5 of the heterocyclic ring gave only one ^1H NMR signal in all solvents except for benzene- d_6 and toluene- d_8 (Figure 4.3). Therefore, it was concluded that in aromatic solvents like benzene- d_6 and toluene- d_8 both **E** and **Z** isomers exist whereas in polar solvents only one isomer, probably **Z** is present.

Table 4.1. 400 MHz spectral data for 2-phenylimino-3-phenyl-thiazolidine-4-one in different solvents

Solvent	Protons on C-5 (ppm)	Aromatic (ppm)
DMF- d_7	4.41	7.01-7.72
CDCl_3	3.99	6.90-7.54
Methanol- d_4	3.98	6.77-7.43
Toluene- d_8	2.75 and 2.74	7.16-7.41
Benzene- d_6	2.63 and 2.64	6.59-6.98

^1H NMR spectra of the compound were also taken at various temperatures in order to find out whether the **E** and **Z** isomers are thermally interconvertible. In DMF- d_7 only one ^1H NMR signal was observed at temperatures between $-50\text{ }^\circ\text{C}$ and $110\text{ }^\circ\text{C}$ (Figure 4.4). In toluene- d_8 one ^1H NMR signal was observed from $-70\text{ }^\circ\text{C}$ to $0\text{ }^\circ\text{C}$, but from $15\text{ }^\circ\text{C}$ to $40\text{ }^\circ\text{C}$ a splitting in the peak was observed (Figure 4.5). This result is interpreted in the following way: Here the **Z** to **E** isomerization is being observed (Figure 4.2). k_f and k_r being the rate constants in the forward and the reverse directions and K is the equilibrium constants,

which is determined by the relative populations of the E and Z isomers at a given temperature. At temperatures below 15 °C K is too small to give rise to any observable E isomers in the NMR spectrum. As temperature is increased the equilibrium constant K increases for this endothermic process and the E isomer becomes observable.

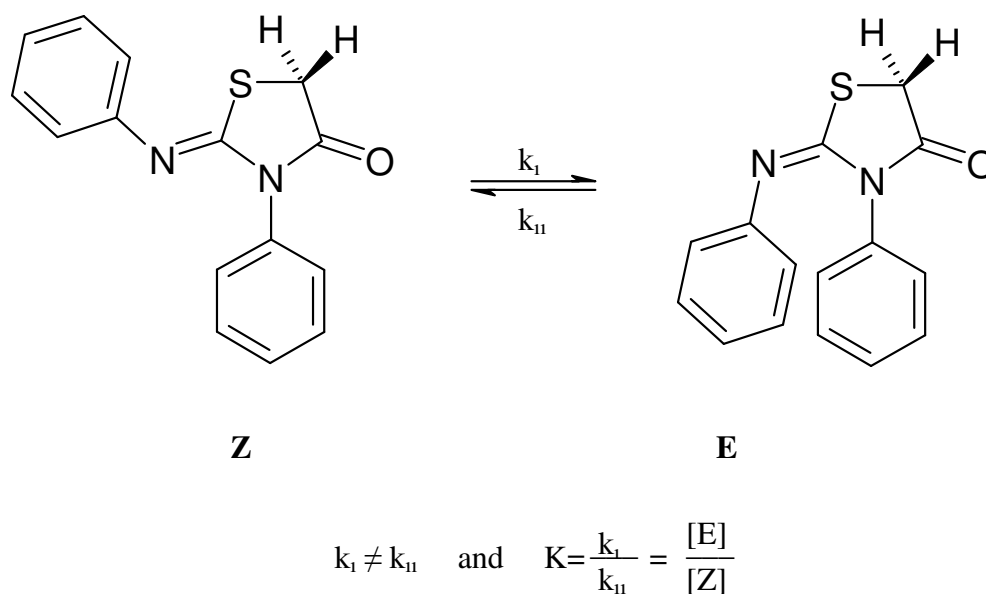


Figure 4.2. The Z to E isomerization of 2-phenylimino-3-phenylthiazolidine-4-one

However, in toluene- d_8 (Figure 4.5) and benzene- d_6 (Figure 4.6) solutions the chemical shift differences of the E and Z isomers were found to be very close to each other. Therefore, depending on the resolution of the instrument sometimes only one peak was observed instead of two and Z to E isomerization could not be analyzed quantitatively. Further heating up to 95°C in toluene- d_8 caused extra splittings (Figure 4.4). These have been thought to occur as a result of either a decrease in resolution of the NMR instrument close to the boiling point of the solvent or due to the partial decomposition of the compound. However, a coalescence of the two signals could not be observed. In benzene- d_6 solutions the integration of the two signal gave E/Z ratio as 3:5. In toluene- d_8 the ratio was found as 2:5. In benzene- d_6 extra splittings were also seen between 60°C and 70°C.

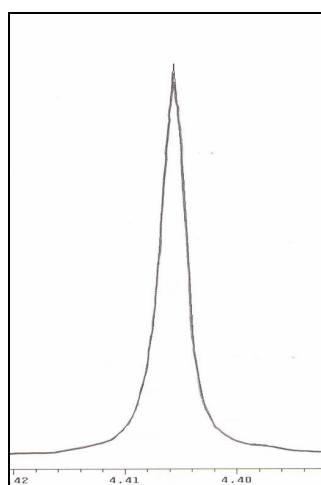
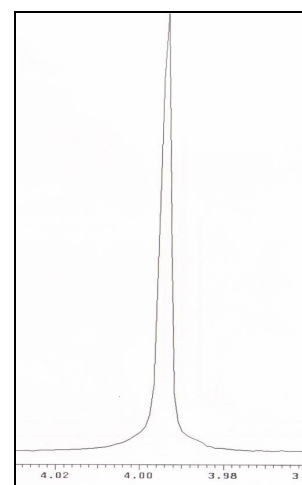
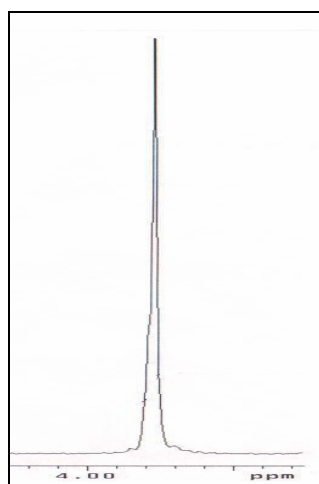
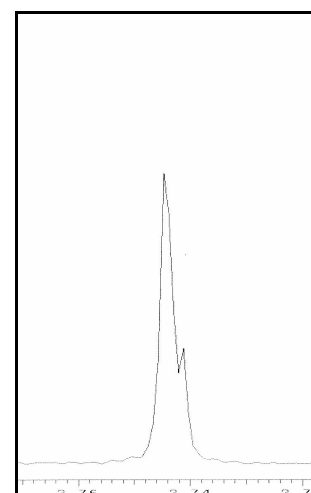
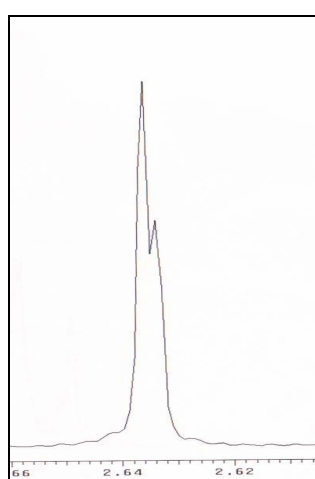
in DMF-d₇in CDCl₃in methanol-d₄in toluene-d₈in benzene-d₆

Figure 4.3. The methylene peak of 2-phenylimino-3-phenyl-thiazolidine-4-one in various solvents at 25 °C

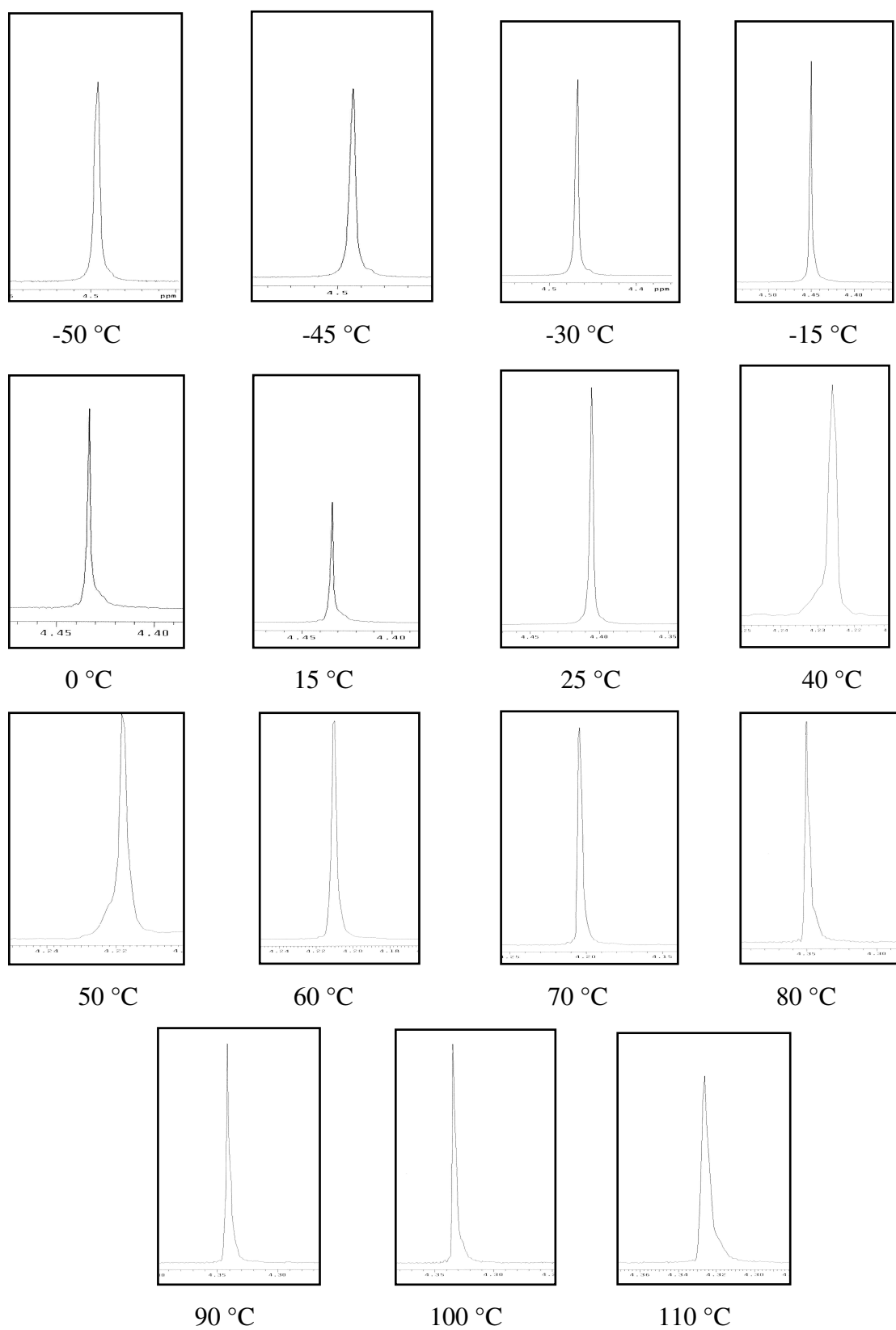


Figure 4.4. ^1H NMR signals of methylene protons on C-5 of 2-phenylimino-3-phenylthiazolidine-4-one at various temperatures in DMF-d_7

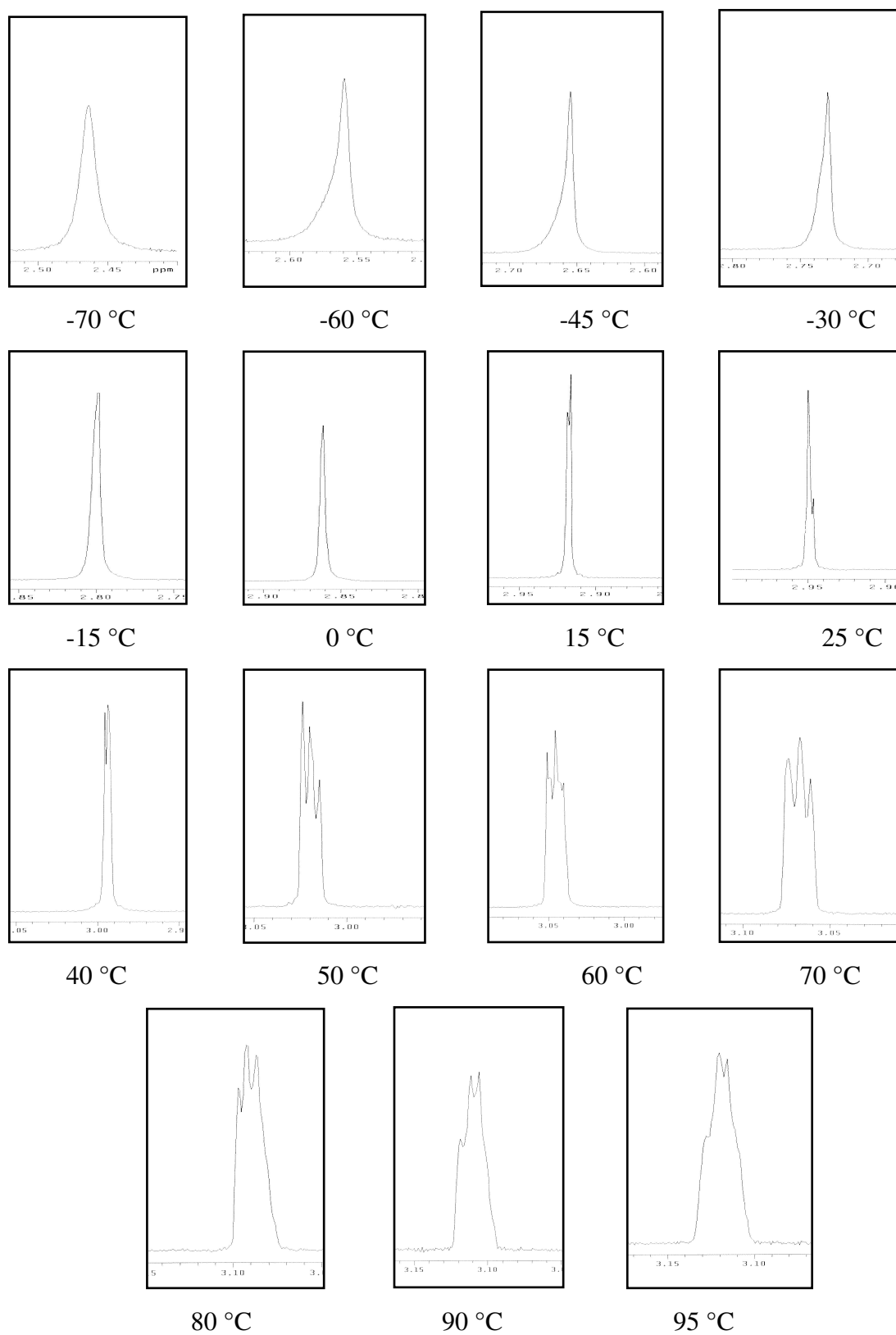


Figure 4.5. ^1H NMR signals of methylene protons on C-5 of 2-phenylimino-3-phenylthiazolidine-4-one at various temperatures in toluene- d_8

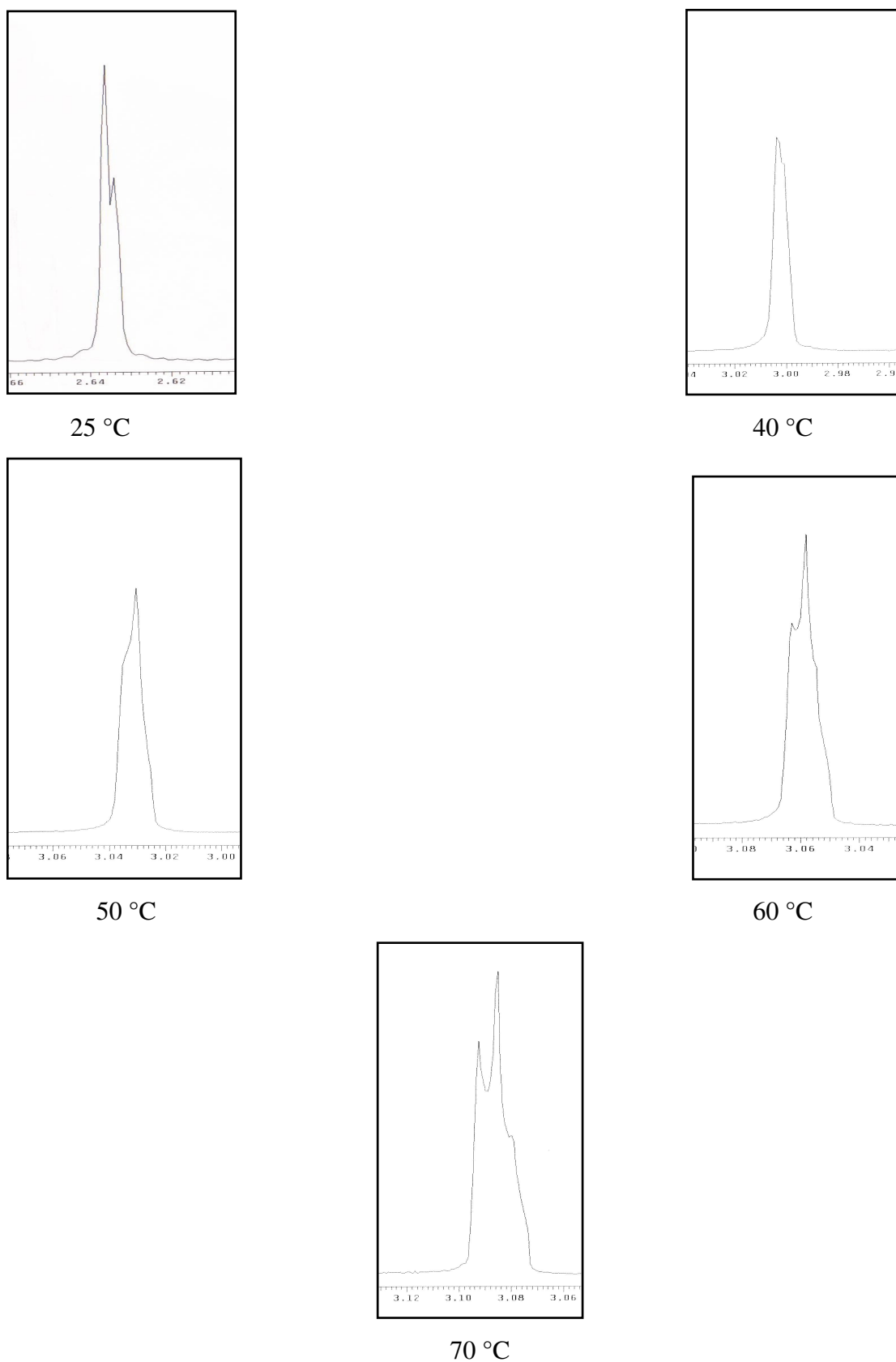


Figure 4.6. ^1H NMR signals of methylene protons on C-5 of 2-phenylimino-3-phenylthiazolidine-4-one at various temperatures in benzene- d_6

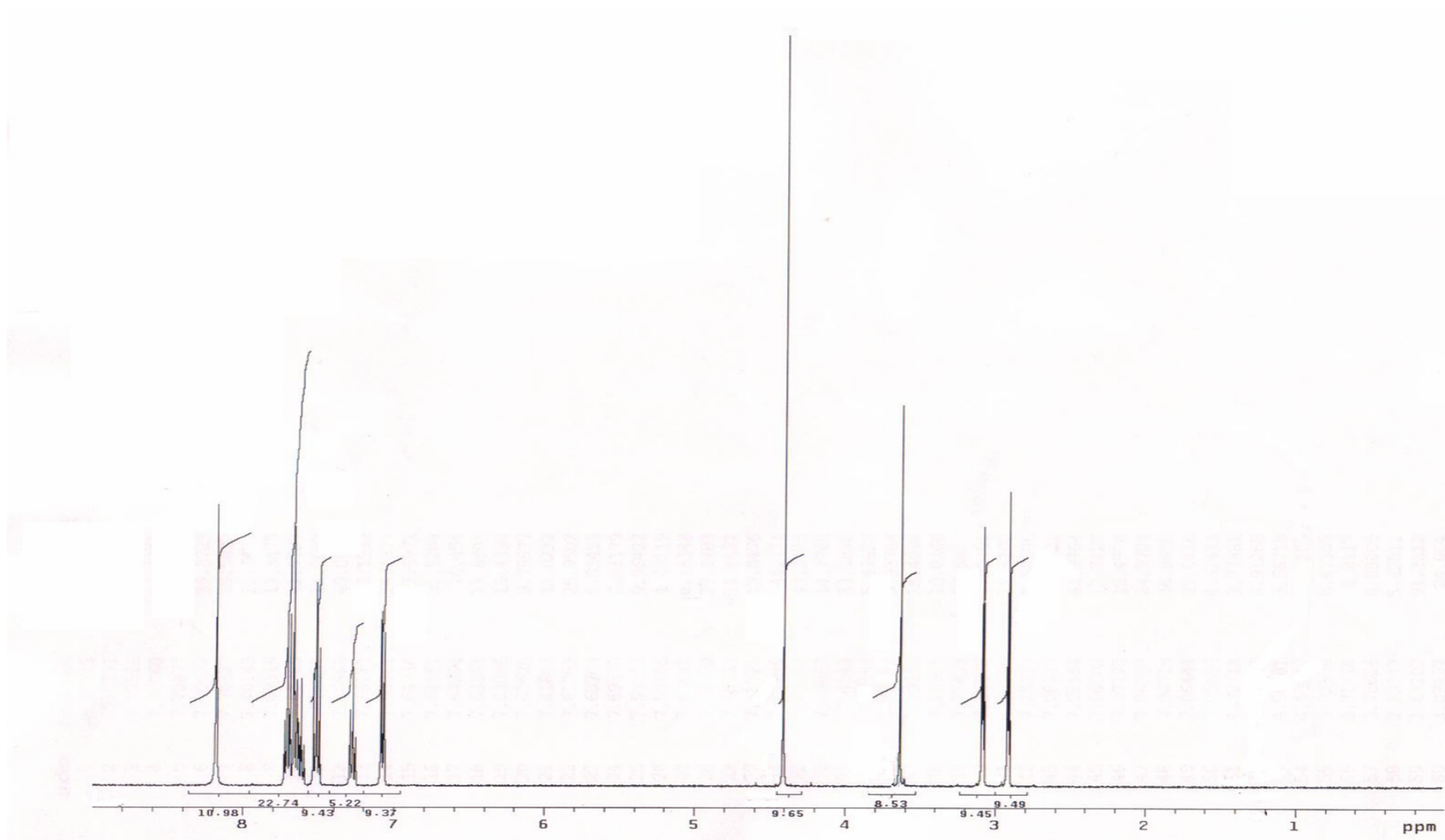


Figure 4.7. The 400 MHz ^1H NMR spectrum of 2-phenylimino-3-phenyl-thiazolidine-4-one in DMF-d_7

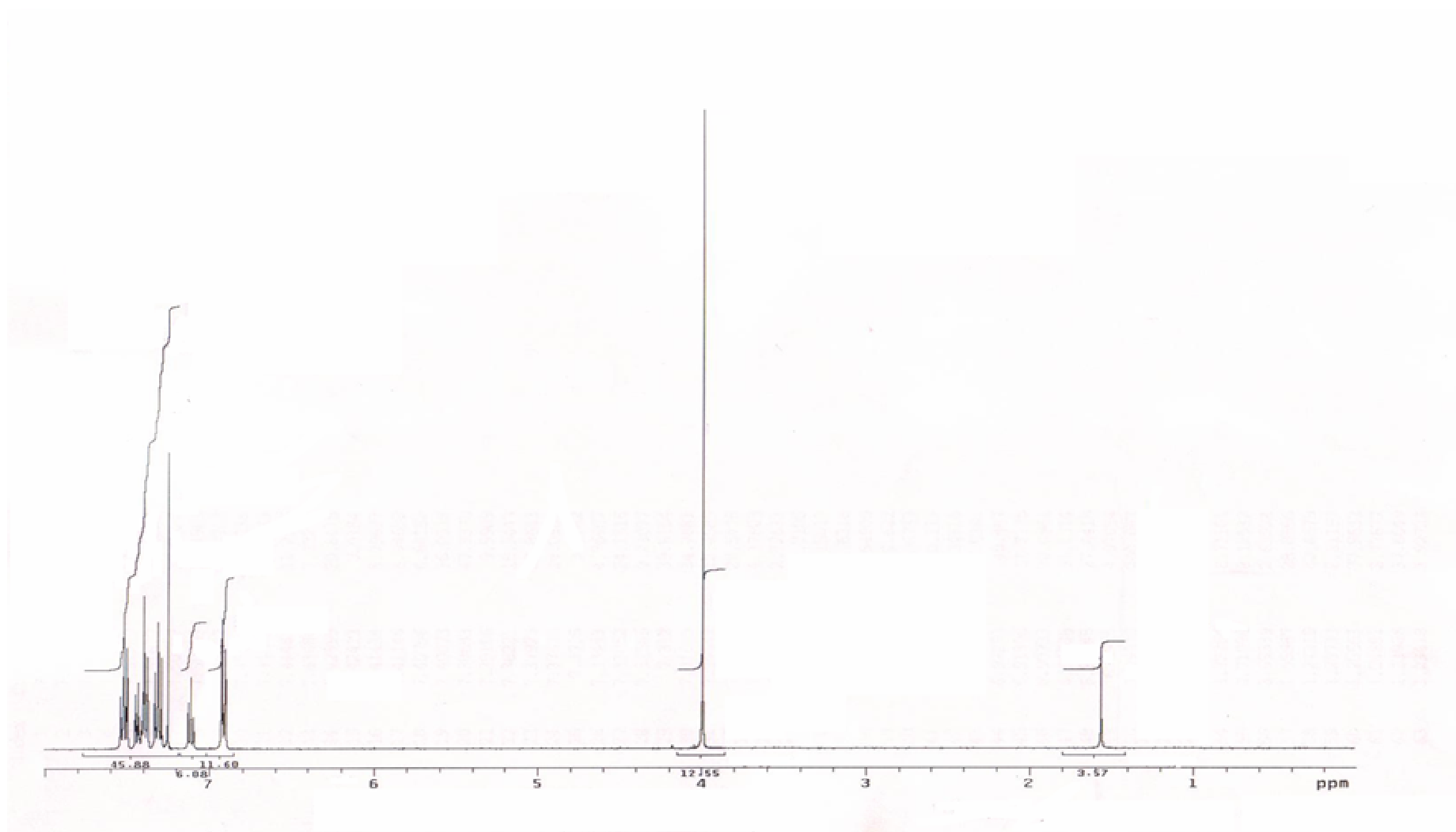


Figure 4.8. The 400 MHz ^1H NMR spectrum of 2-phenylimino-3-phenyl-thiazolidine-4-one in CDCl_3

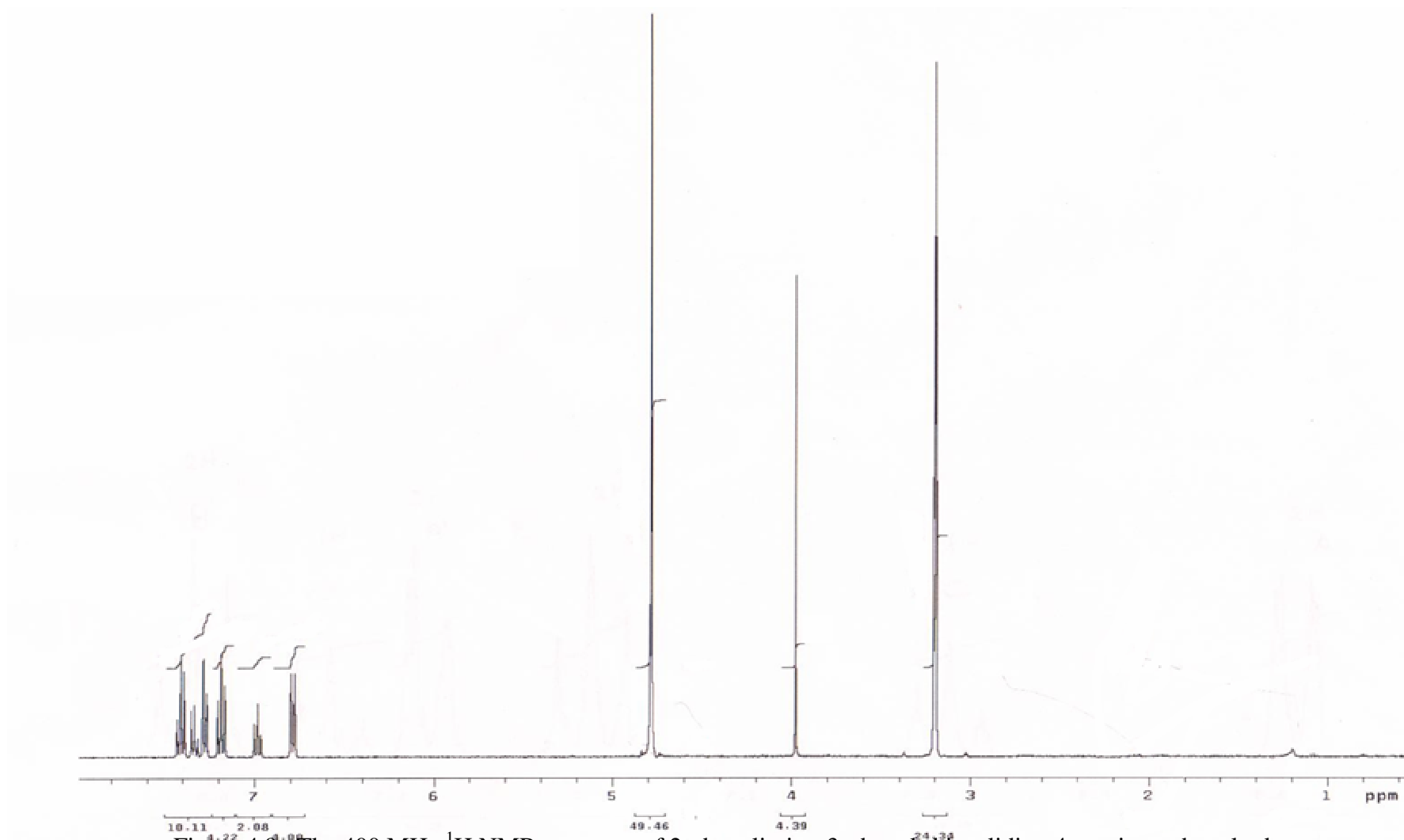


Figure 4.9. The 400 MHz ^1H NMR spectrum of 2-phenylimino-3-phenylthiazolidine-4-one in methanol- d_4

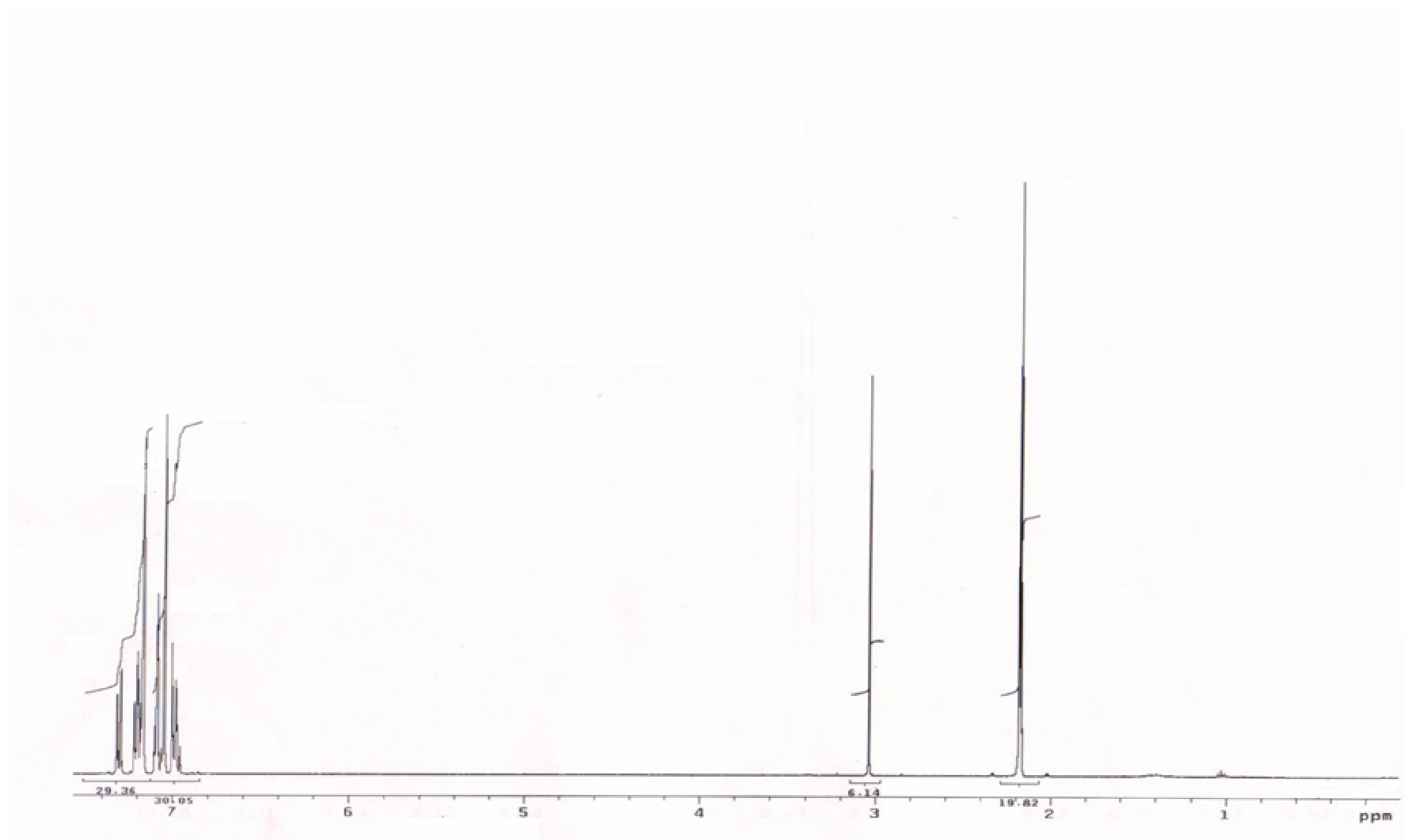


Figure 4.10. The 400 MHz ^1H NMR spectrum of 2-phenylimino-3-phenyl-thiazolidine-4-one in toluene-d_8

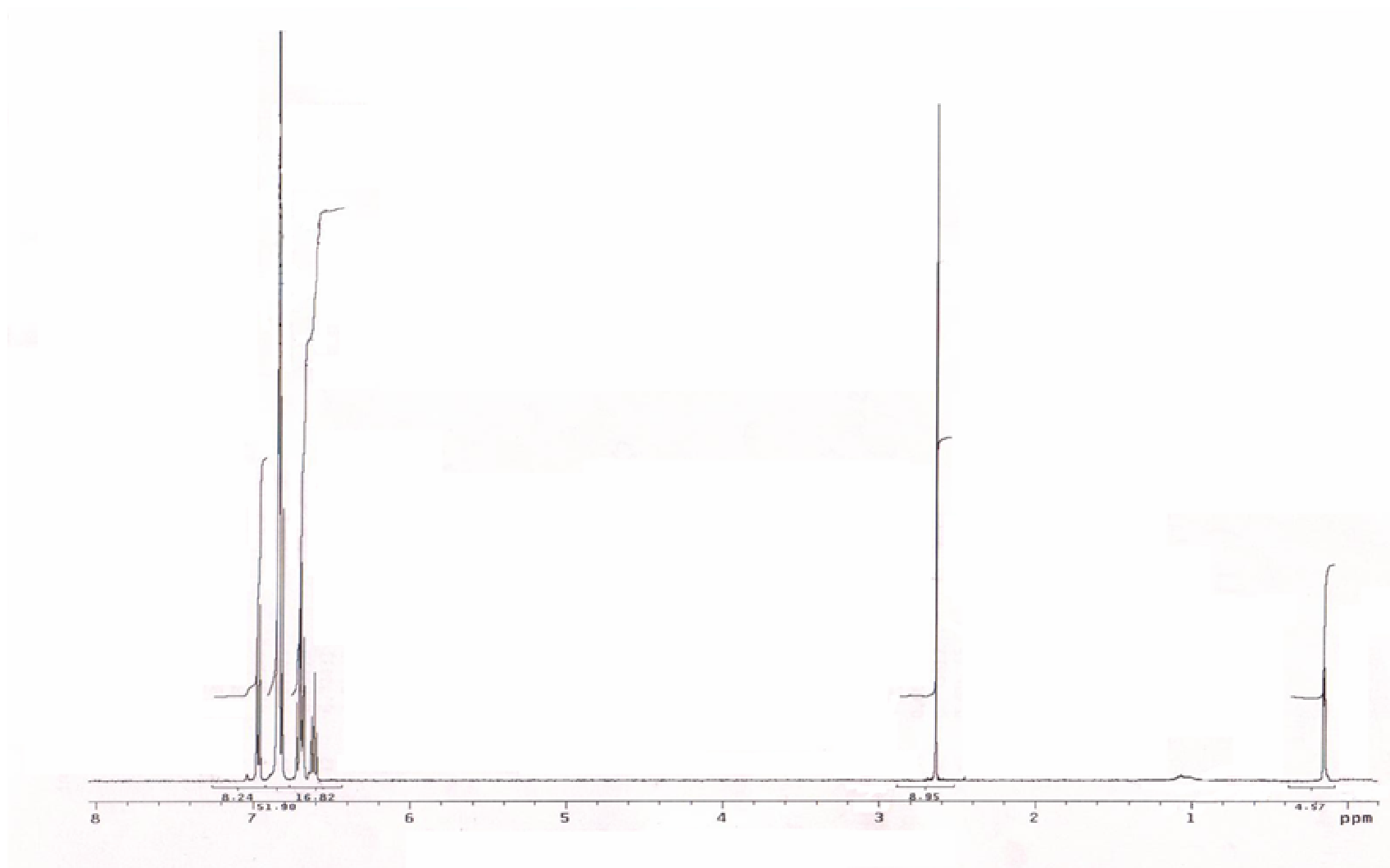


Figure 4.11. The 400 MHz ^1H NMR spectrum of 2-phenylimino-3-phenyl-thiazolidine-4-one in benzene- d_6

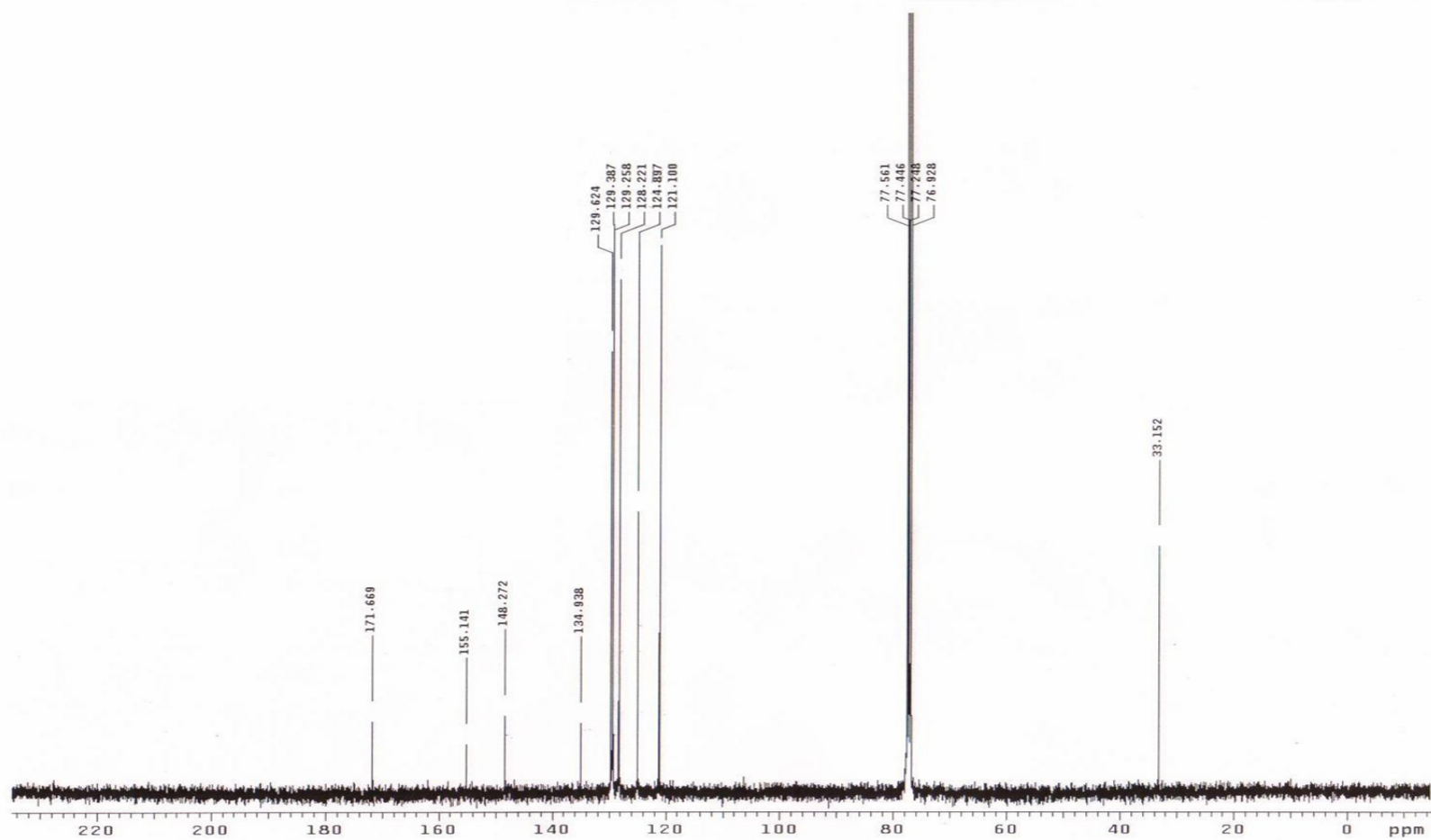


Figure 4.12. The ^{13}C NMR spectrum of 2-phenylimino-3-phenyl-thiazolidine-4-one in CDCl_3

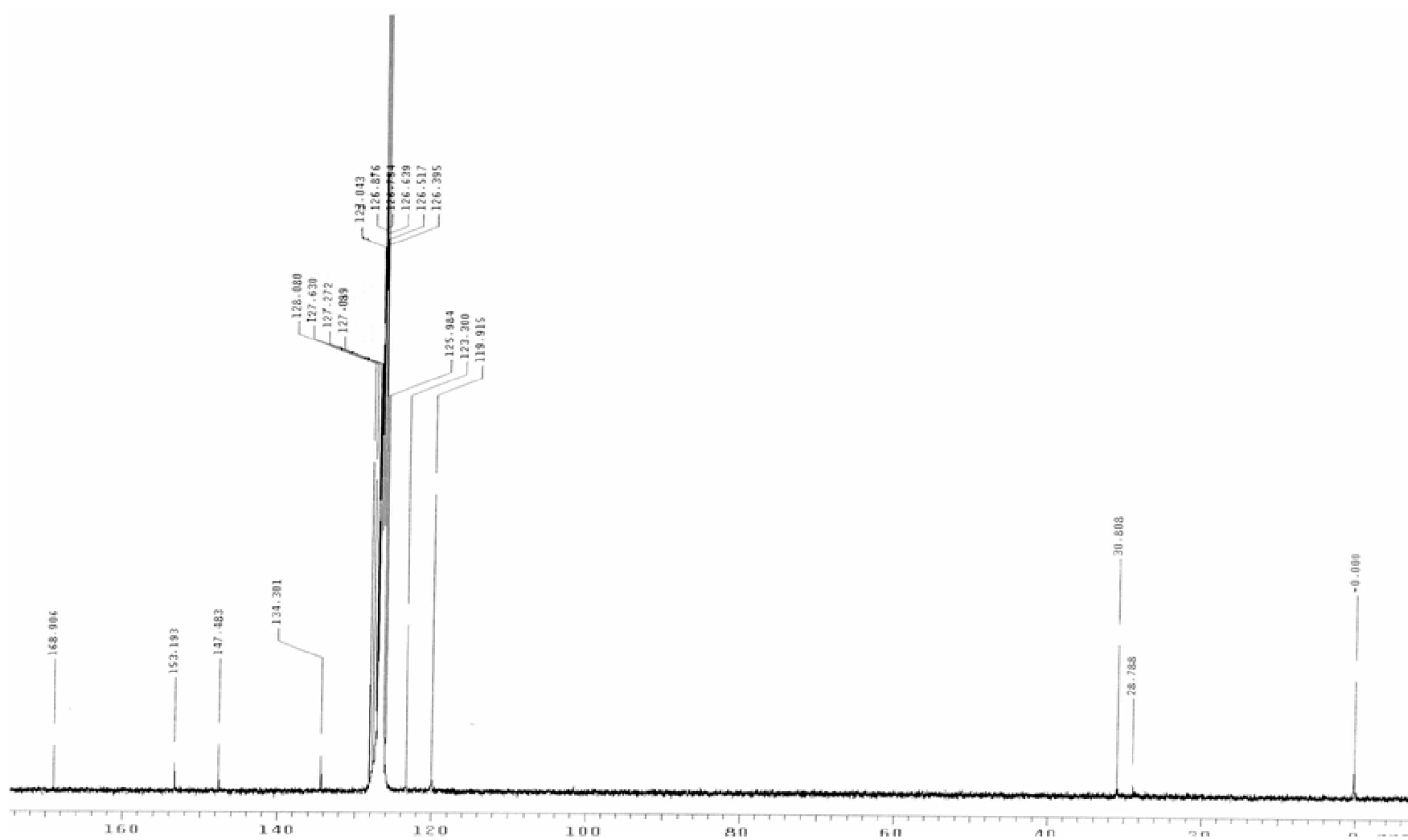


Figure 4.13. The ^{13}C NMR spectrum of 2-phenylimino-3-phenyl-thiazolidine-4-one in benzene- d_6

4.1.2. ^{13}C NMR Spectra of 2-phenylimino-3-phenyl-thiazolidine-4-one

^{13}C NMR spectrum of 2-phenylimino-3-phenyl-thiazolidine-4-one in CDCl_3 was examined for identification of the compound (Figure 4.12). The C-2 carbon, which belongs to the imino carbon gave a peak at 155.1 ppm. The C-4 carbon, which is the carbonyl carbon of the heterocyclic ring resonated at 171.7 ppm and the C-5 carbon gave a signal at 33.2 ppm. Aromatic carbons resonated between 121.1-148.3 ppm.

In benzene- d_6 two different chemical shifts for C-5 protons were observed in ^1H NMR spectrum. Therefore, ^{13}C NMR spectrum of 2-phenylimino-3-phenyl-thiazolidine-4-one in benzene- d_6 (Figure 4.13) was also examined. It was observed that two different chemical shifts for C-5 carbon at 30.8 ppm and 28.8 ppm exist in the ^{13}C NMR spectrum. The peak observed at 30.8 ppm belongs to the C-5 carbon of **Z** isomer due to the higher intensity and the peak observed at 28.8 ppm belongs to the C-5 carbon of **E** isomer. The C-4 carbon and the C-2 carbon resonated at 168.9 ppm and 153.2 ppm, respectively. Aromatic protons gave peaks between 119.9-147.5 ppm.

4.1.3. 2D-NOESY and 2D-COSY spectra of 2-phenylimino-3-phenyl-thiazolidine-4-one in Benzene- d_6 and DMF- d_7

In DMF- d_7 two different NMR chemical shifts for C-5 protons of the heterocyclic ring were not observed in the ^1H NMR spectrum in the range between $-50\text{ }^\circ\text{C}$ to $100\text{ }^\circ\text{C}$ (Figure 4.4), which means that either one isomer exists or the interconversion between two isomers is fast with respect to the NMR time scale. 2D-NOESY spectrum of 2-phenylimino-3-phenyl-thiazolidine-4-one in DMF- d_7 was examined to gain information about the stereochemistry of the C=N bond.

If the C=N bond has a **Z** configuration (Figure 4.14) no crosspeak are expected between the two rings. However, if the configuration is **E**, crosspeaks may be expected between the two rings. The DMF- d_7 was chosen as solvent because in this solvent the two phenyl rings were very well resolved. The assignments of the ^1H NMR peaks of the phenyl rings have been done in the following way:

As can be seen from the resonance structures (Figure 4.15), N_{imino} -aryl ring has a higher electron density than N_3 -aryl ring, thus the peaks due to N_{imino} -aryl ring are expected to appear relatively more shielded. Among the protons of the N_{imino} -aryl ring, the *ortho*-protons and the *para*-proton have higher electron density than the *meta*-protons, which gave rise to different resonances in the spectrum.

In 2D-NOESY spectrum (Figure 4.16), the most shielded peak which corresponds to 2H, and appears as a doublet belongs to the *ortho*-protons (A), next peak (1H, triplet due to the three bond coupling with two equivalent *meta*-protons) which is slightly more deshielded belongs to the *para*-proton (C), and the next peak belongs to the *meta*-protons (B). The most deshielded overlapping peaks belong to the protons of N_3 -aryl ring because of the lower electron density.

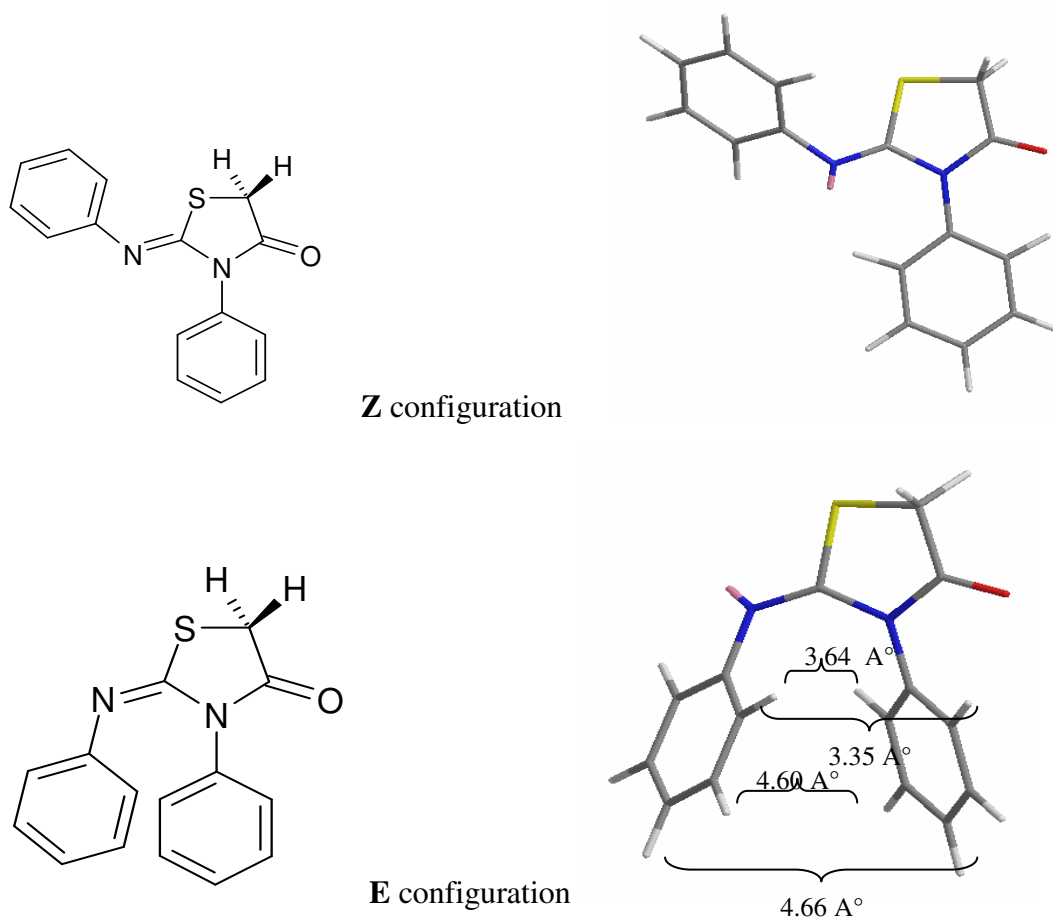


Figure 4.14 The 3D structure of 2-phenylimino-3-phenyl-thiazolidine-4-one

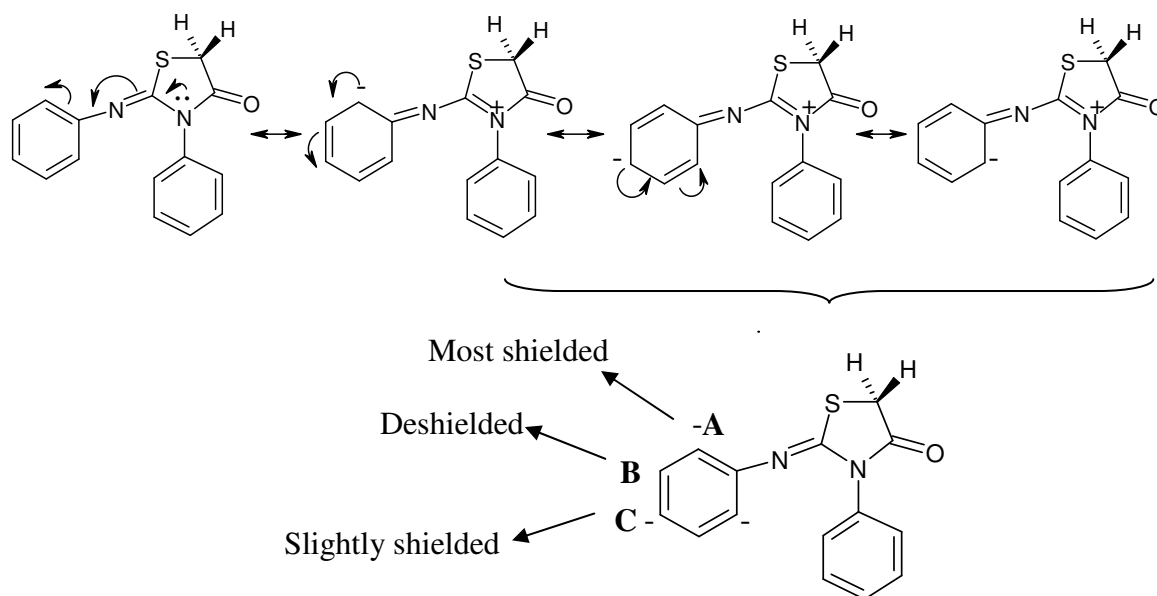


Figure 4.15. The resonance structure of 2-phenylimino-3-phenyl-thiazolidine-4-one

It can be seen from 2D-NOESY spectrum in DMF (Figure 4.15) that there are interactions only between the neighboring protons, A and B; B and C. Any interaction between two rings was not observed. Therefore, it was concluded that either phenyl derivative has *Z* configuration or due to fast rotation about the N-C_{aryl} bonds a close proximity between the rings could not be achieved.

2D-NOESY spectrum of 2-phenylimino-3-phenyl-thiazolidine-4-one in benzene-d₆ (Figure 4.18) was also examined because a splitting was observed in the ¹H NMR signal of C-5 hydrogens in this solvent. Besides the 2D-NOESY spectrum, 2D-COSY spectrum of the compound in benzene-d₆ (Figure 4.17) was also examined due to the fact that 2D-NOESY experiment shows through space interactions (< 4Å^o apart) as well as interactions between the neighboring protons, while 2D-COSY experiment shows only interactions between the neighboring protons, and thus the difference between two spectra gives only the spatial interactions.

In 2D-COSY spectrum of 2-phenylimino-3-phenyl-thiazolidine-4-one (Figure 4.17) the most shielded peak which corresponds to 1H and appears as triplet due to the three bond coupling with two equivalent the *meta*-protons belongs to the *para*-proton (C) of the

N_{imino} -aryl ring. The next peak corresponding to three protons was assigned to the *ortho*-protons of the N_{imino} -aryl ring (A) and the *para*-proton of the N_3 -aryl ring (C'). The next peak which corresponds to 4H belongs to the *meta*-protons of both rings. The most deshielded peak corresponding to 2H belongs to the the *ortho*-protons of the N_3 -aryl ring (A'). As can be seen from the 2D-COSY spectrum there are interactions between A and B; B and C; A' and B'and B' and C' protons.

The 2D-NOESY spectrum in benzene- d_6 (Figure 4.18) was compared to the 2D-COSY spectrum in benzene- d_6 (Figure 4.17) in order to see spatial interactions. However, the crosspeaks observed in the 2D-NOESY spectrum were the same as the crosspeaks observed in the 2D-COSY spectrum, so it was concluded that no inter-ring through space interactions were present, which may be due to long inter-ring distances developed while the molecules adopt various conformations during fast rotations around $N-C_{\text{phenyl}}$ bonds

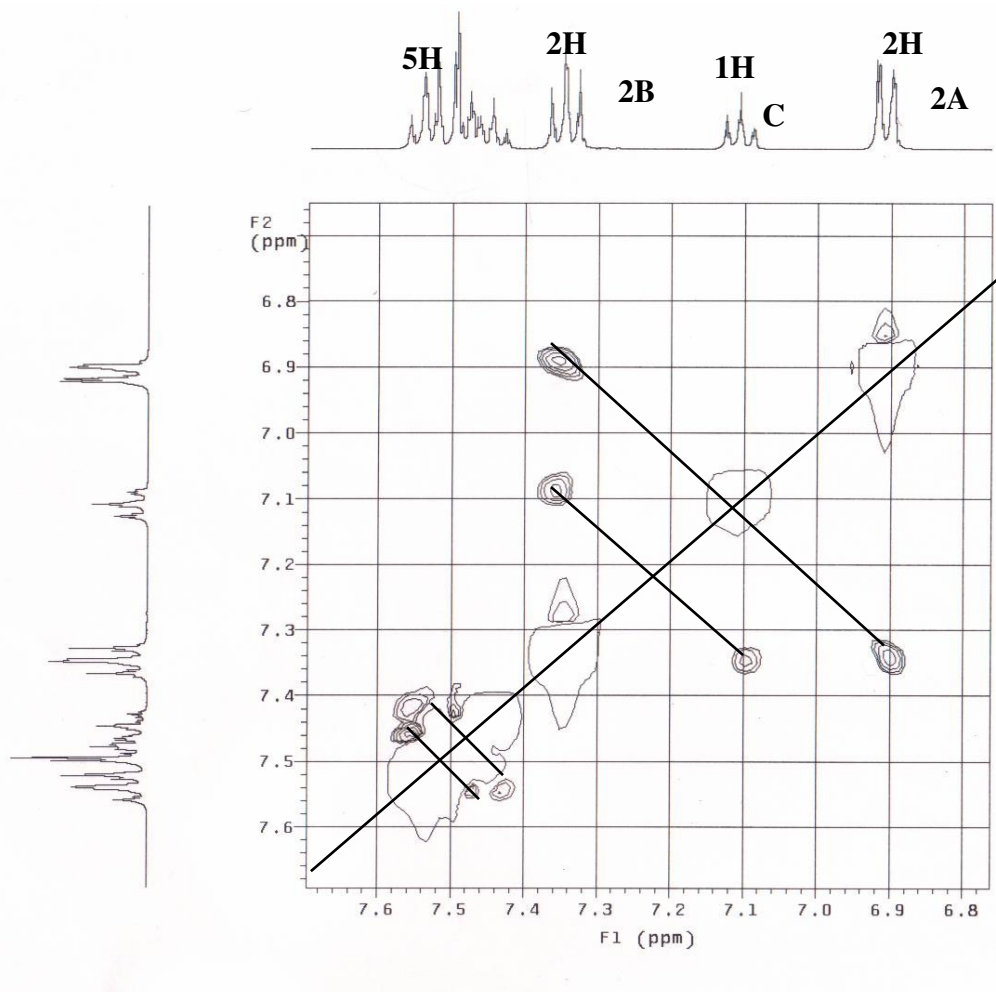


Figure 4.16. Aromatic region of the 2D-NOESY spectrum of 2-phenylimino-3-phenyl-4-thiazolidinone in $DMF-d_7$

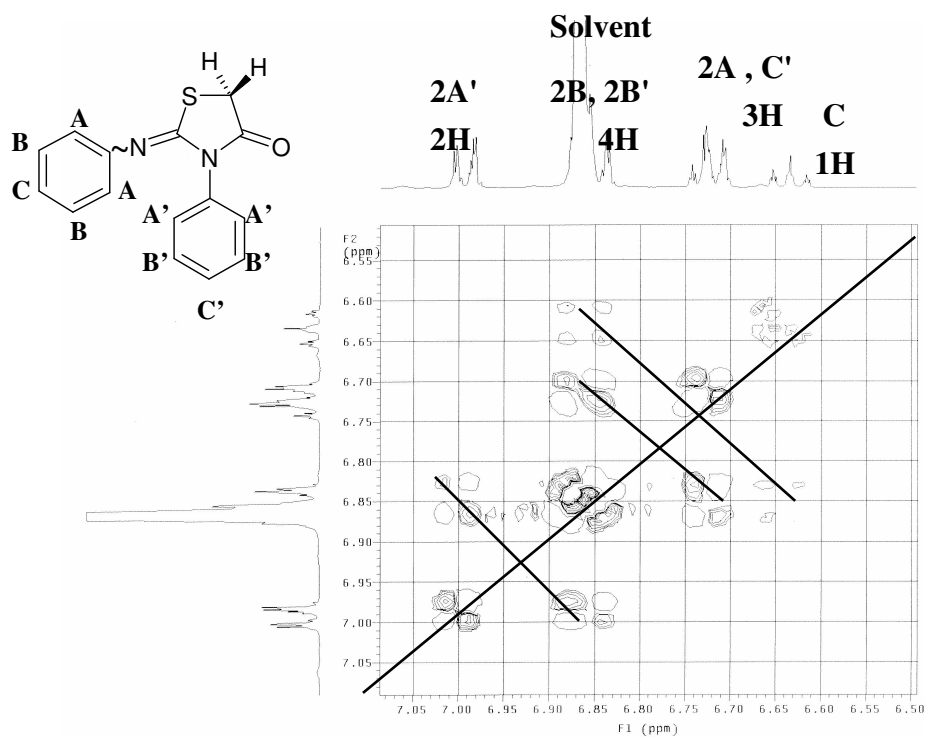


Figure 4.17. Aromatic region of 2D-COSY spectrum of 2-phenylimino-3-phenylthiazolidine-4-one in benzene- d_6

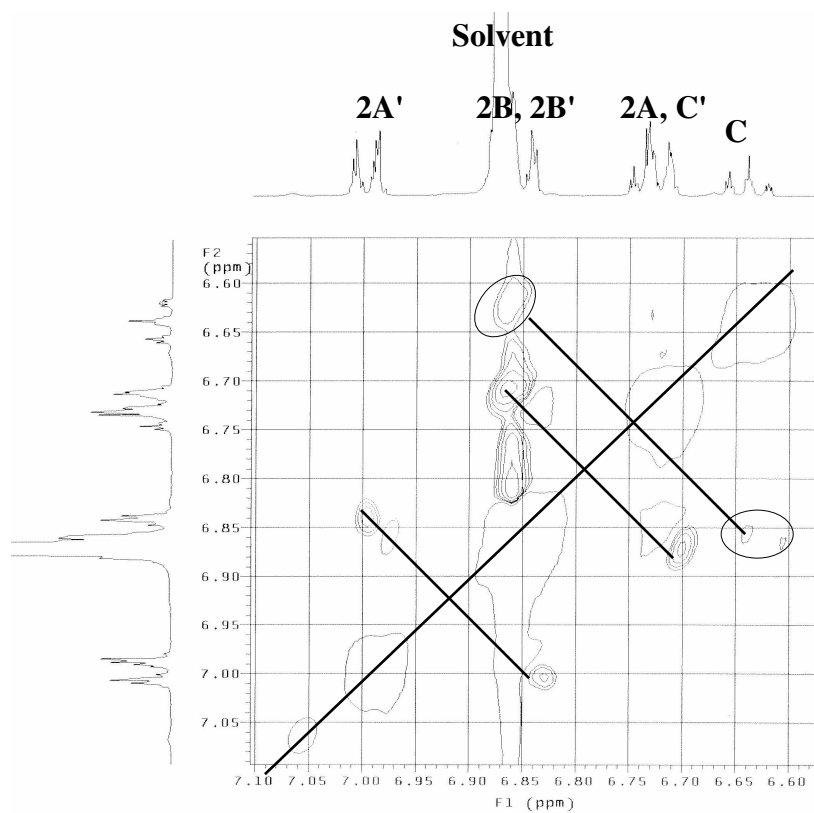


Figure 4.18 Aromatic region of 2D-NOESY spectrum of 2-phenylimino-3-phenylthiazolidine-4-one in benzene- d_6

4.2. 2-(*o*-Tolyl)imino-3-(*o*-tolyl)-thiazolidine-4-one

4.2.1. ^1H NMR spectra of 2-(*o*-tolyl)imino-3-(*o*-tolyl)-thiazolidine-4-one

The N_3 -aryl bond of the 2-(*o*-tolyl)imino-3-(*o*-tolyl)-thiazolidine-4-one (Figure 4.19) is a chiral axis, which gives rise to AB type splitting for the diastereotopic protons on C-5. The presence of the further AB type splittings in ^1H NMR spectrum would indicate that either N_{imino} -aryl bond is chiral axis and/or E and Z isomerization of C=N bond exists.

The ^1H NMR spectral assignments of 2-(*o*-tolyl)imino-3-(*o*-tolyl)-thiazolidine-4-one in various solvents are given in Table 4.2 (Figure 4.22, 4.23, 4.24, 4.25).

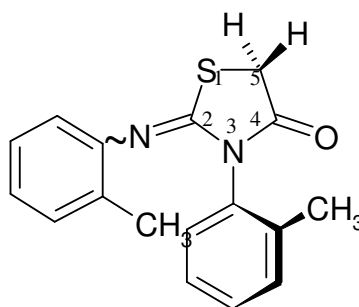


Figure 4.19. The structure of 2-(*o*-tolyl)imino-3-(*o*-tolyl)-thiazolidine-4-one

Table 4.2. 400 MHz spectral data for 2-(*o*-tolyl)imino-3-(*o*-tolyl)-thiazolidine-4-one in various solvents

Solvents	Protons on C-5 (ppm)	<i>o</i> -methyl's(ppm)	Aromatic (ppm)
DMF	$\delta_{\text{A}}=4.51$ $\delta_{\text{B}}=4.42$	2.46 and 2.25	6.96-7.58
Methanol	$\delta_{\text{A}}=4.15$ $\delta_{\text{B}}=4.12$	2.29 and 2.09	6.78-7.41
CDCl_3	$\delta_{\text{A}}=4.02$ $\delta_{\text{B}}=4.01$	2.32 and 2.11	6.79-7.38
Toluene	$\delta_{\text{A}}=3.03$ $\delta_{\text{B}}=2.98$ $\delta_{\text{A}}=3.03$ $\delta_{\text{B}}=2.97$	1.94 and 1.84	6.80-7.05

One AB splitting in DMF-d_7 , methanol-d_4 and CDCl_3 was observed for diastereotopic methylene protons on C-5 carbon, but in toluene-d_6 two AB splittings were observed

(Figure 4.20). In this case one AB results from hindered rotation about N₃-aryl bond, the other AB is thought to result from the E-Z isomerization of the C=N double bond analogous to 2-phenylimino-3-phenyl-thiazolidine-4-one.

¹H NMR spectra of the compounds were also taken at various temperatures in toluene-d₈ (Figure 4.21) One AB splitting was observed at temperatures between -60°C and 0°C, but at higher temperatures up to 100°C two AB splittings were observed, which did not give to a coalescence of the E-Z isomers in the temperature range studied.

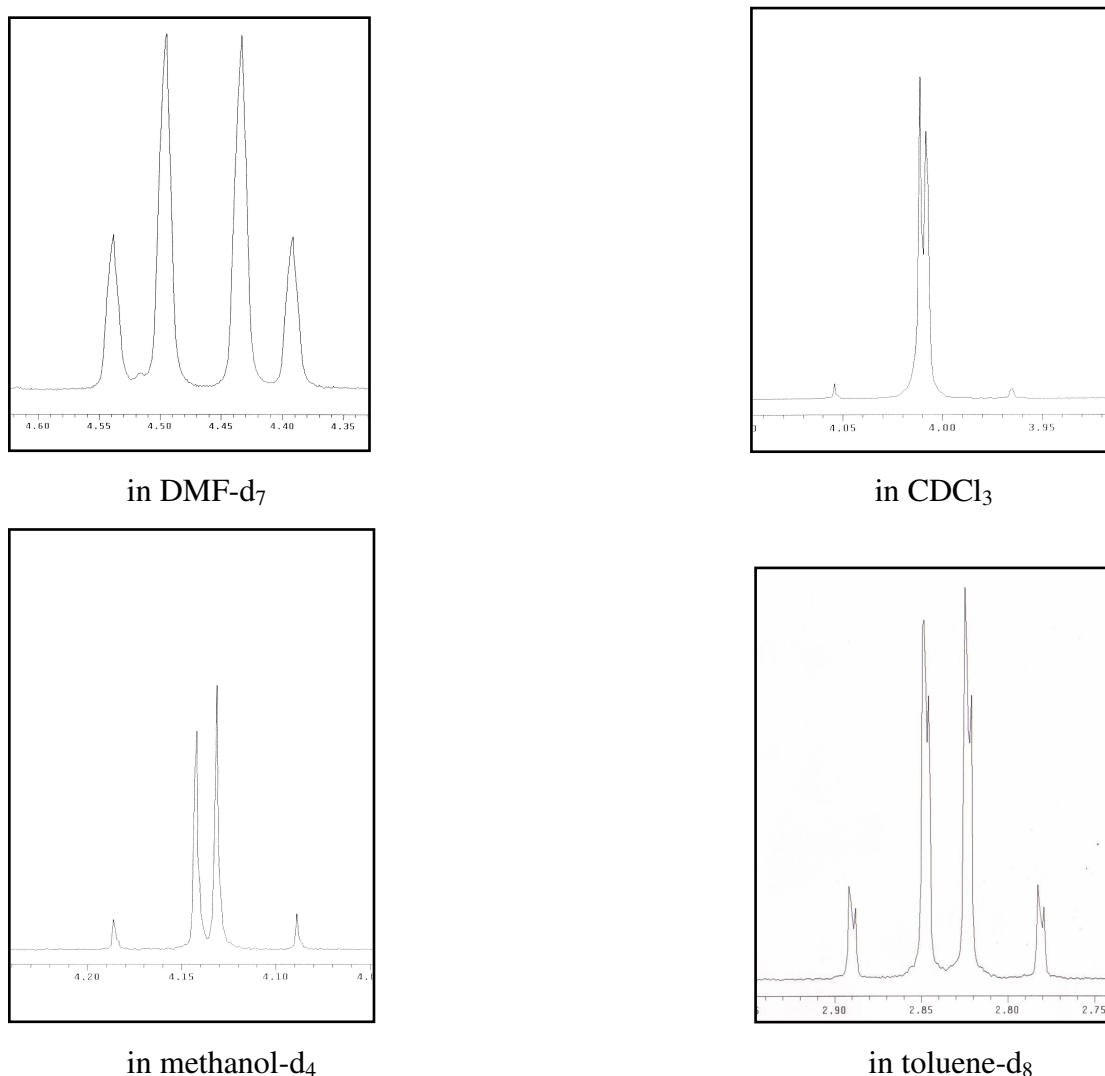


Figure 4.20. The AB spectra of diastereotopic methylene protons on the C-5 of 2-(*o*-tolyl)imino-3-(*o*-tolyl)-thiazolidine-4-one in various solvents at 25 °C

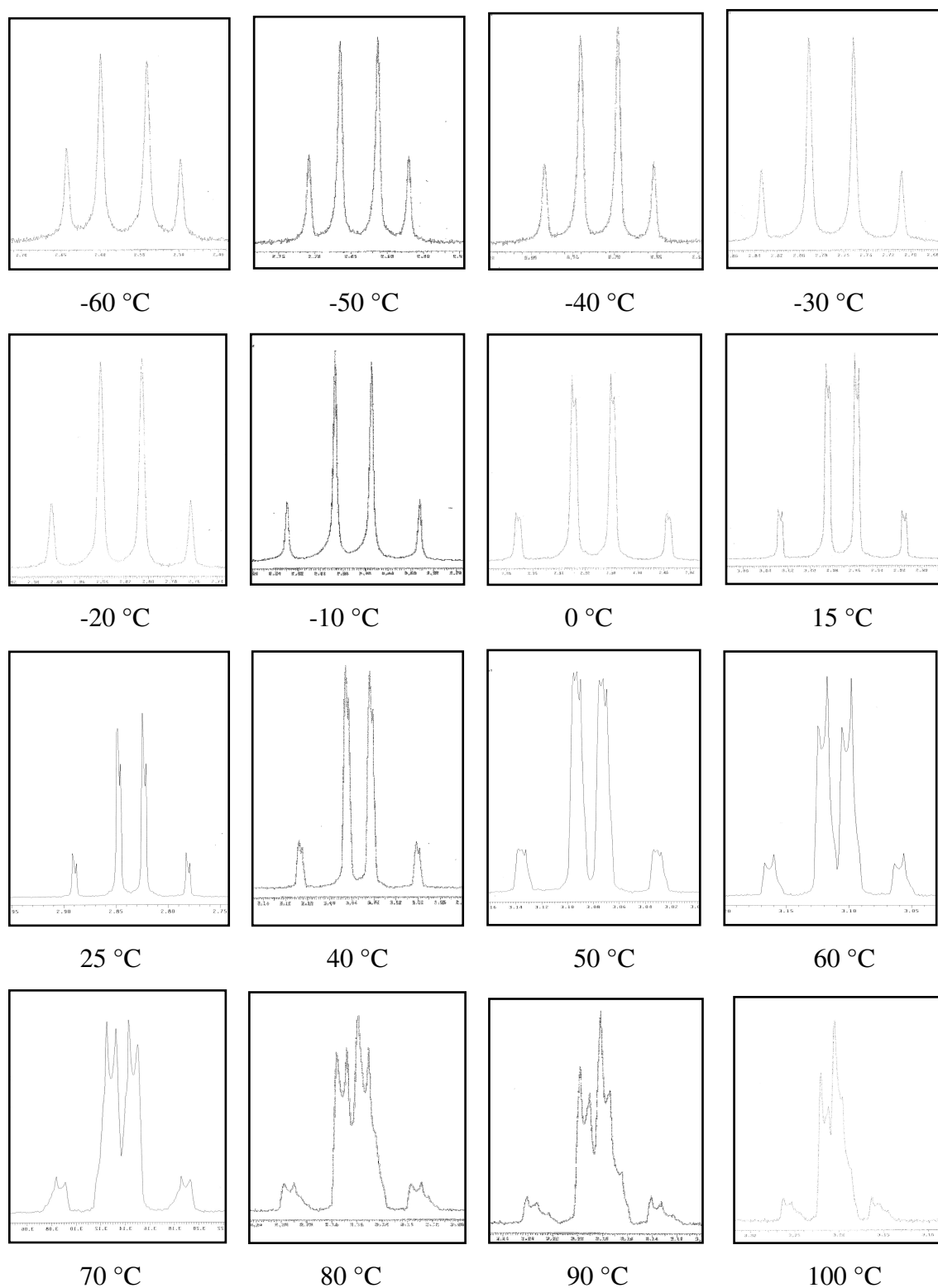


Figure 4.21 ^1H NMR signals for diastereotopic methylene protons on C-5 of 2-(*o*-tolyl)imino-3-(*o*-tolyl)thiazolidine-4-one at various temperatures in toluene-d_8

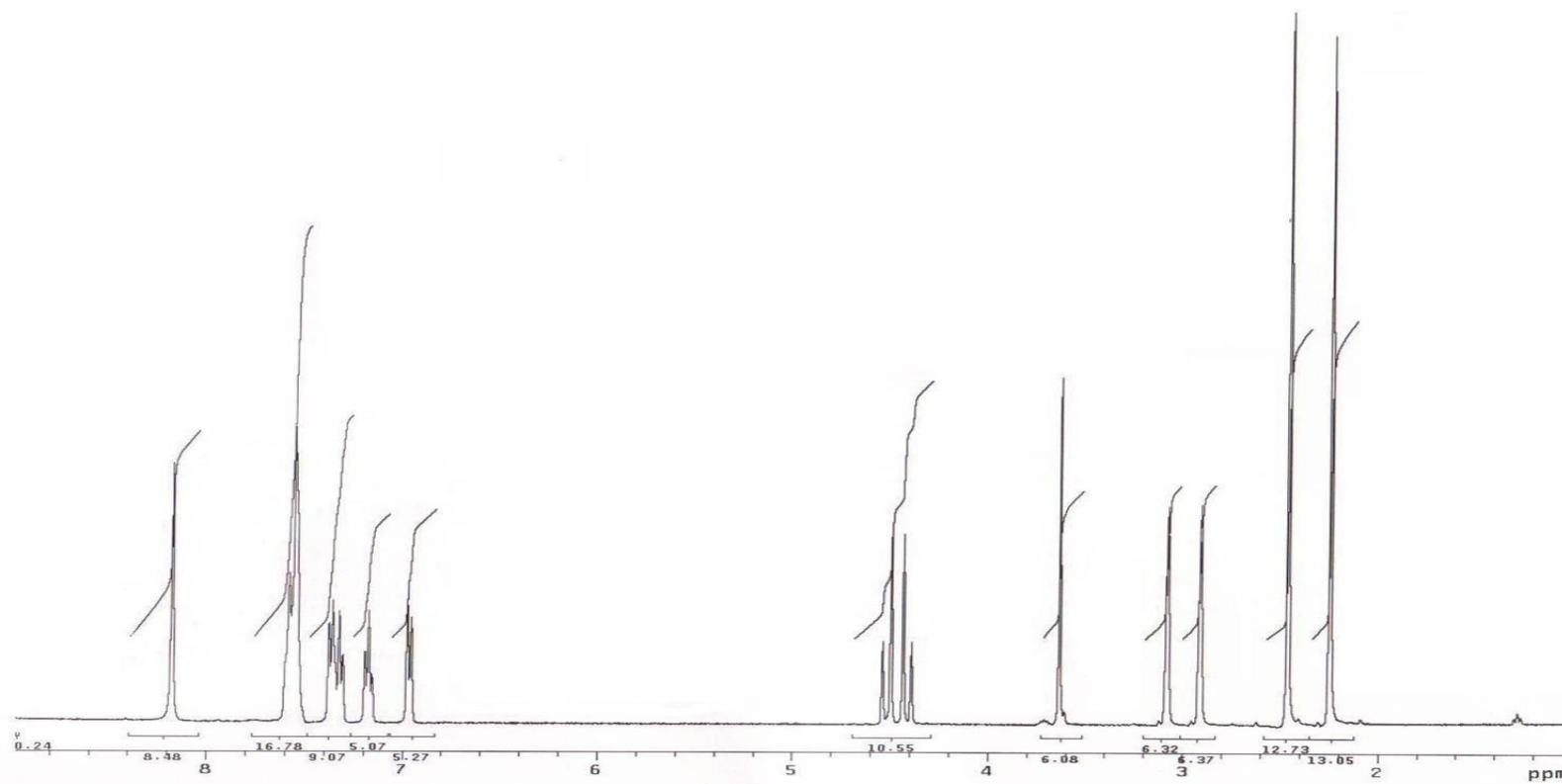


Figure 4.22. The 400 MHz ^1H NMR spectrum of 2-(*o*-tolyl)imino-3-(*o*-tolyl)-thiazolidine-4-one in DMF-d_7

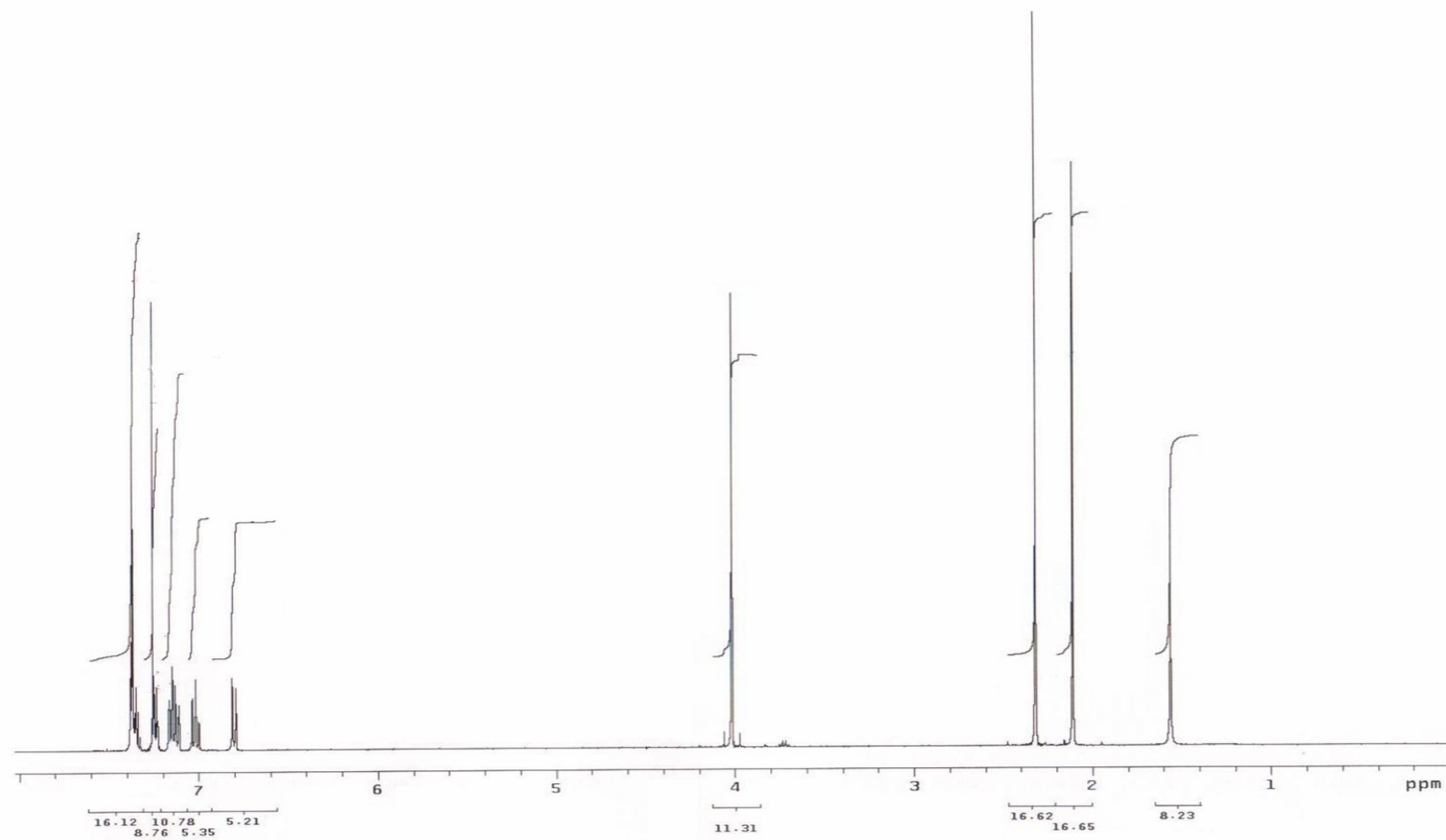


Figure 4.23. The 400 MHz ^1H NMR spectrum of 2-(*o*-tolyl)imino-3-(*o*-tolyl)-thiazolidine-4-one in CDCl_3

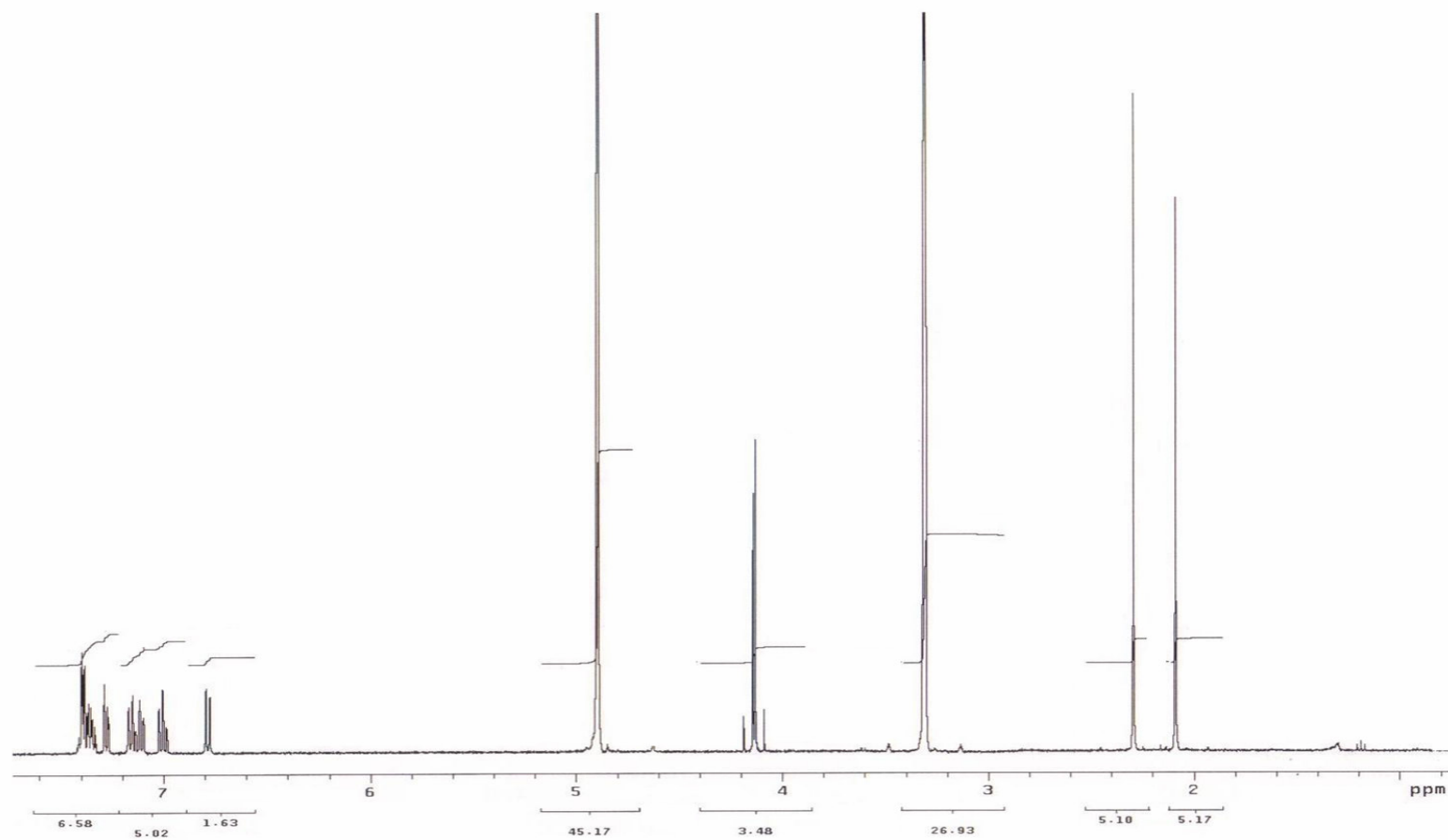


Figure 4.24. The 400 MHz ^1H NMR spectrum of 2-(*o*-tolyl)imino-3-(*o*-tolyl)-thiazolidine-4-one in methanol- d_4

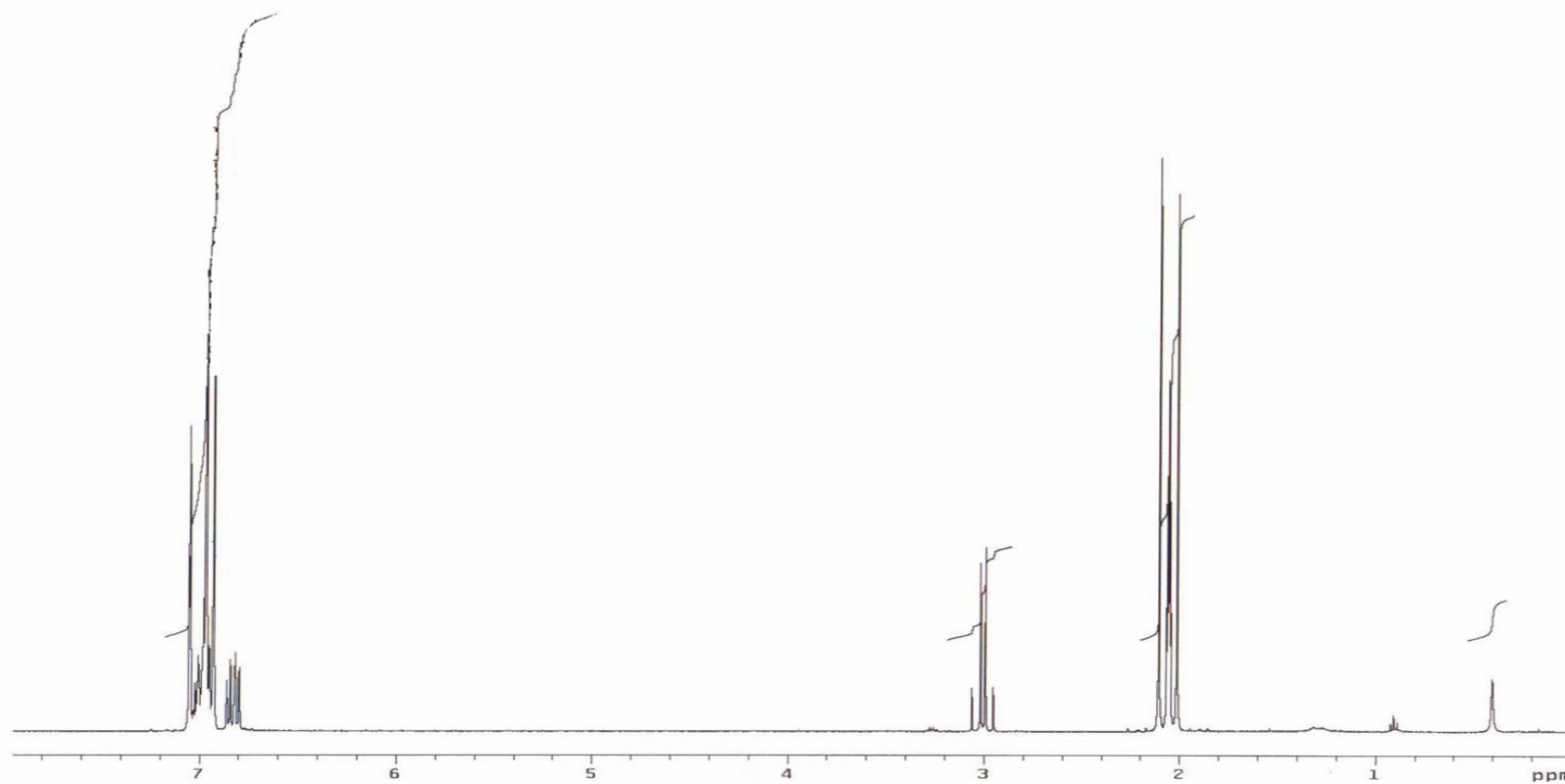


Figure 4.25. The 400 MHz ^1H NMR spectrum of 2-(*o*-tolyl)imino-3-(*o*-tolyl)-thiazolidine-4-one in CDCl_3

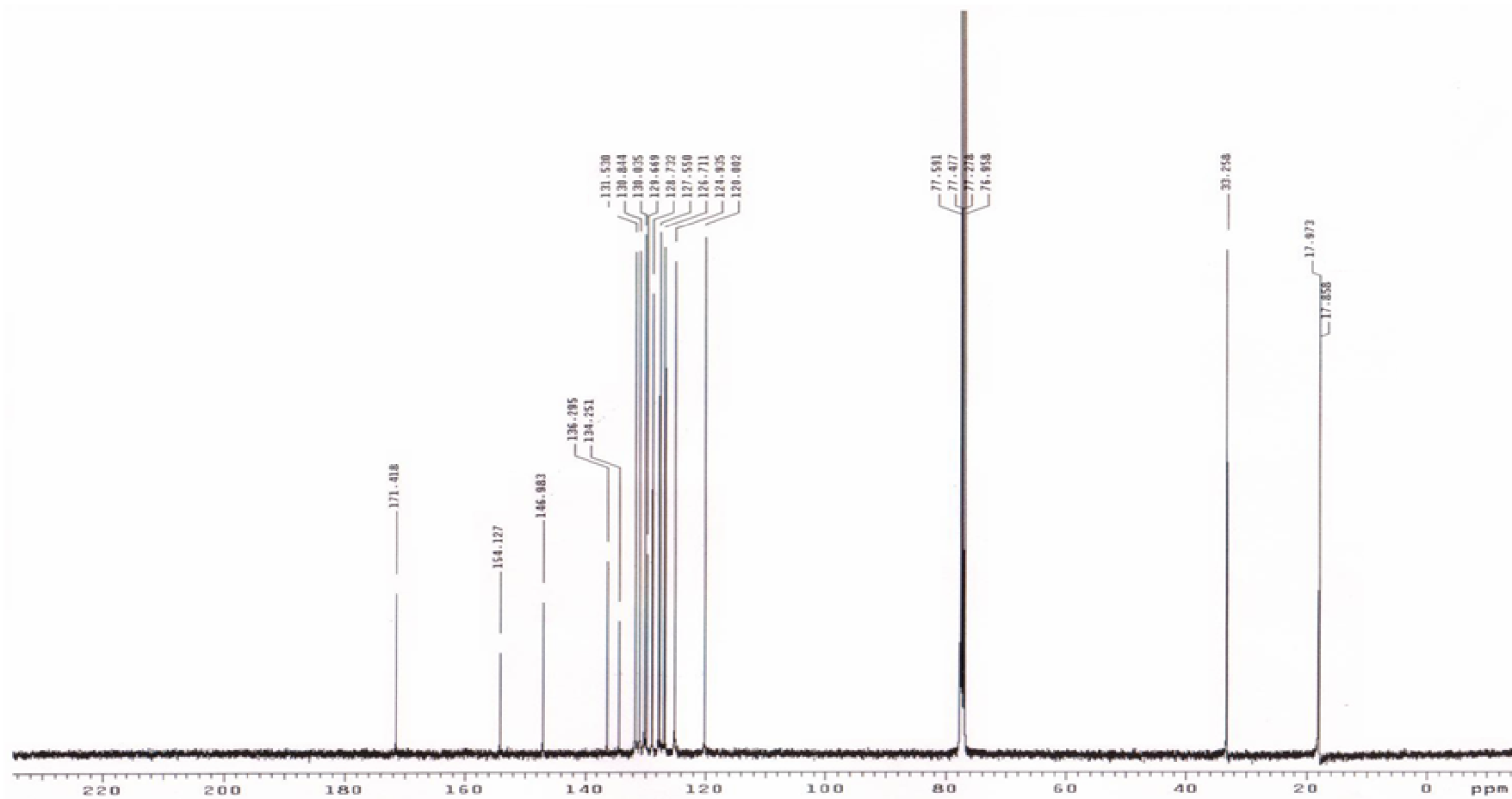


Figure 4.26. The ^{13}C NMR spectrum of 2-(*o*-tolyl)imino-3-(*o*-tolyl)-thiazolidine-4-one in CDCl_3

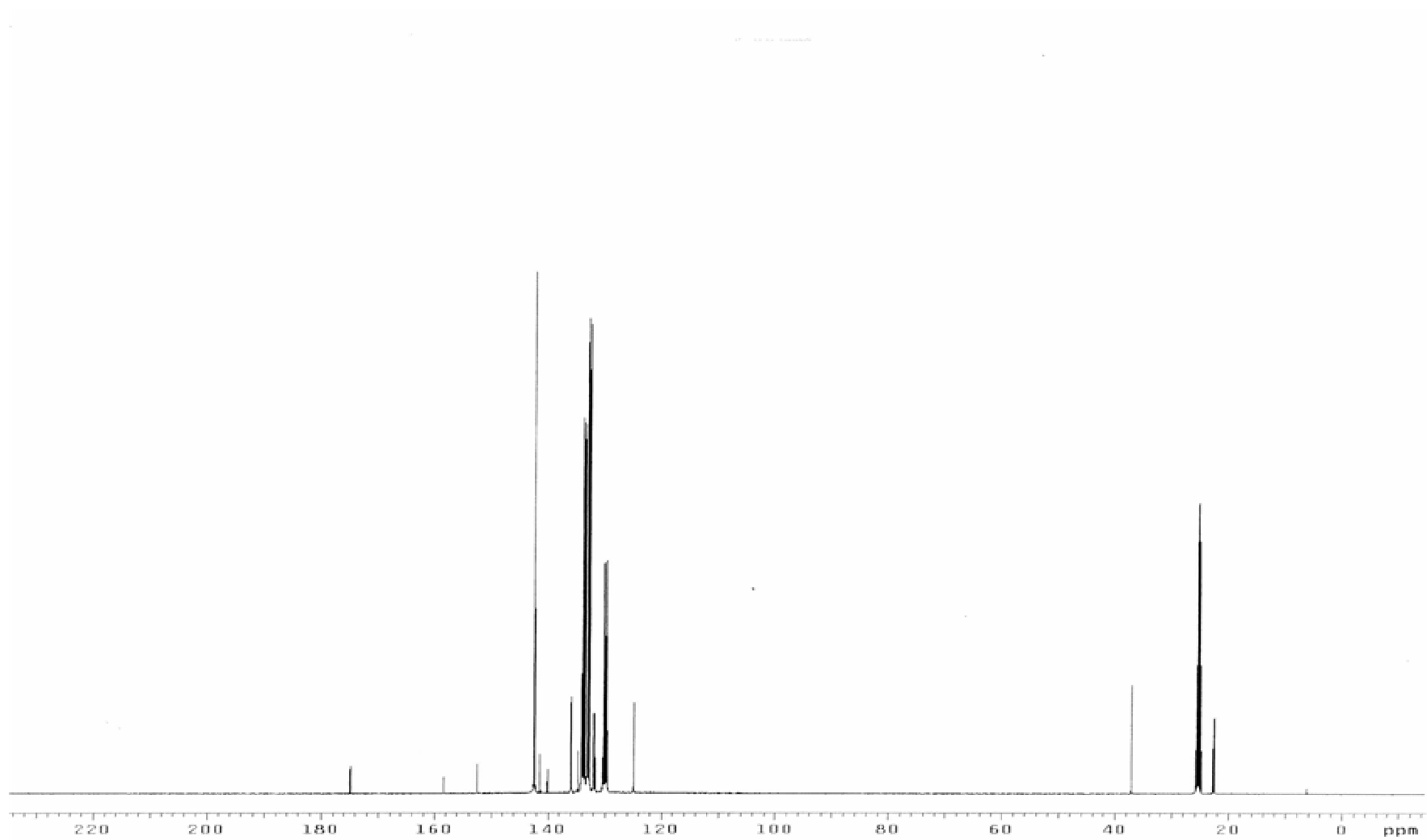


Figure 4.27. The ^{13}C NMR spectrum of 2-(*o*-tolyl)imino-3-(*o*-tolyl)-thiazolidine-4-one in toluene- d_8

4.2.2. ^{13}C NMR Spectra of 2-(*o*-tolyl)imino-3-(*o*-tolyl)-thiazolidine-4-one

^{13}C NMR spectrum of the compound was taken in CDCl_3 (Figure 4.26). The C-2 carbon, which belongs to the imino carbon resonated at 154.13 ppm. The C-4 carbon, which is the carbonyl carbon of the heterocyclic ring, and the C-5 carbon gave peaks at 171.42 ppm and 33.26 ppm, respectively. The *o*-methyl carbons resonated at 17.97 ppm and 17.86 ppm. Aromatic carbons resonated between 120.0-146.98 ppm.

^{13}C NMR spectrum of the compound was also examined in toluene- d_8 (Figure 4.27). Although it was expected to observe two chemical shifts in ^{13}C NMR spectrum for C-5 carbons of the two diastereomers (two AB splittings were observed in ^1H NMR spectrum), only one signals was observed. The C-4 carbon and the C-2 carbon resonated at 174.9 ppm and 158.4 ppm, respectively. The C-5 carbon gave a peak at 37.1 ppm and the *o*-methyl carbons resonated at 22.7 ppm and 22.5 ppm. Aromatic carbons gave peaks between 124.8-152.4 ppm.

4.2.3. 2D-NOESY and 2D-COSY Spectra of 2-(*o*-tolyl)imino-3-(*o*-tolyl)-thiazolidine-4-one in CDCl_3 and Toluene- d_8

In 2D-NOESY spectrum of 2-(*o*-tolyl)imino-3-(*o*-tolyl)-thiazolidine-4-one in CDCl_3 (Figure 4.28), the most shielded peak which corresponds to 1H and appears as a doublet belongs to the *ortho*-proton of N_{imino} -aryl ring (A), the next peak corresponding 1H belongs to the *para*-proton of N_{imino} -aryl ring (C), and the next peak which corresponds to 2H belongs to the *meta*-protons N_{imino} -aryl ring (B and D). The next peak belongs to the *ortho*-proton of N_3 -aryl ring (A') and the most deshielded overlapping peaks corresponding 3H belong to the other protons (B', C', D'). It can be seen from the 2D-NOESY spectrum in CDCl_3 (Figure 4.28) that there are interactions only between the neighboring protons. Any through space interactions between two ring was not present. In addition, 2D-NOESY spectrum of the compound in CDCl_3 was compared to the 2D-COSY spectrum of the compound in CDCl_3 (Figure 4.29). It was found that interactions between the protons observed in both spectra are the same. Therefore, it was concluded that through space interactions between the two ring are not present.

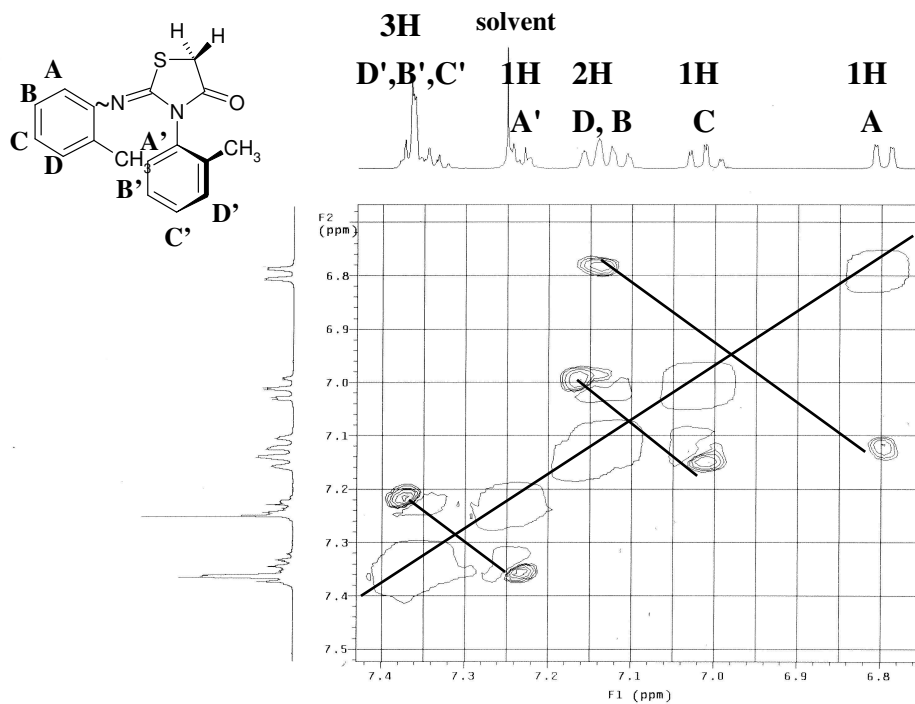


Figure 4.28. Aromatic part of 2D-NOESY spectrum of 2-(*o*-tolyl)imino-3-(*o*-tolyl)thiazolidine-4-one in CDCl₃

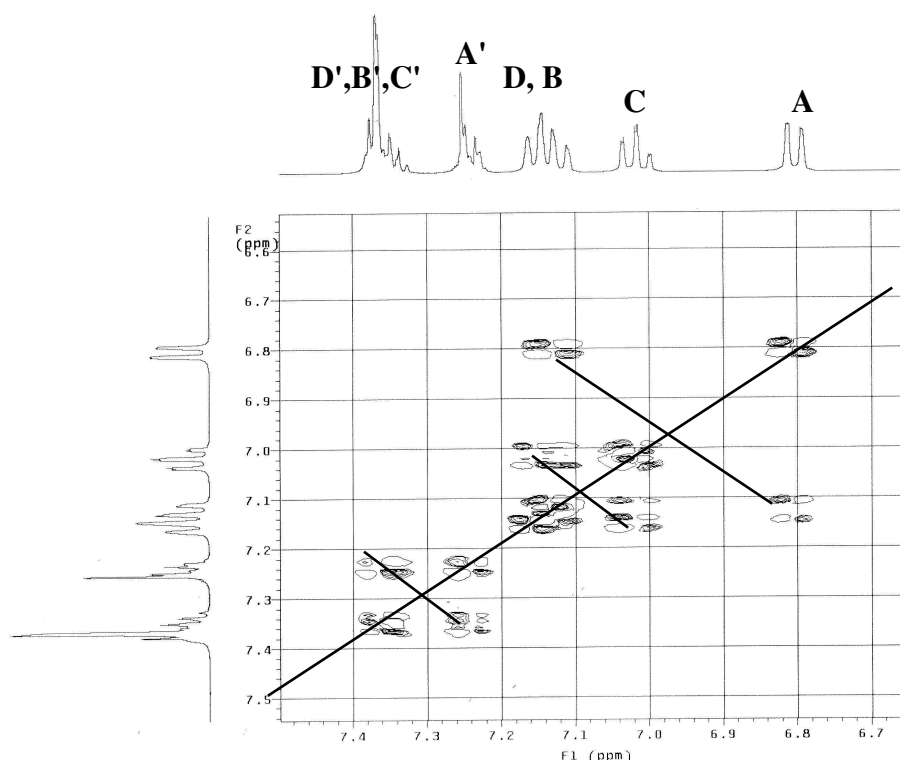


Figure 4.29. Aromatic part of 2D-COSY spectrum of 2-(*o*-tolyl)imino-3-(*o*-tolyl)thiazolidine-4-one in CDCl₃

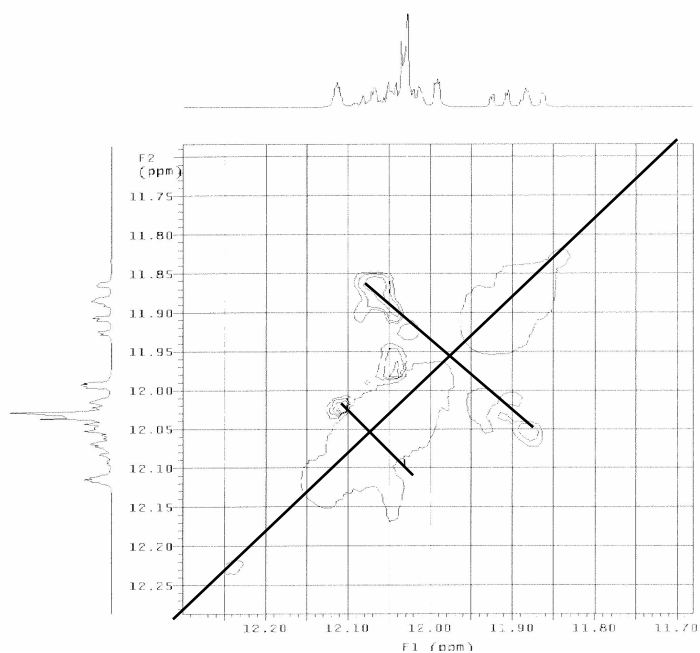


Figure 4.30. Aromatic part of 2D-NOESY spectrum of 2-(*o*-tolyl)imino-3-(*o*-tolyl)thiazolidine-4-one in toluene- d_8

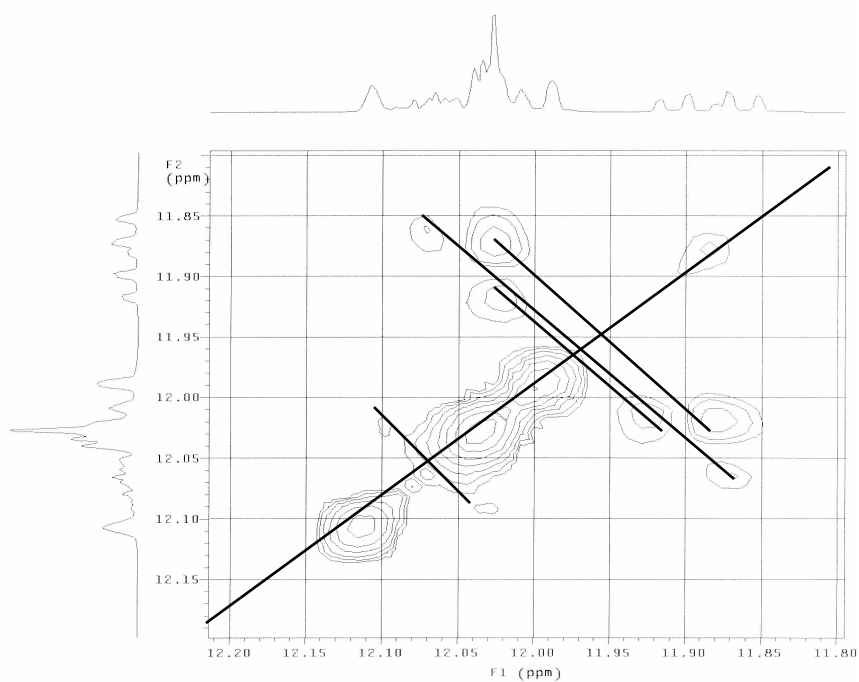


Figure 4.31. Aromatic part of 2D-COSY spectrum of 2-(*o*-tolyl)imino-3-(*o*-tolyl)thiazolidine-4-one in toluene- d_8

2D-NOESY and 2D-COSY spectra of the compound in toluene- d_8 (Figure 4.30 and 4.31) were also compared because in this solvent two AB splittings for diastereotopic C-5 protons were observed in ^1H NMR spectrum, which means that both E and Z isomers exist. The peaks of the solvent in these spectra overlapped with the aromatic part of the spectrum. However, because it was found that interactions between the protons observed in both spectra are the same, it was concluded that there are no through space interactions between the two rings.

4.2.4. Barrier to Rotation about N_3 -aryl bond of 2-(*o*-tolyl)imino-3-(*o*-tolyl)-thiazolidine-4-one

Barrier to rotation about N_3 -aryl bond of the compound was determined by thermal racemization method which was performed in the following way: The isomers of the compound were separated by liquid chromatography on Chiralcel OD-H column and each fraction was collected separately. The eluent used was 95:5 hexane:ethanol mixture. The column temperature was 7°C and the flow rate was 0.6 ml/min. As soon as the fraction was collected, the solvent was evaporated by blowing nitrogen gas to the sample. This procedure was repeated successively until about 0.2 mg of each isomer was collected. Then the solid was dissolved in 200 μl of absolute ethanol, and 30 μl of the solution was injected into the column to determine the initial concentration. The solution left was kept in a constant temperature oil bath at 60°C , and the racemization process was followed by taking 30 μl of the sample at certain time intervals. This process was repeated until equilibrium was reached. At the end, the relative per cent composition of each isomer, which had been recorded by following the integral ratio of the peaks (Figure 4.32), was used in the reversible first order kinetical calculation. The relative per cent composition values of the first eluted isomer were substituted into Equation 2.9 and a graph of the obtained results versus time (Figure 4.32) was plotted.

$$\ln ([M]-[M]_{\text{eq}}/[M]_0-[M]_{\text{eq}})=-2kt \quad (2.9)$$

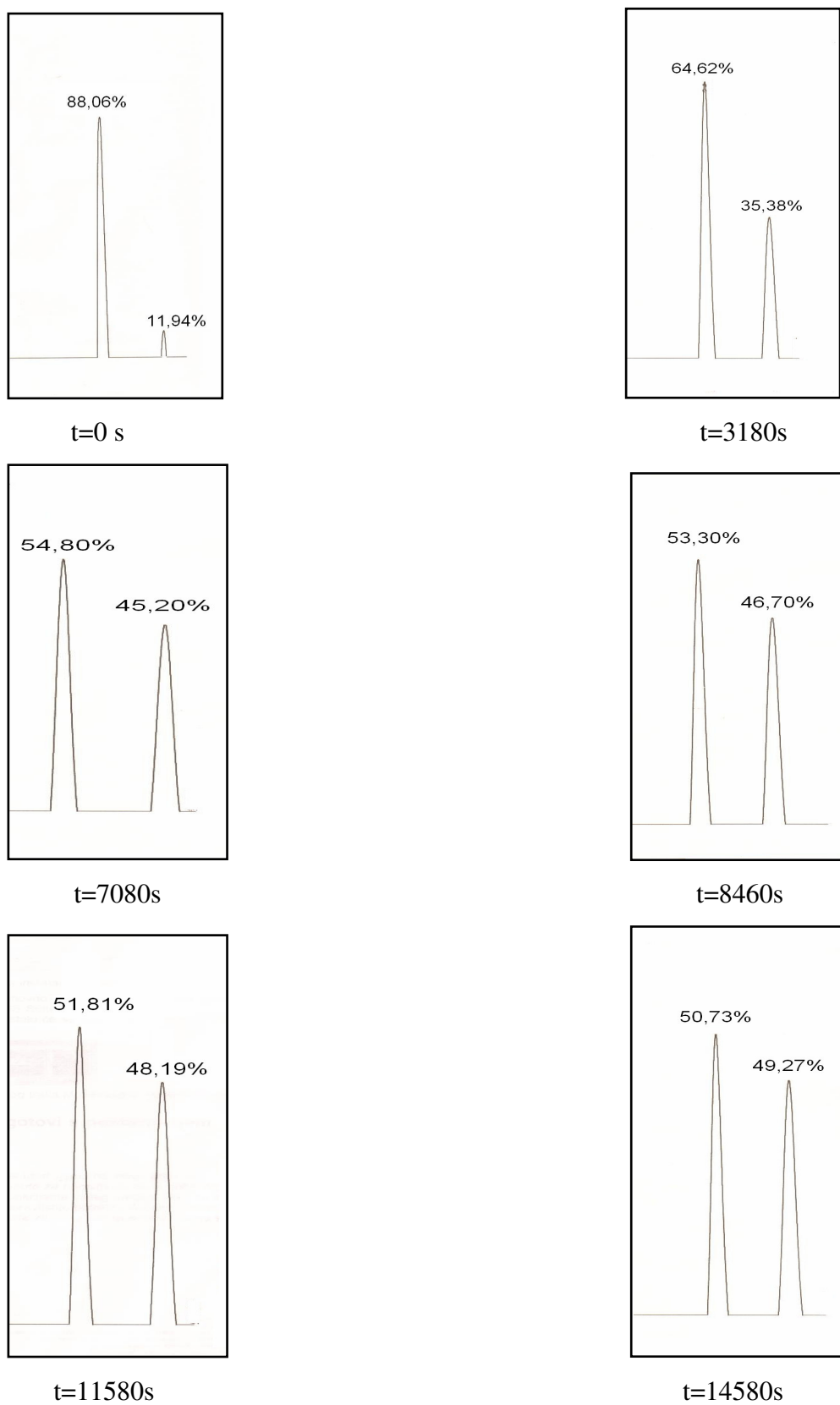


Figure 4.32. The chromatograms taken to follow thermal racemization process of 2-(*o*-tolyl)imino-3-(*o*-tolyl)-thiazolidine-4-one

From the slope of the graph shown in Figure 4.33, the first order rate constant, k was calculated to be 0.00015 s^{-1} . this value was substituted into Equation 2.10 and the energy barrier of 2-(*o*-tolyl)imino-3-(*o*-tolyl)-thiazolidine-4-one was found to be 106,2 kJ/mole.

$$\Delta G^\ddagger = RT \ln(k_b \cdot T / k \cdot h) \quad (2.10)$$

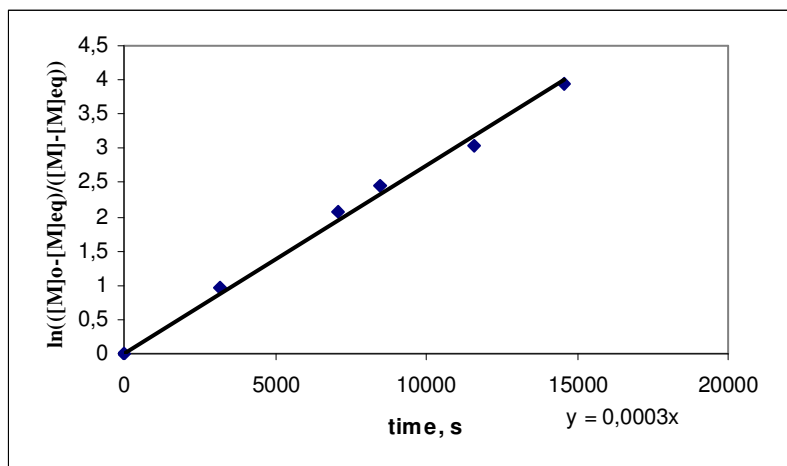
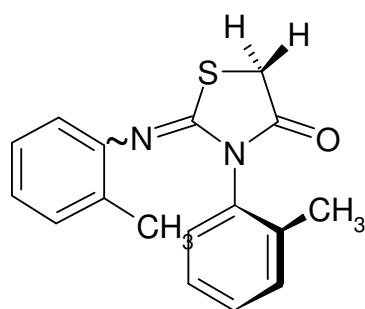


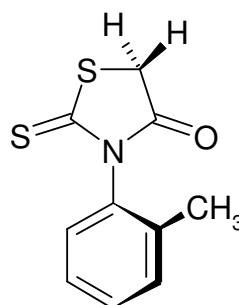
Figure 4.33. The plot of $\ln([M]_0/[M]_{eq}/([M]-[M]_{eq}))$ versus time at 333 K for 2-(*o*-tolyl)imino-3-(*o*-tolyl)-thiazolidine-4-one

4.2.5. Comparison of the Energy Barrier of 2-(*o*-tolyl)imino-3-(*o*-tolyl)-thiazolidine-4-one with Structurally Related Compound

Energy barrier of 2-(*o*-tolyl)imino-3-(*o*-tolyl)-thiazolidine-4-one was compared with that of 3-(*o*-tolyl)rhodanine [10]. It was thought that if 2-(*o*-tolyl)imino-3-(*o*-tolyl)-thiazolidine-4-one has **Z** configuration, there may be no big energy difference in the energy barriers between 2-(*o*-tolyl)imino-3-(*o*-tolyl)-thiazolidine-4-one and 3-(*o*-tolyl)rhodanine because the imino nitrogen would not hinder the rotation about N_3 -aryl more than sulfur. If the compound has **E** configuration, the other aryl gives rise to more hinderence, thus the barrier will be expected to be higher than that of 3-(*o*-tolyl)rhodanine. Energy barriers and the structures of the compounds are given in the Figure 4.34 and 4.35. Comparison of the barriers showed that barrier of the compound studied is lower than that of 3-(*o*-tolyl)rhodanine, which supports assignment of **Z** configuration to the C=N bond.

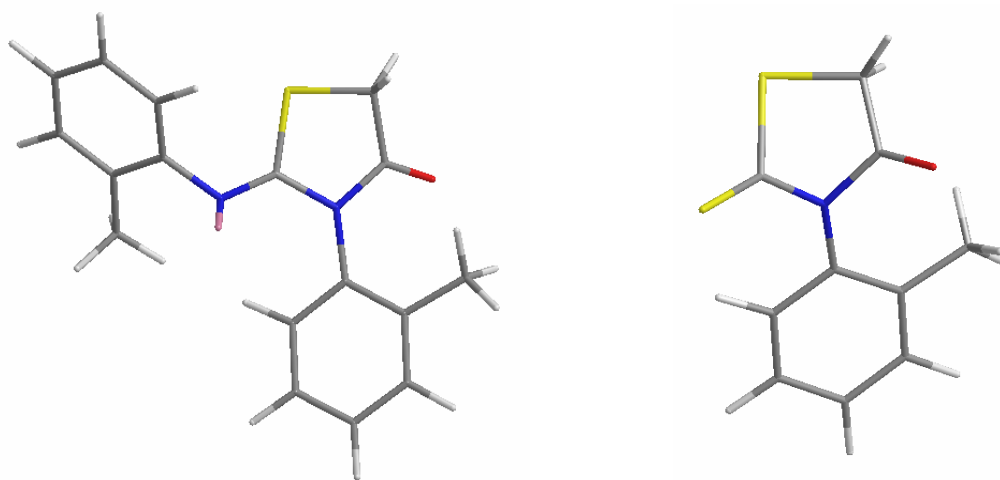


2-(*o*-tolyl)imino-3-(*o*-tolyl)-thiazolidine-4-one
106.2 kJ/mole



3-(*o*-tolyl)rhodanine
114.4 kJ/mole

Figure 4.34 The energy barriers and the structures of 2-(*o*-tolyl)imino-3-(*o*-tolyl)-thiazolidine-4-one and 3-(*o*-tolyl)rhodanine



2-(*o*-tolyl)imino-3-(*o*-tolyl)-thiazolidine-4-one

3-(*o*-tolyl)rhodanine

Figure 4.35 3D structures of 2-(*o*-tolyl)imino-3-(*o*-tolyl)-thiazolidine-4-one and 3-(*o*-tolyl)rhodanine

4.3. 2-(α -Naphthyl)imino-3-(α -naphthyl)-thiazolidine-4-one

4.3.1. ^1H NMR spectra of 2-(α -naphthyl)imino-3-(α -naphthyl)-thiazolidine-4-one

The ^1H NMR spectral assignments of 2-(α -naphthyl)imino-3-(α -naphthyl)-thiazolidine-4-one (Figure 4.36) in various solvents are given in Table 4.3 (Figure 4.40, 4.41, 4.42 and 4.43).

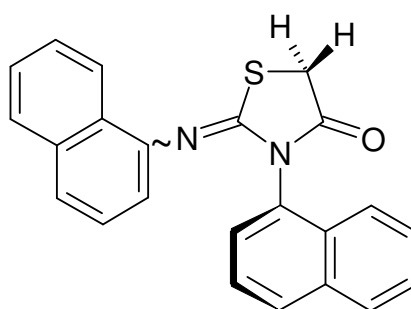


Figure 4.36. The structure of 2-(α -naphthyl)imino-3-(α -naphthyl)-thiazolidine-4-one

Table 4.3. 400 MHz spectral data for 2-(α -naphthyl)imino-3-(α -naphthyl)-thiazolidine-4-one in various solvents

Solvents	Protons on C-5 (ppm)		Aromatic protons (ppm)
DMF-d ₇	$\delta_A=4.69$	$\delta_B=4.53$	7.19-8.30
Methanol-d ₄	$\delta_A=4.32$	$\delta_B=4.23$	7.01-8.08
CDCl ₃	$\delta_A=4.09$	$\delta_B=4.05$	6.93-7.92
Toluene-d ₈	$\delta_A=3.26$	$\delta_B=3.20$	7.05-7.94

In all solvents one AB splitting was observed for the diastereotopic methylene protons on the C-5 (Figure 4.37), which means that N₃-C_{naphthyl} bond rotation is hindered, N₃-C_{naphthyl} being the chiral axis and as far as the imino C=N bond is concerned, only one, probably the Z isomer exists.

One AB splitting for the ^1H NMR signal of protons on the C-5 carbon in DMF-d₇ was observed at temperatures between -50 °C and 100 °C (Figure 4.38). Moreover, in

toluene-d₈ the methylene protons at C-5 carbon of the heterocyclic ring showed one AB splitting in the 75°C to -70°C range (Figure 4.39).

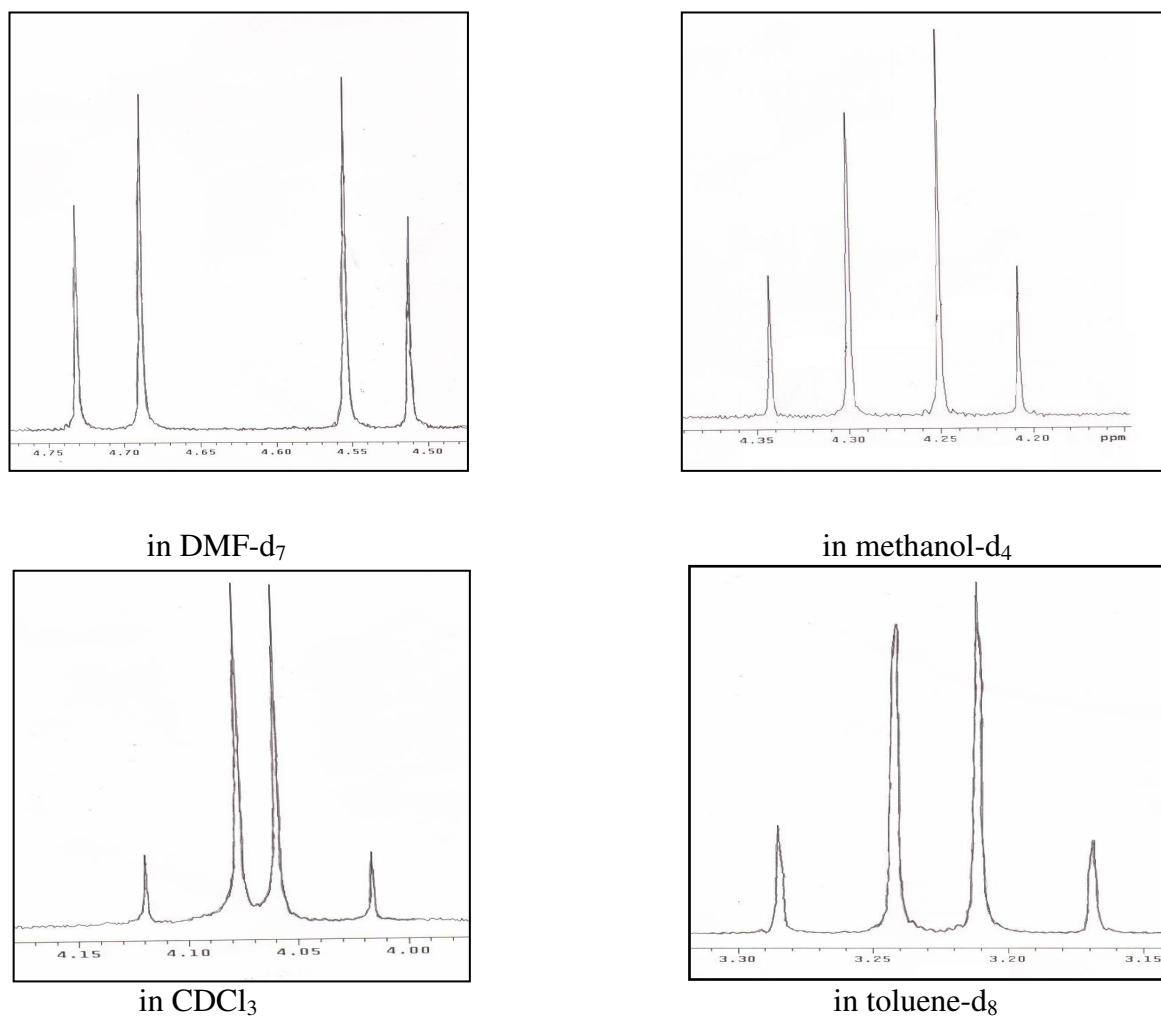


Figure 4.37. The AB spectra of diastereotopic methylene protons on the C-5 of 2-(α-naphthyl)imino-3-(α-naphthyl)-thiazolidine-4-one in various solvents at 25 °C

4.3.2. ¹³C NMR Spectra of 2-(α-naphthyl)imino-3-(α-naphthyl)-thiazolidine-4-one

¹³C NMR spectrum of 2-(α-naphthyl)imino-3-(α-naphthyl)-thiazolidine-4-one was taken in CDCl₃ (Figure 4.44). The C-2, C-4 and C-5 carbons gave peaks at 166.4 ppm, 171.9 ppm and 33.4 ppm, respectively. The aromatic carbons resonated between 115.3-144.50 ppm. ¹³C NMR spectrum of the compound was also taken in toluene-d₈ (Figure 4.45). The C-2, C-4 and C-5 carbons resonated at 159.7 ppm, 175.3 ppm and 37.3 ppm, respectively. The aromatic carbons resonated between 119.9-150.0 ppm.

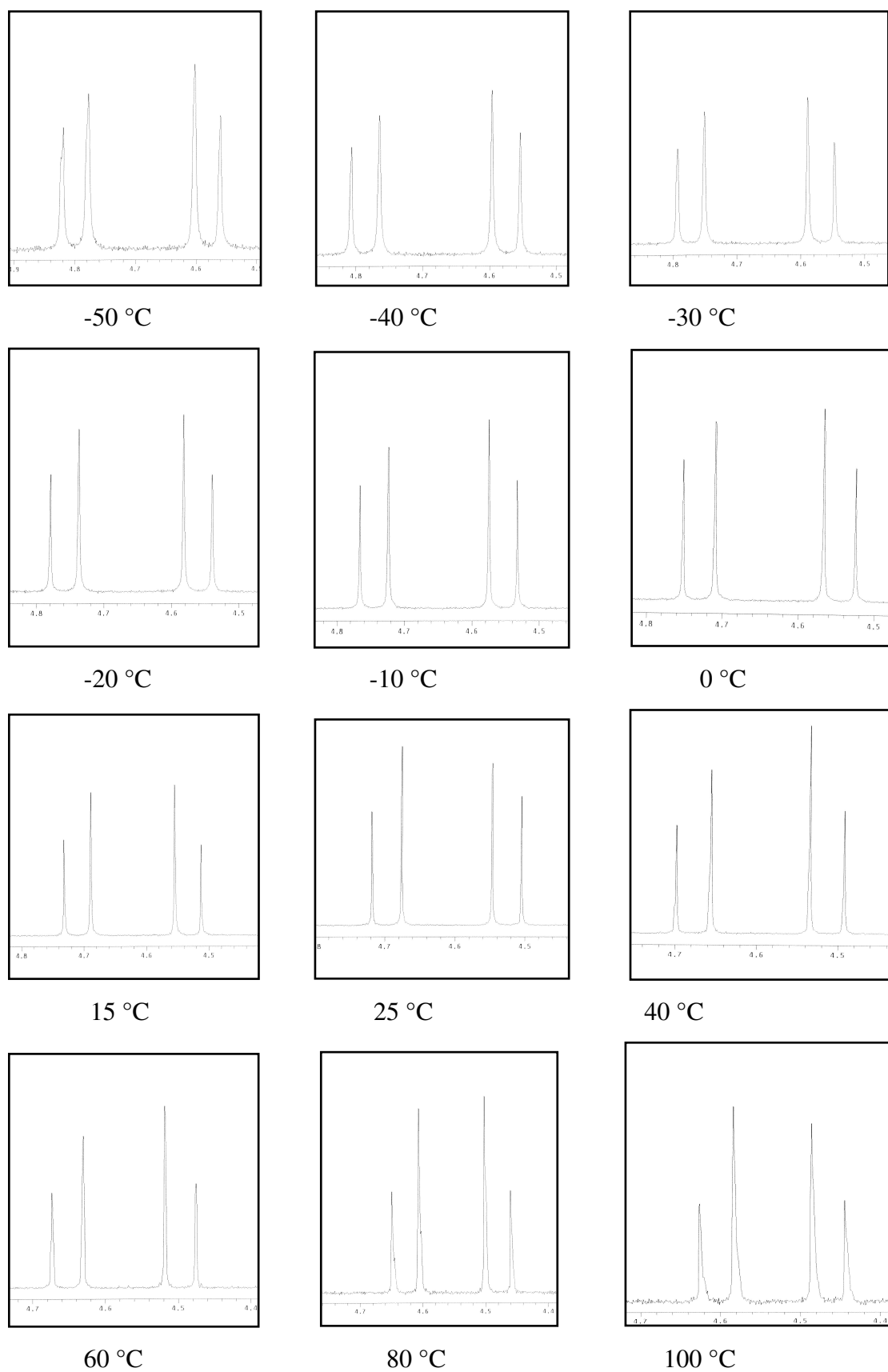


Figure 4.38. ^1H NMR signals for diastereotopic methylene protons on C-5 of 2-(α -naphthyl)imino-3-(α -naphthyl)-thiazolidine-4-one at various temperatures in DMF-d_7

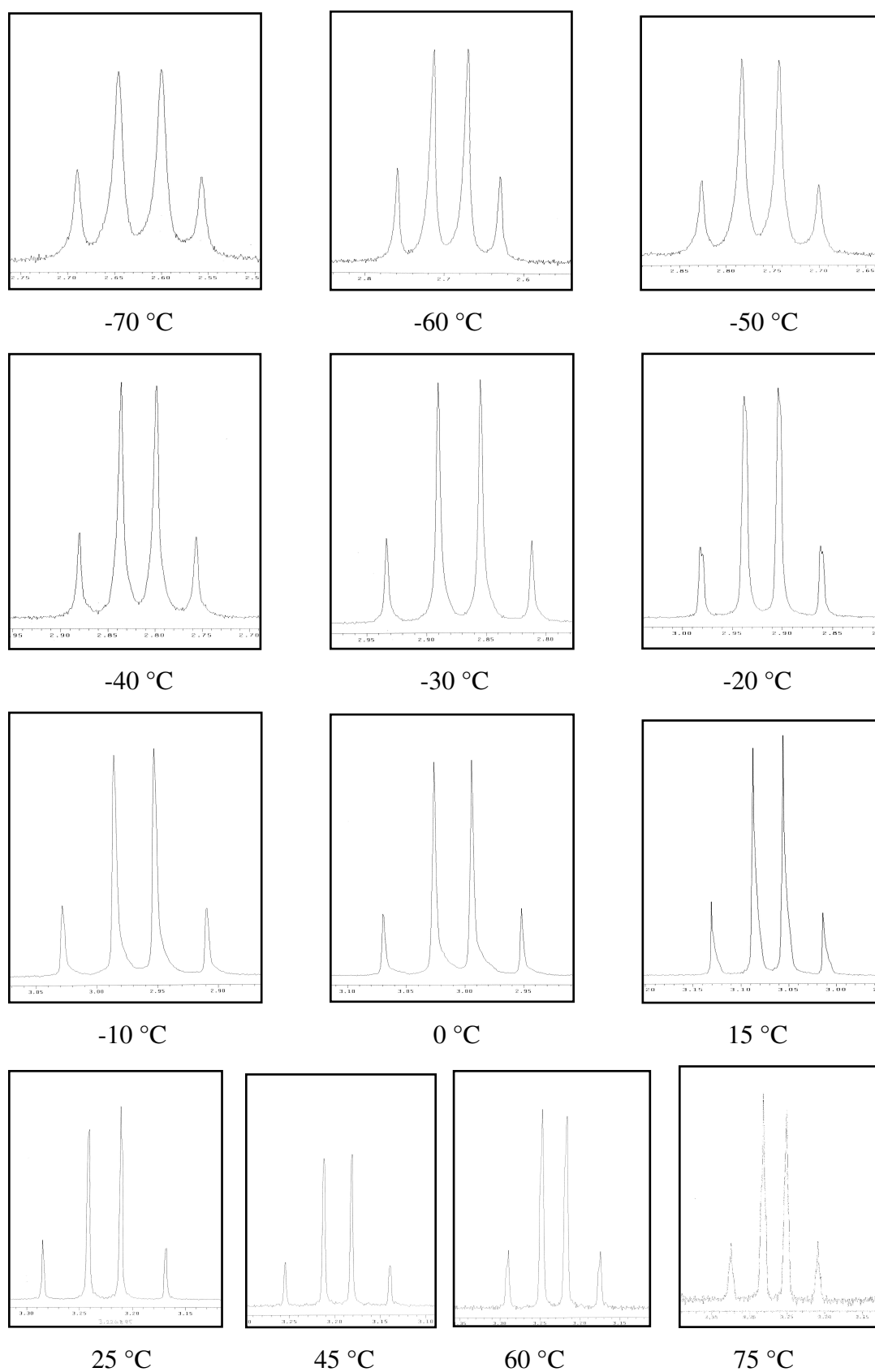


Figure 4.39. ^1H NMR signals for diastereotopic methylene protons on C-5 of 2-(α -naphthyl)imino-3-(α -naphthyl)-thiazolidine-4-one at various temperatures in toluene- d_8

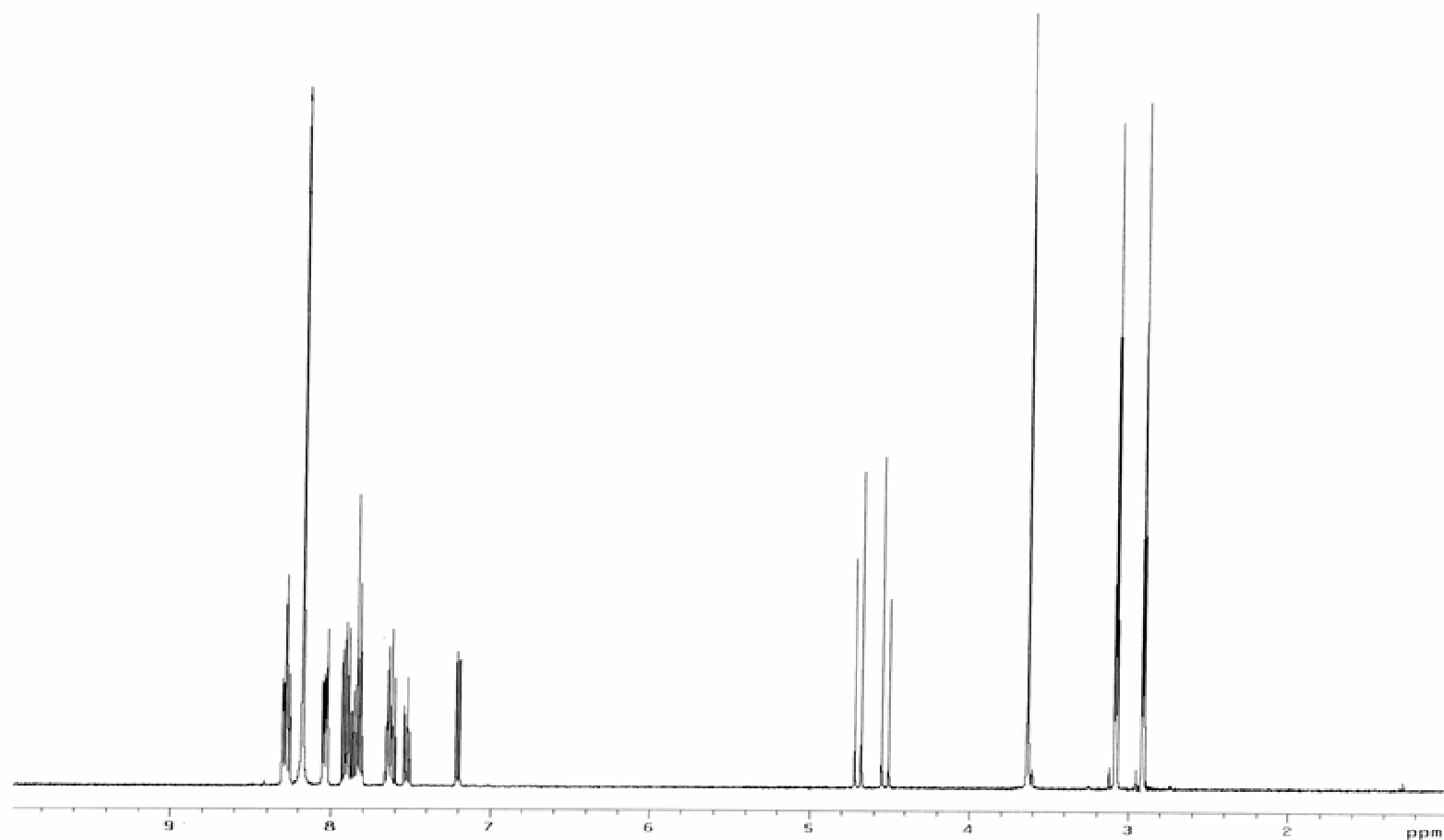


Figure 4.40. The 400 MHz ¹H NMR spectrum of 2-(α-naphthyl)imino-3-(α-naphthyl)-thiazolidine-4-one in DMF-d₇

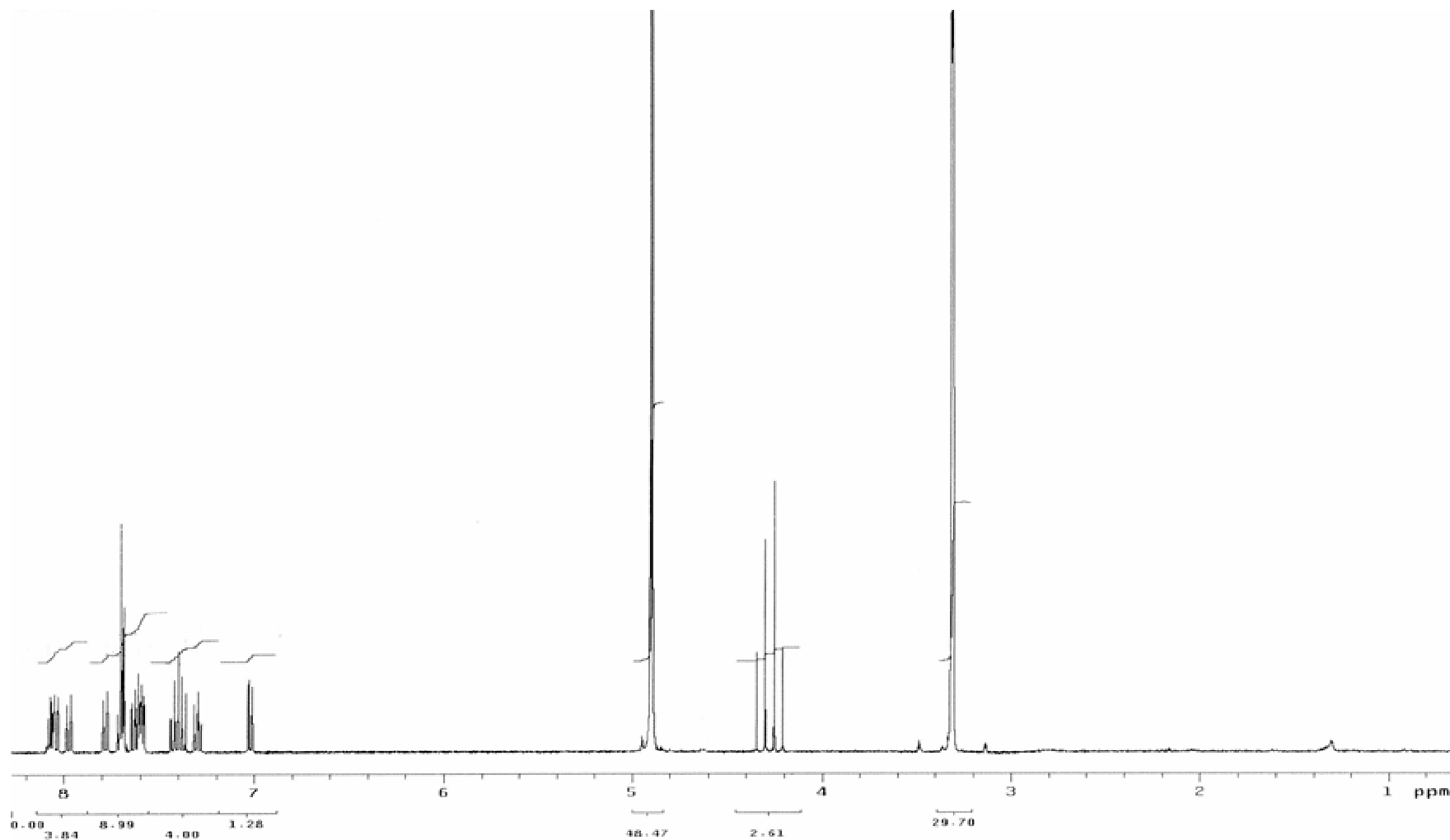


Figure 4.41. The 400 MHz ^1H NMR spectrum of 2-(α -naphthyl)imino-3-(α -naphthyl)-thiazolidine-4-one in methanol- d_4

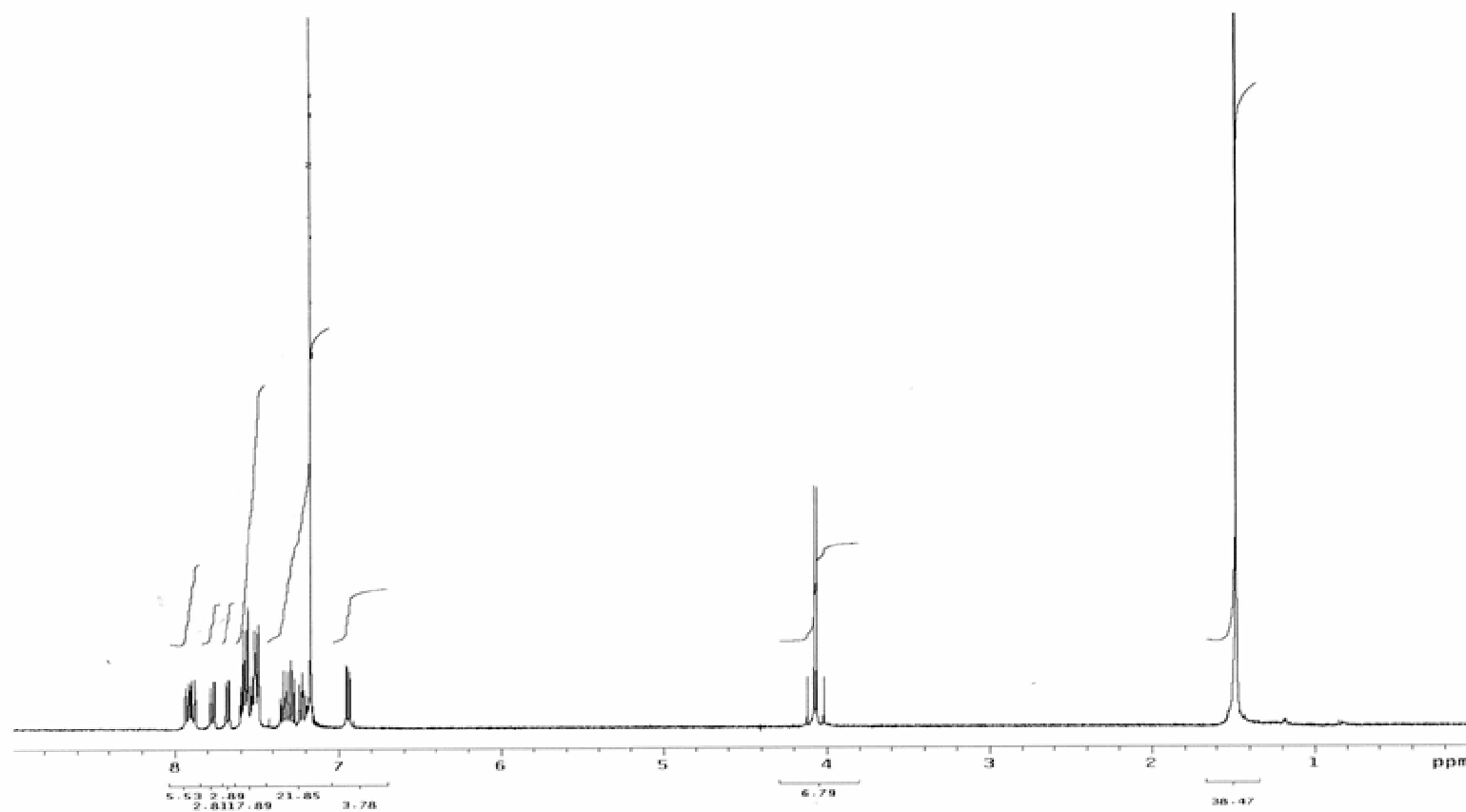


Figure 4.42. The 400 MHz ¹H NMR spectrum of 2-(α-naphthyl)imino-3-(α-naphthyl)-thiazolidine-4-one in CDCl₃

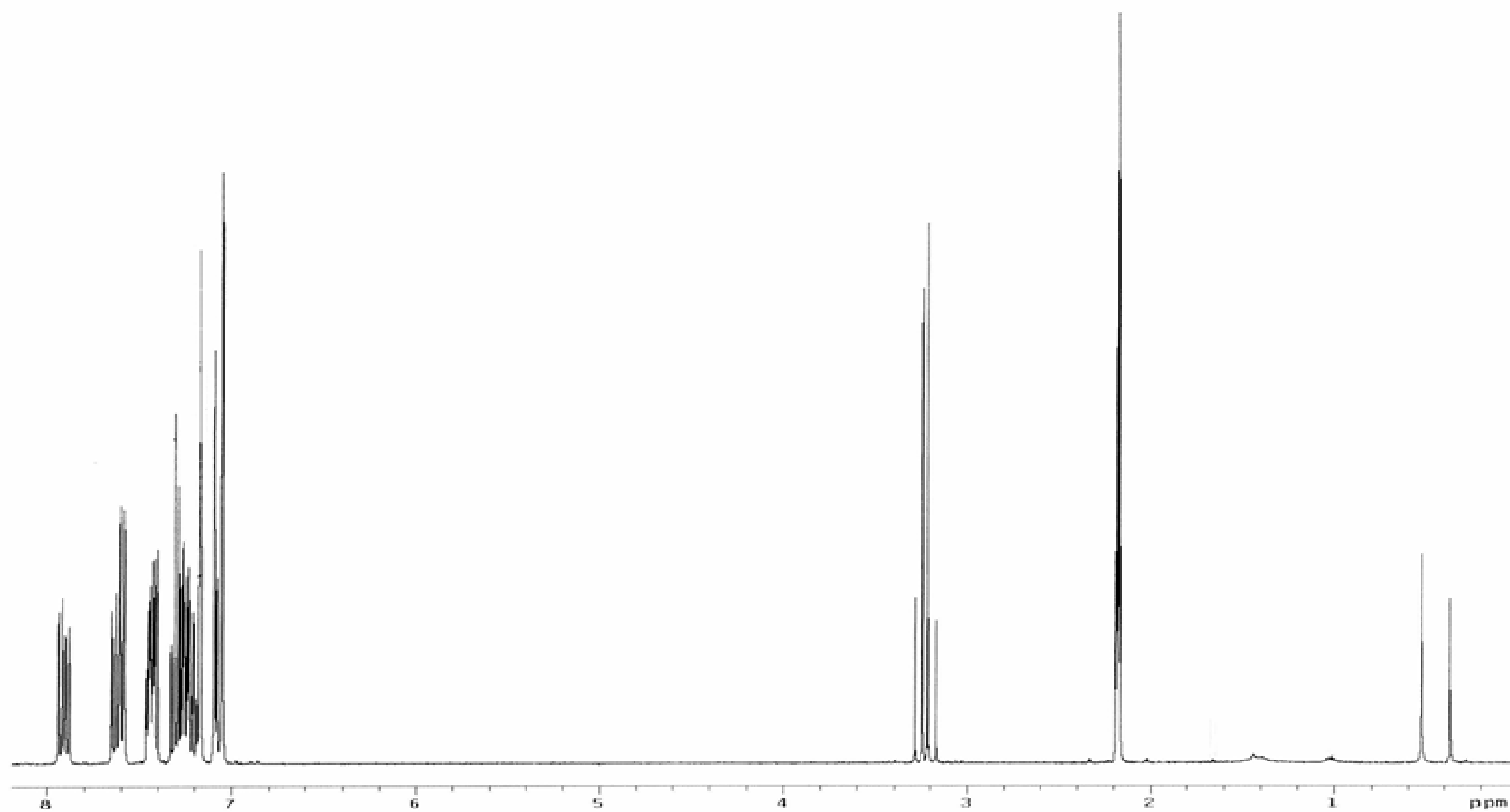


Figure 4.43. The 400 MHz ¹H NMR spectrum of 2-(α-naphthyl)imino-3-(α-naphthyl)-thiazolidine-4-one in toluene-d₈

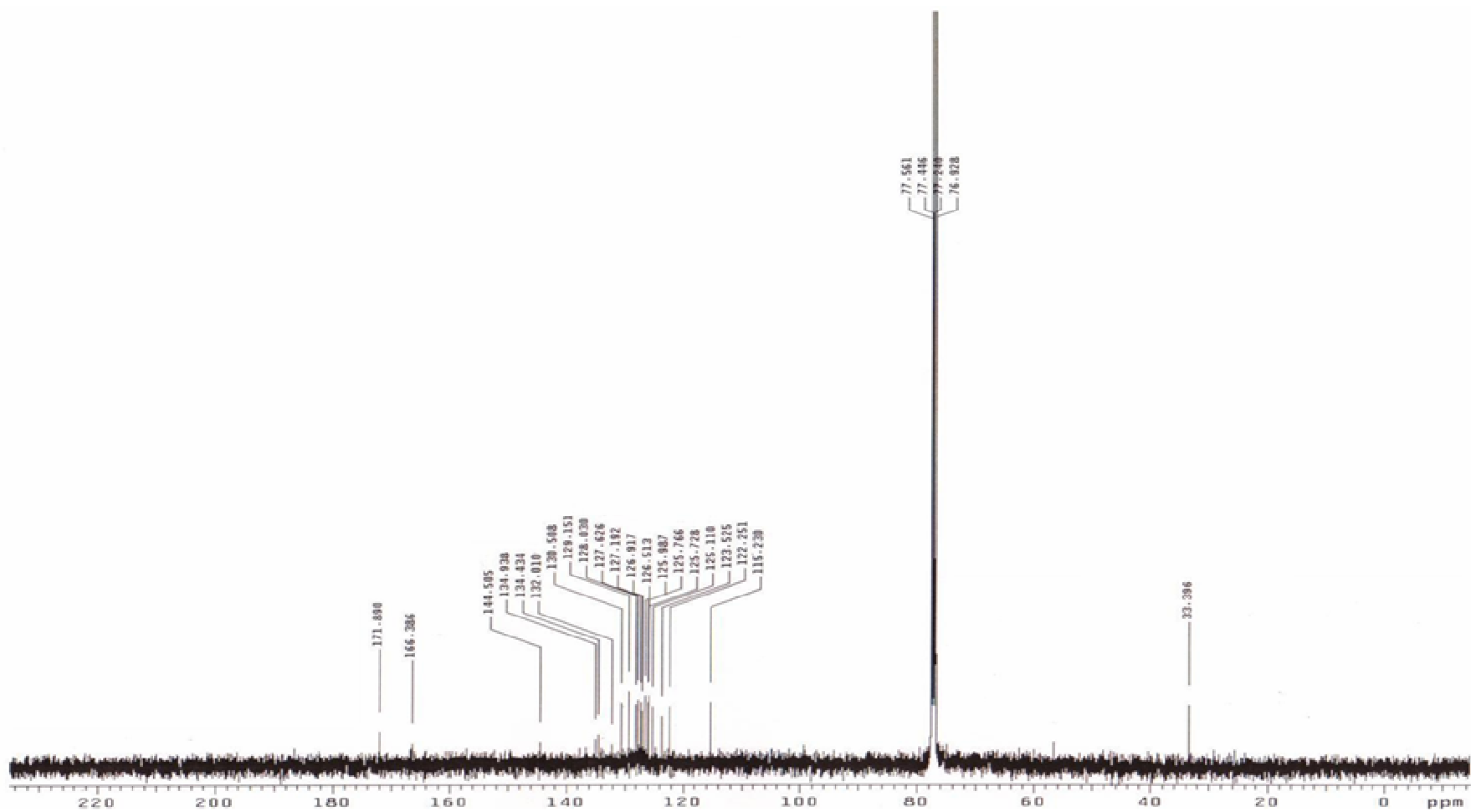


Figure 4.44. The ^{13}C NMR spectrum of 2-(α -naphthyl)imino-3-(α -naphthyl)-thiazolidine-4-one in CDCl_3

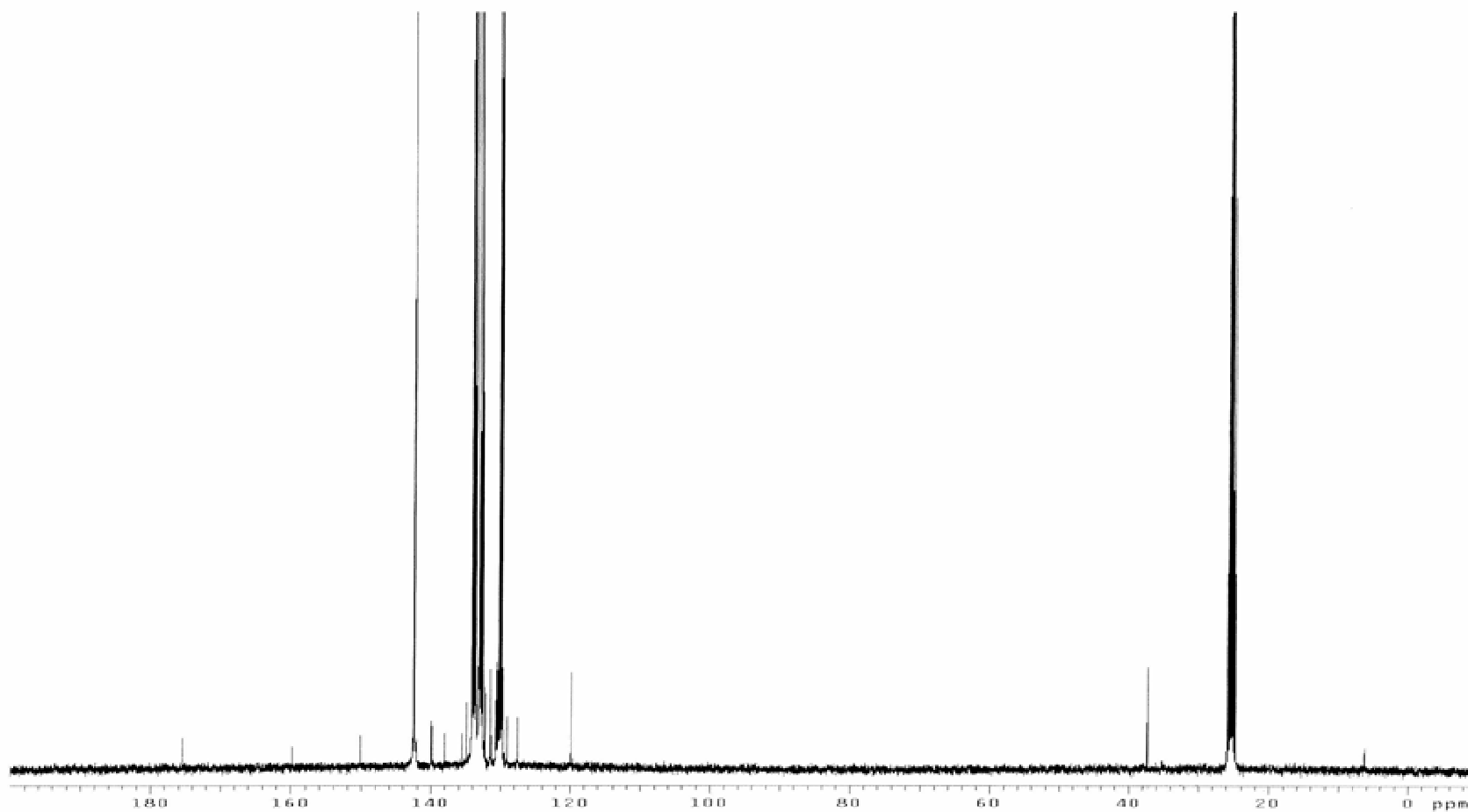


Figure 4.45. The ^{13}C NMR spectrum of 2-(α -naphthyl)imino-3-(α -naphthyl)-thiazolidine-4-one in toluene- d_8

4.3.3. 2D-NOESY and 2D-COSY spectra of 2-(α -naphthyl)imino-3-(α -naphthyl)-thiazolidine-4-one

2D-NOESY spectrum of compound in CDCl_3 (Figure 4.46) was compared to the 2D-COSY spectrum of compound in CDCl_3 (Figure 4.47) in order to gain information about the spacial interactions. In this case, due to the complexity of the spectrum, it was not possible to do an assignment for each peak in the aromatic region of the ^1H NMR spectrum. However, it was found that interactions between the protons observed in the 2D-COSY spectrum are the same as that found in the 2D-NOESY spectrum of the compound, which means that through space interactions between the two rings are not present.

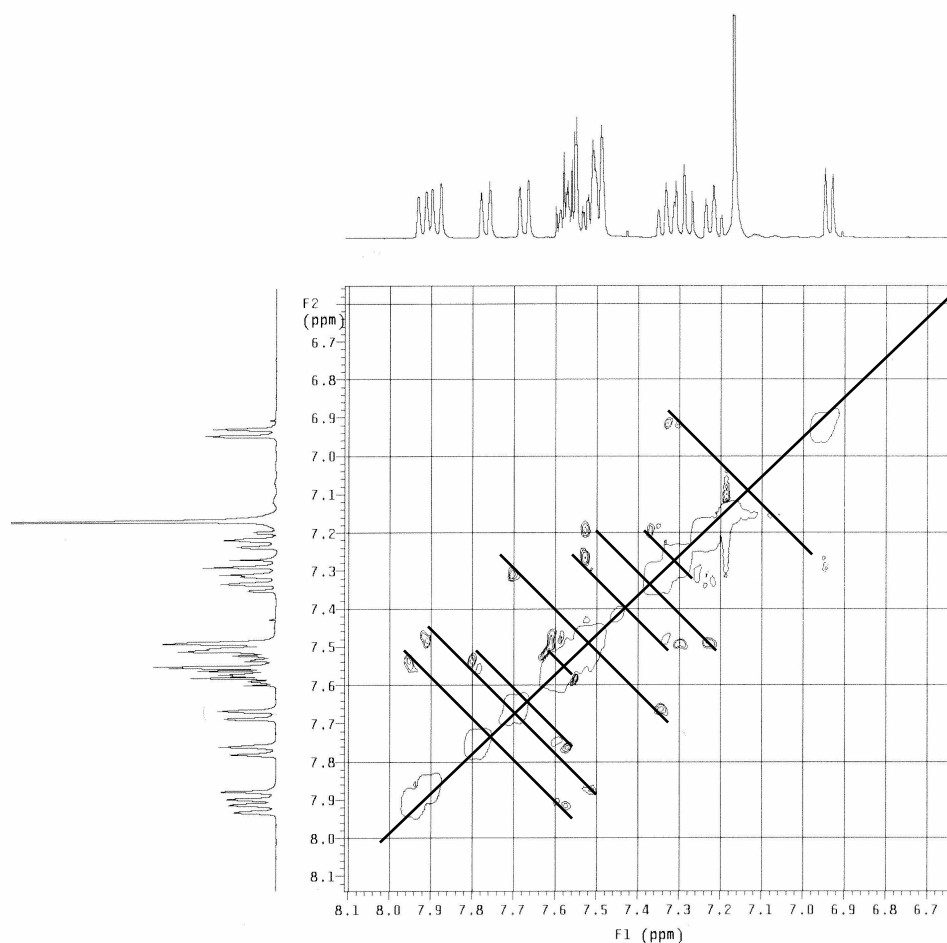


Figure 4.46. Aromatic region of 2D-NOESY spectrum of 2-(α -naphthyl)imino-3-(α -naphthyl)-thiazolidine-4-one in CDCl_3

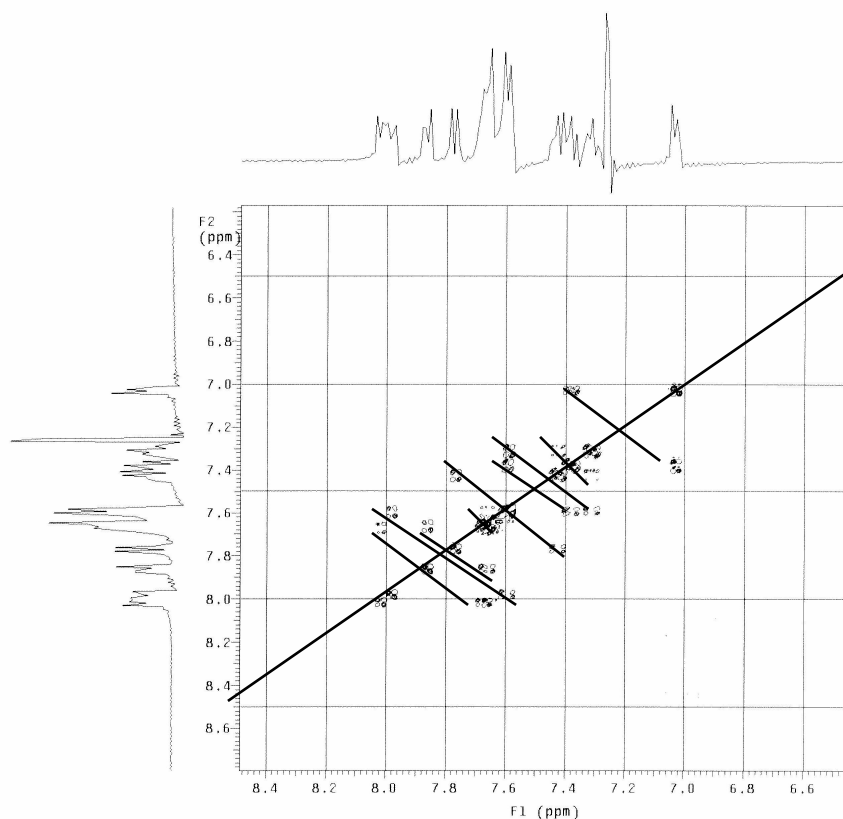


Figure 4.47. Aromatic region of 2D-COSY spectrum of 2-(α -naphthyl)imino-3-(α -naphthyl)-thiazolidine-4-one in CDCl_3

4.3.4. Barrier to Rotation about N_3 -aryl bond of 2-(α -naphthyl)imino-3-(α -naphthyl)-thiazolidine-4-one

Barrier to rotation about N_3 -aryl bond of the compound was determined by thermal racemization method. Separation of the isomers was attempted on Chiralpak AD-H column. The eluent used was 70:30 ethanol:hexane. The column temperature was 7°C and the flow rate was 0.5 ml/min. After the isomers were separated, one of them was subjected to the thermal racemization experiment which had been explained in detail in section 4.2.4. The graph of obtained results (Figure 4.48) versus time is given in Figure 4.49. From the slope of the graph the rate constant, k was calculated to be $2.5 \cdot 10^{-5} \text{ s}^{-1}$. Rotational barrier was found to be 111.2 kJ/mole.

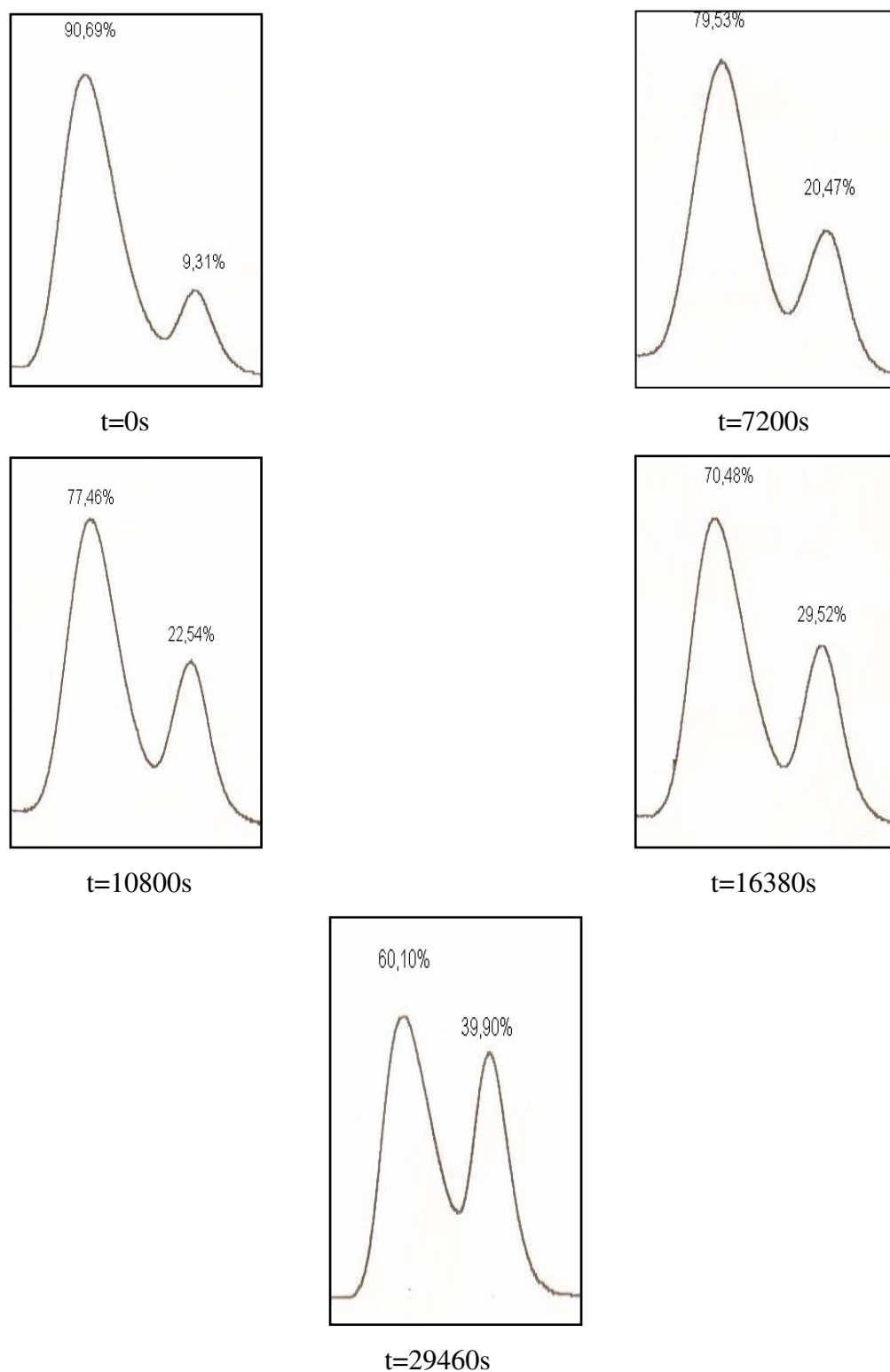


Figure 4.48. The chromatograms taken to follow thermal racemization process of 2-(α -naphthyl)imino-3-(α -naphthyl)-thiazolidine-4-one

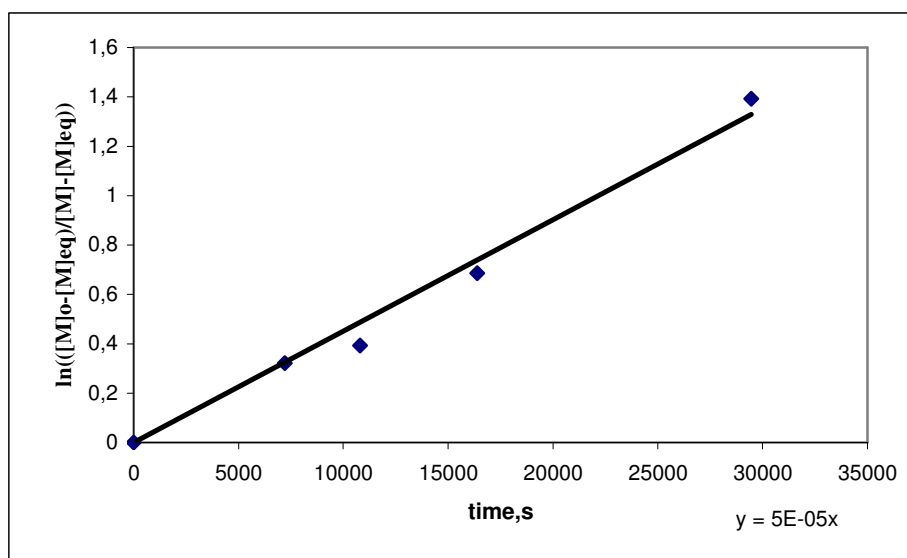


Figure 4.49. The plot of $\ln\left(\frac{[M]_0 - [M]_{eq}}{[M] - [M]_{eq}}\right)$ versus time at 333 K for 2-(α -naphthyl)imino-3-(α -naphthyl)-thiazolidine-4-one

4.3.5. Comparison of the Energy Barrier of 2-(α -naphthyl)imino-3-(α -naphthyl)-thiazolidine-4-one with Structurally Related Compounds

Energy barrier of 2-(α -naphthyl)imino-3-(α -naphthyl)-thiazolidine-4-one was compared with that of 3-(α -naphthyl)-2,4-thioazolidinedione[18] and with that of 3-(α -naphthyl)rhodanine [18] to get information about the stereochemistry of the C=N double bond. It is thought that there may be no big difference in the energy barriers between 2-(α -naphthyl)imino-3-(α -naphthyl)-thiazolidine-4-one and structurally related compounds if 2-(α -naphthyl)imino-3-(α -naphthyl)-thiazolidine-4-one has **Z** configuration because the imino nitrogen would not hinder the rotation about N₃-aryl more than the oxygen and the sulfur. Energy barriers and the structures of compounds are given in the Figure 4.50 and Figure 4.51. Comparison of the energy barriers of the structurally related compounds reveal that the barrier is higher than expected from the steric requirement for a nitrogen atom. Therefore, the arylimino ring is also contributing to the barrier to rotation in these compounds.

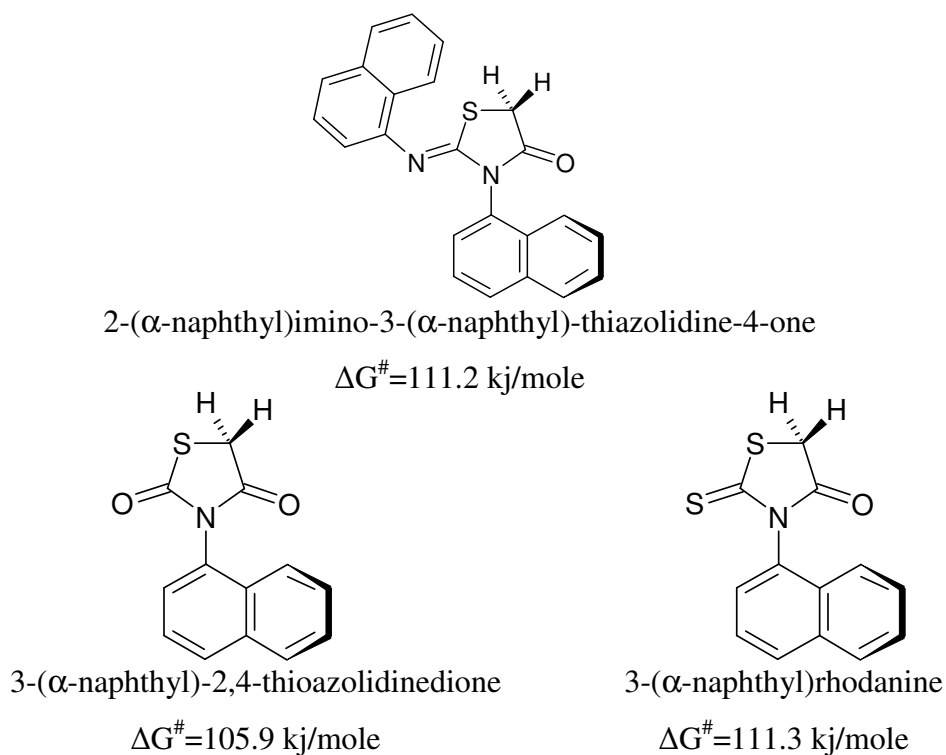


Figure 4.50. The energy barriers and the structures of 2-(α -naphthyl)imino-3-(α -naphthyl)-thiazolidine-4-one, 3-(α -naphthyl)-2,4 thioazolidinedione, 3-(α -naphthyl)rhodanine

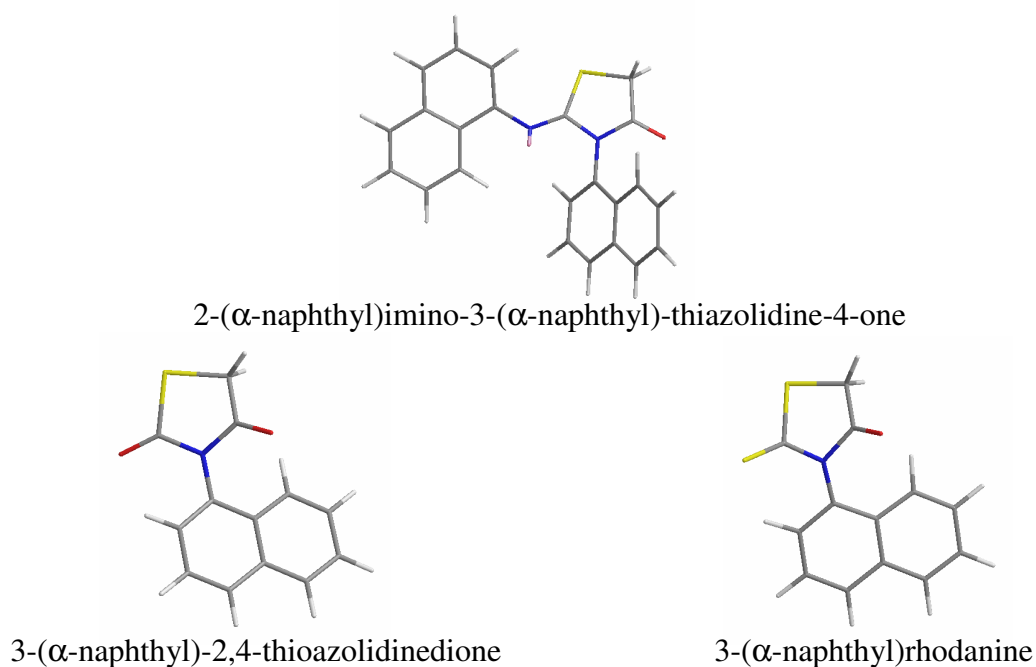


Figure 4.51. 3D structures of 2-(α -naphthyl)imino-3-(α -naphthyl)-thiazolidine-4-one, 3-(α -naphthyl)-2,4 thioazolidinedione and 3-(α -naphthyl)rhodanine

4.4. 2-(*o*-Chlorophenyl)imino-3-(*o*-chlorophenyl)-thiazolidine-4-one

4.4.1. ¹H NMR Spectra of 2-(*o*-chlorophenyl)imino-3-(*o*-chlorophenyl)-thiazolidine-4-one

The ¹H NMR spectral assignments of 2-(*o*-chlorophenyl)imino-3-(*o*-chlorophenyl)-thiazolidine-4-one (Figure 4.52) in various solvents are given in Table 4.4. (Figure 4.55, 4.56, 4.57, 4.58 and 4.59).

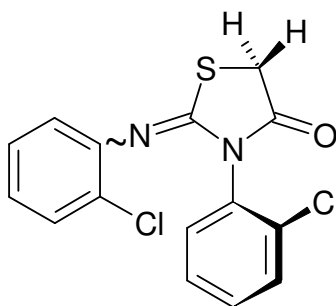


Figure 4.52. The general structure of 2-(*o*-chlorophenyl)imino-3-(*o*-chlorophenyl)-thiazolidine-4-one

In the solvents such as DMF-d₇, CDCl₃ one AB splitting was observed for diastereotopic methylene protons on C-5 (Figure 4.53). In methanol-d₄ the diastereotopic protons were not resolved. In toluene-d₈ one AB splitting for diastereotopic methylene protons on C-5 was observed in the 25°C to 95°C range (Figure 4.54).

Table 4.4. 400 MHz spectral data for 2-(*o*-chlorophenyl)imino-3-(*o*-chlorophenyl)-thiazolidine-4-one in various solvents

Solvents	Protons on C-5 (ppm)		Aromatic protons (ppm)
DMF-d ₇	δ _A =4.45	δ _B =4.38	7.01-7.75
CDCl ₃	δ _A =4.11	δ _B =4.04	6.93-7.60
Methanol-d ₄	δ=4.09		6.85-7.52
Toluene-d ₈	δ _A =3.06	δ _B =2.90	6.60-7.29
Benzene-d ₆	δ _A =2.76	δ _B =2.58	6.29-7.06

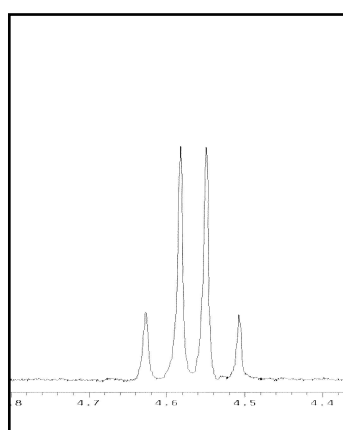
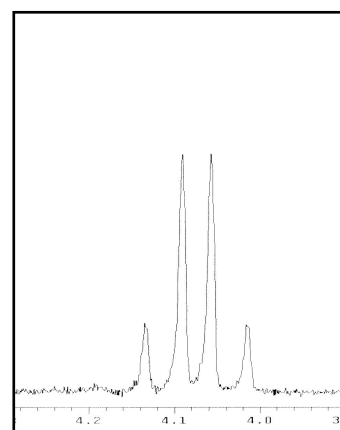
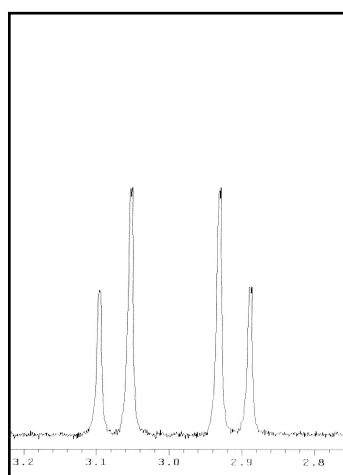
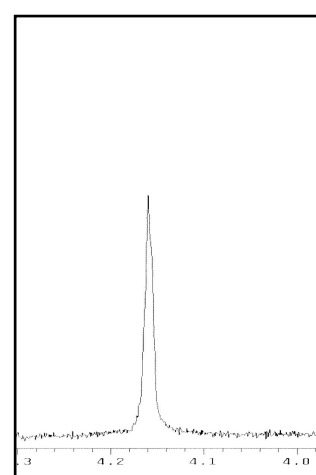
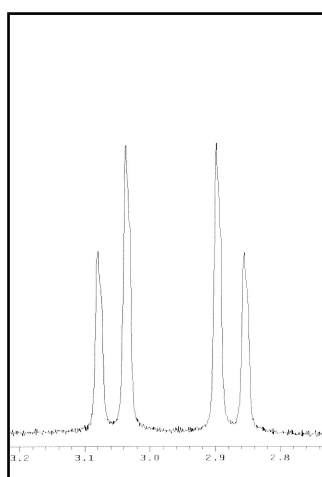
in DMF-d₇in CDCl₃in toluene-d₈in methanol-d₄in benzene-d₆

Figure 4.53. The AB spectra of diastereotopic methylene protons on the C-5 of 2-(*o*-chlorophenyl)imino-3-(*o*-chlorophenyl)thiazolidine-4-one in various solvents at 25 °C

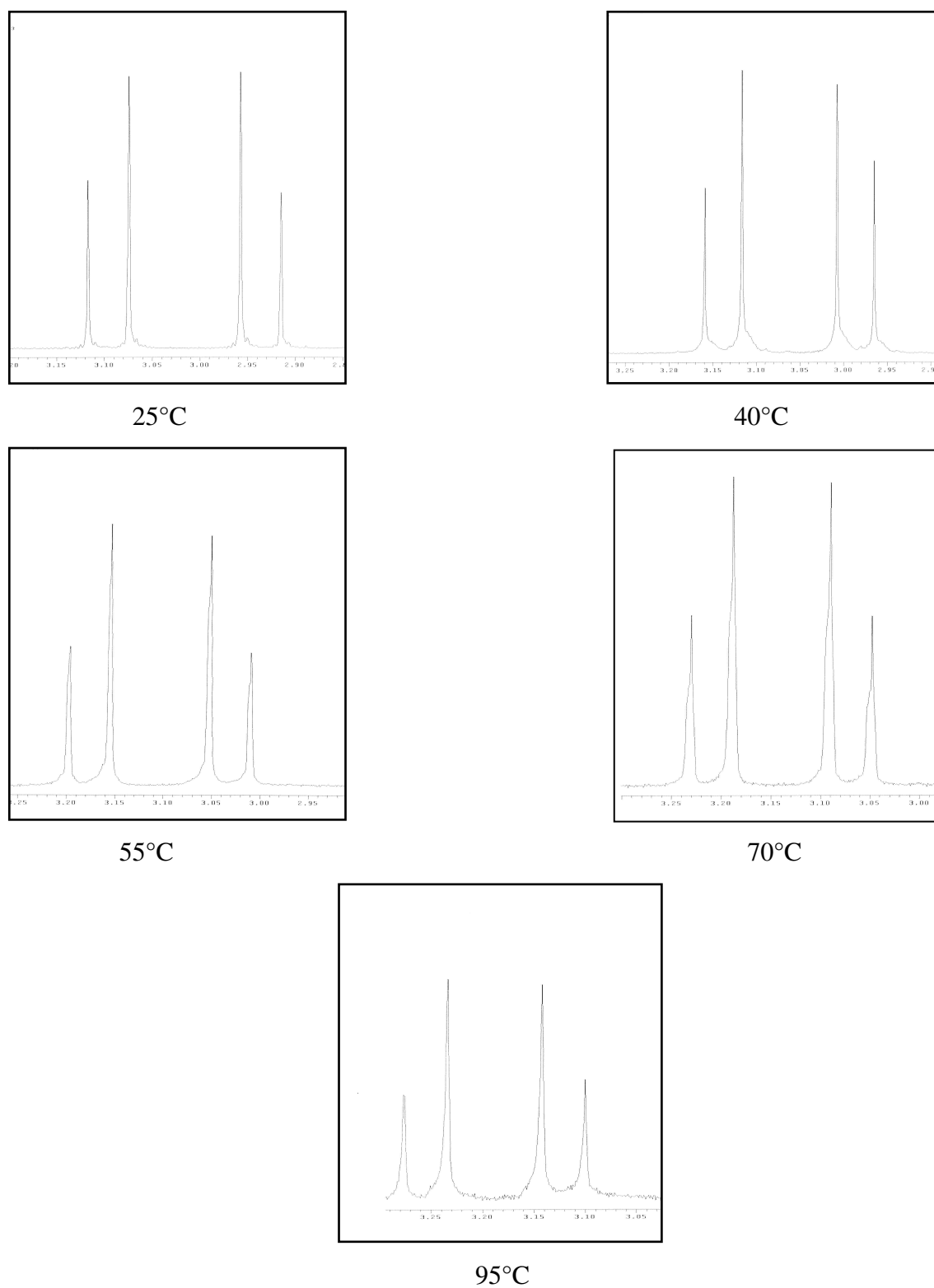


Figure 4.54. ^1H NMR signals for diastereotopic methylene protons on the C-5 of 2-(*o*-chlorophenyl)imino-3-(*o*-chlorophenyl)-thiazolidine-4-one at various temperatures in toluene-d_8

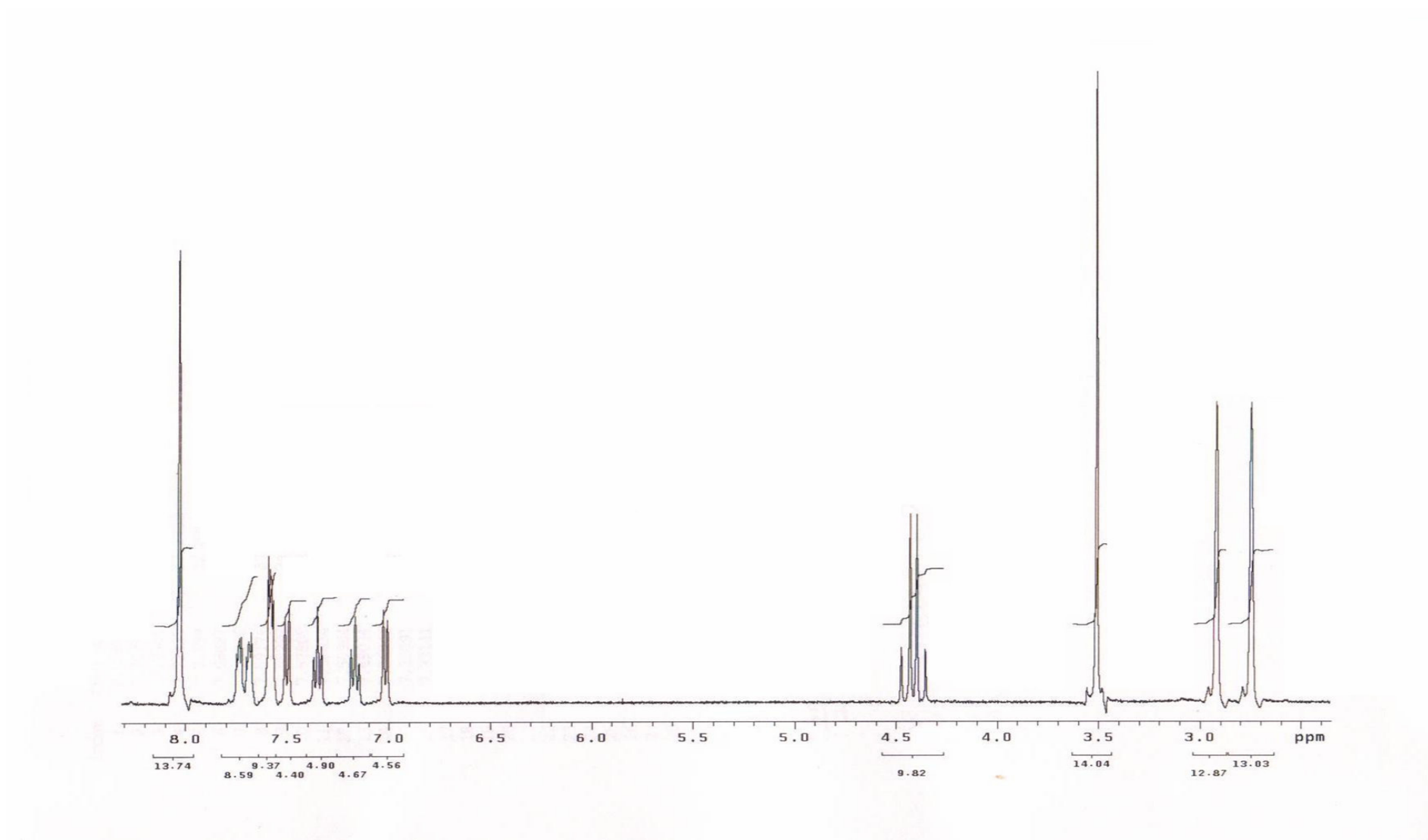


Figure 4.55. The 400 MHz ^1H NMR spectrum of 2-(*o*-chlorophenyl)imino-3-(*o*-chlorophenyl)-thiazolidine-4-one in DMF-d_7

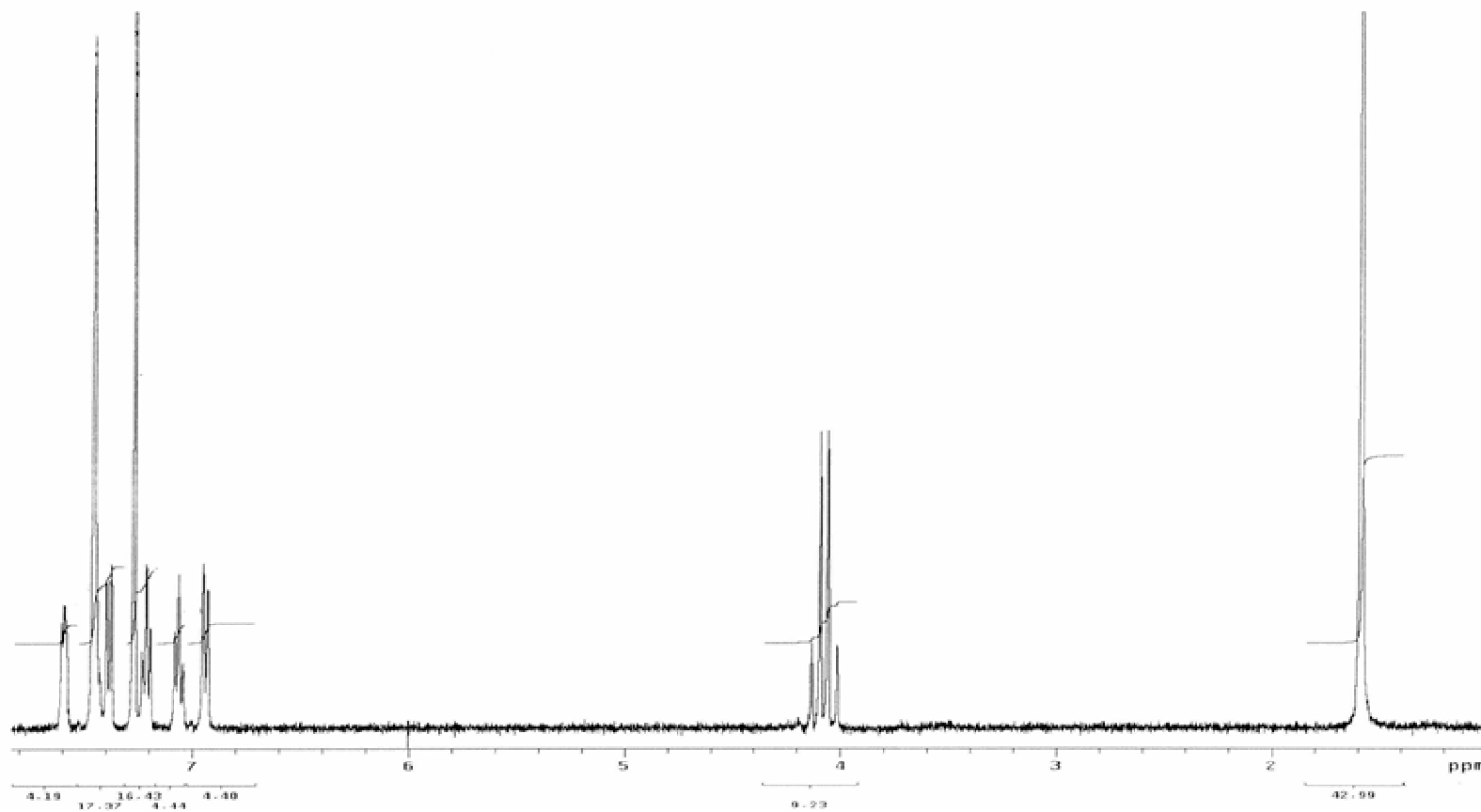


Figure 4.56. The 400 MHz ¹H NMR spectrum of 2-(*o*-chlorophenyl)imino-3-(*o*-chlorophenyl)-thiazolidine-4-one in CDCl₃

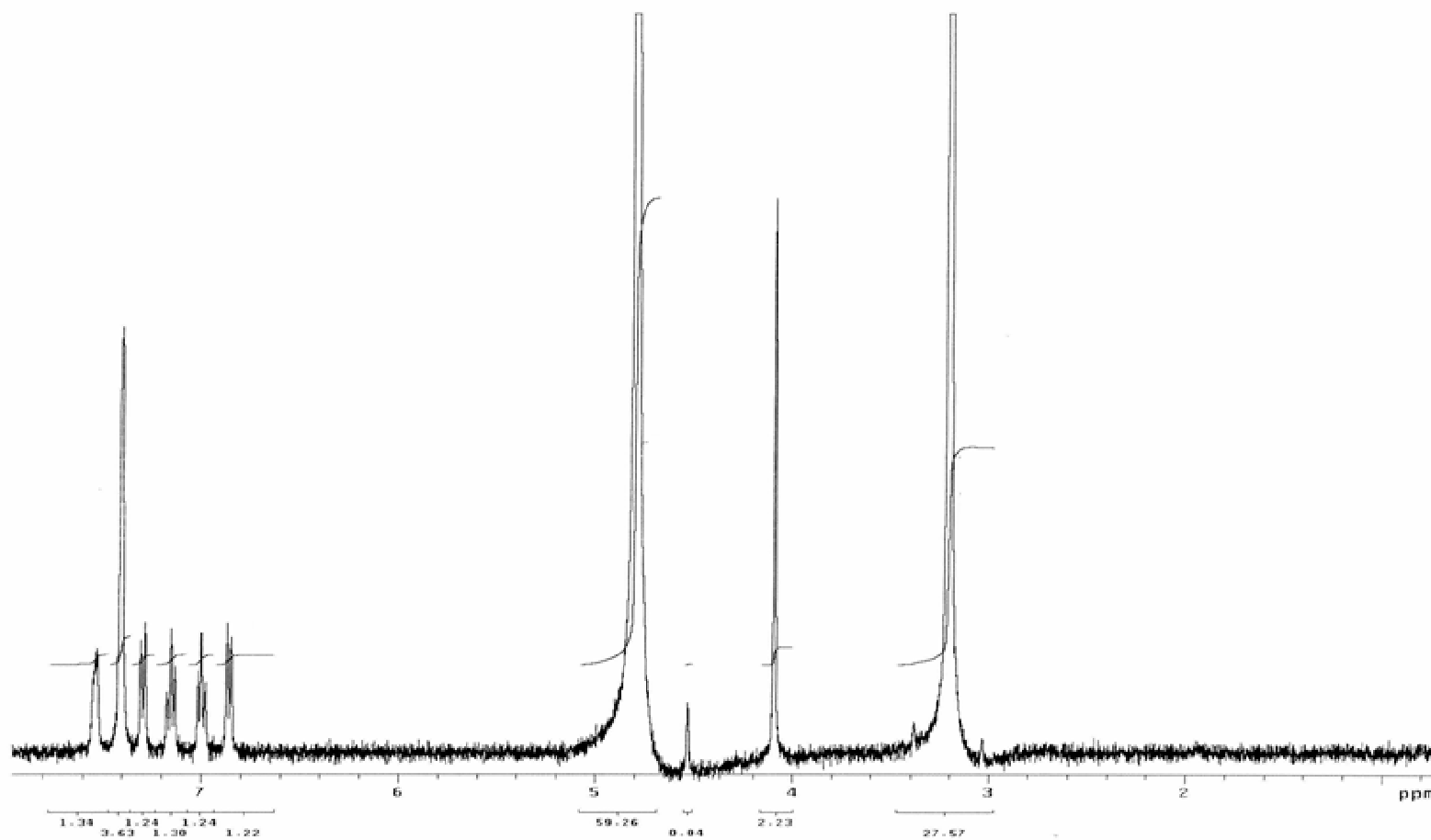


Figure 4.57. The 400 MHz ^1H NMR spectrum of 2-(*o*-chlorophenyl)imino-3-(*o*-chlorophenyl)-thiazolidine-4-one in methanol- d_4

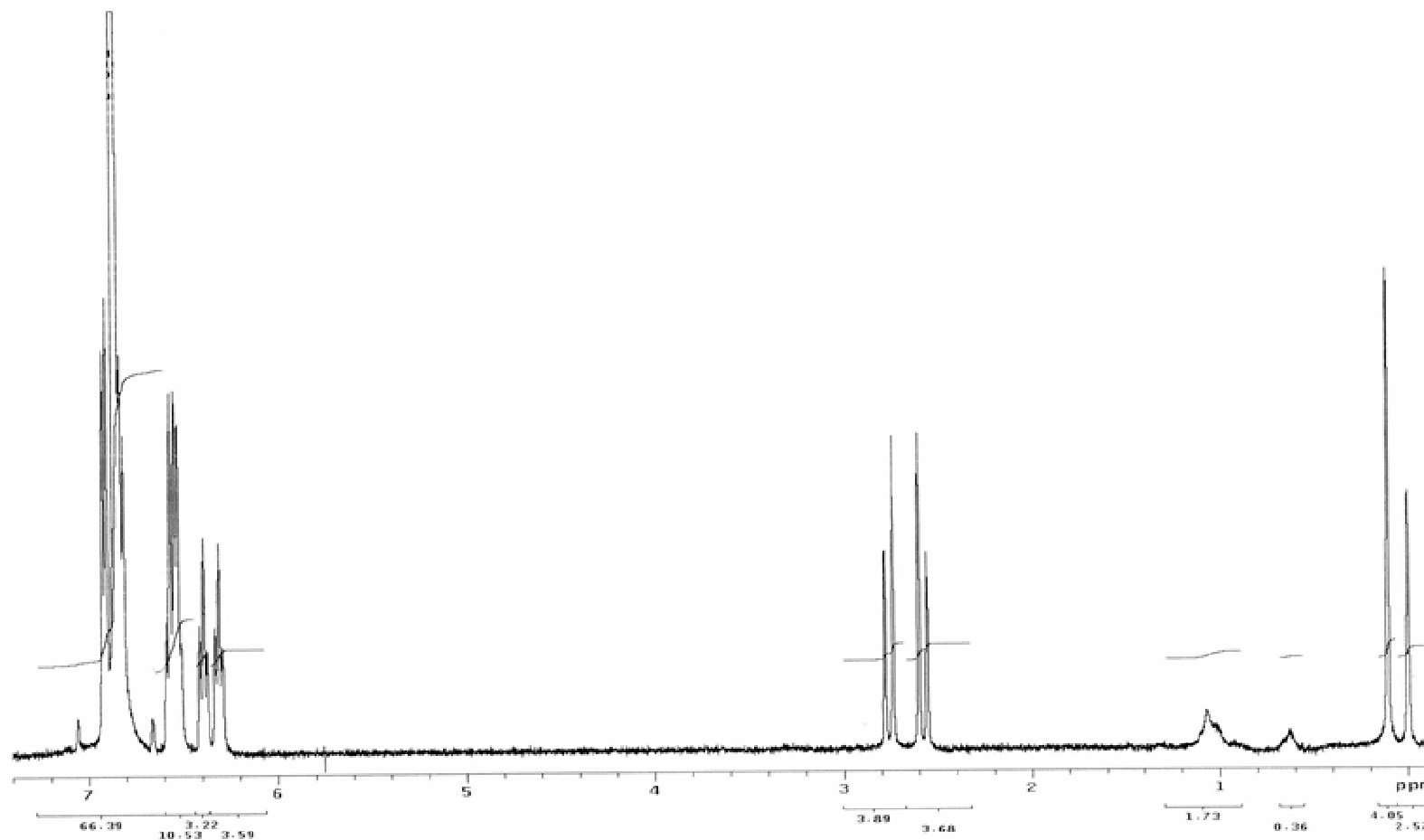


Figure 4.59. The 400 MHz ^1H NMR spectrum of 2-(*o*-chlorophenyl)imino-3-(*o*-chlorophenyl)-thiazolidine-4-one in benzene- d_4

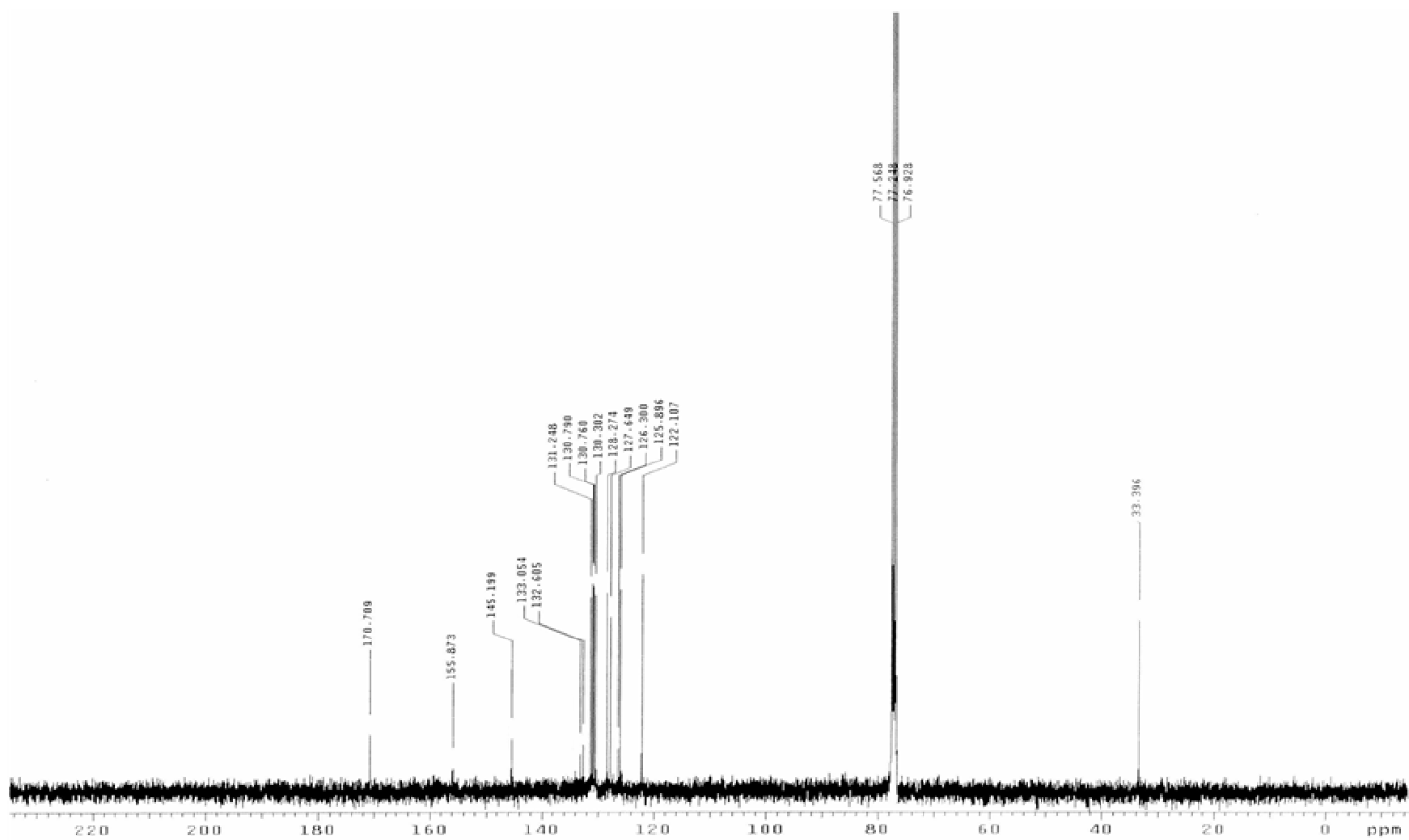


Figure 4.60. The ^{13}C NMR spectrum of 2-(*o*-chlorophenyl)imino-3-(*o*-chlorophenyl)-thiazolidine-4-one in CDCl_3

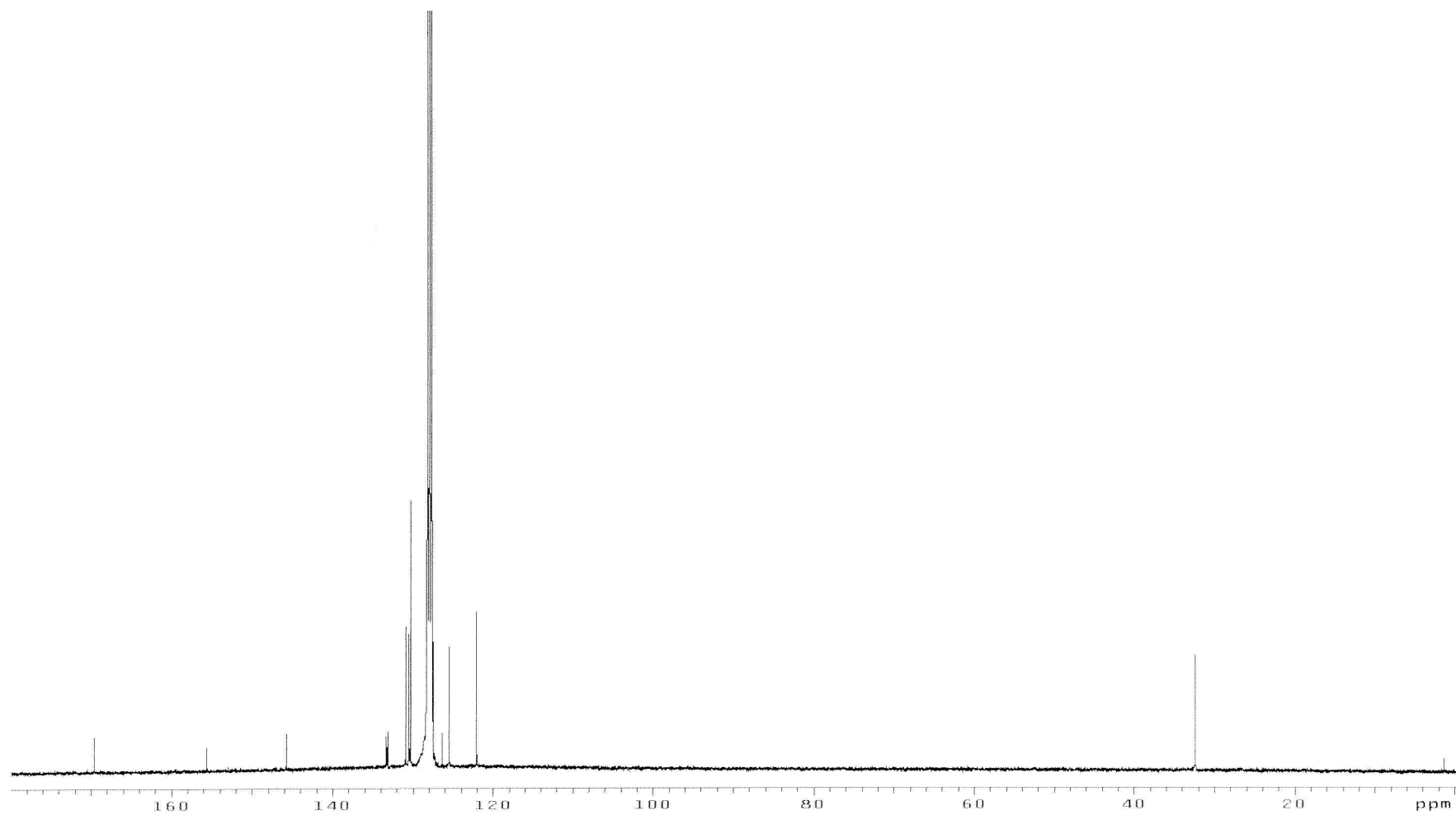


Figure 4.61. The ^{13}C NMR spectrum of 2-(*o*-chlorophenyl)imino-3-(*o*-chlorophenyl)-thiazolidine-4-one in toluene- d_8

4.4.2. ^{13}C NMR Spectra of 2-(*o*-chlorophenyl)imino-3-(*o*-chlorophenyl)-thiazolidine-4-one

^{13}C NMR spectrum of the compound was taken in CDCl_3 (Figure 4.60). The C-2 carbon resonated at 155.9 ppm. The C-4 and C-5 carbons gave peaks at 170.7 ppm and 33.4 ppm, respectively. The aromatic carbons resonated between 122.1-145.2 ppm. ^{13}C NMR spectrum of the compound was also taken in benzene- d_6 (Figure 4.61). The C-2 carbon resonated at 155.6 ppm. The C-4 and C-5 carbons gave peaks at 169.6 ppm and 32.4 ppm, respectively. The aromatic carbons resonated between 122.0-145.7 ppm.

4.4.3. 2D-COSY and 2D-NOESY Spectra of 2-(*o*-chlorophenyl)imino-3-(*o*-chlorophenyl)-thiazolidine-4-one

2D-COSY and 2D-NOESY spectra of the compound in benzene- d_6 (Figure 4.62 and Figure 4.63) were compared to each other to in order to obtain information about through space interactions between two rings. It was found that interactions found in the 2D-COSY spectrum are the same as that observed in the 2D-NOESY spectrum. Therefore, it was concluded that through space interactions between two rings are not present.

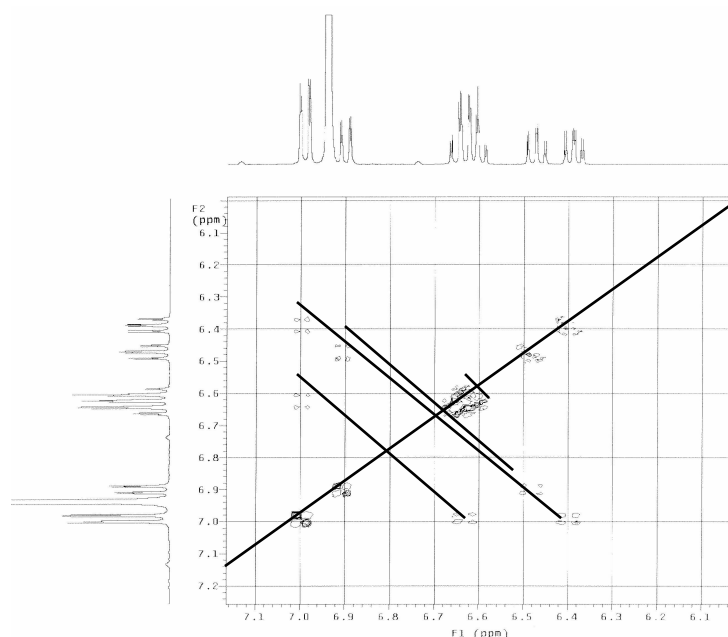


Figure 4.62. Aromatic region of the 2D-COSY spectrum of 2-(*o*-chlorophenyl)imino-3-(*o*-chlorophenyl)-thiazolidine-4-one in benzene- d_6

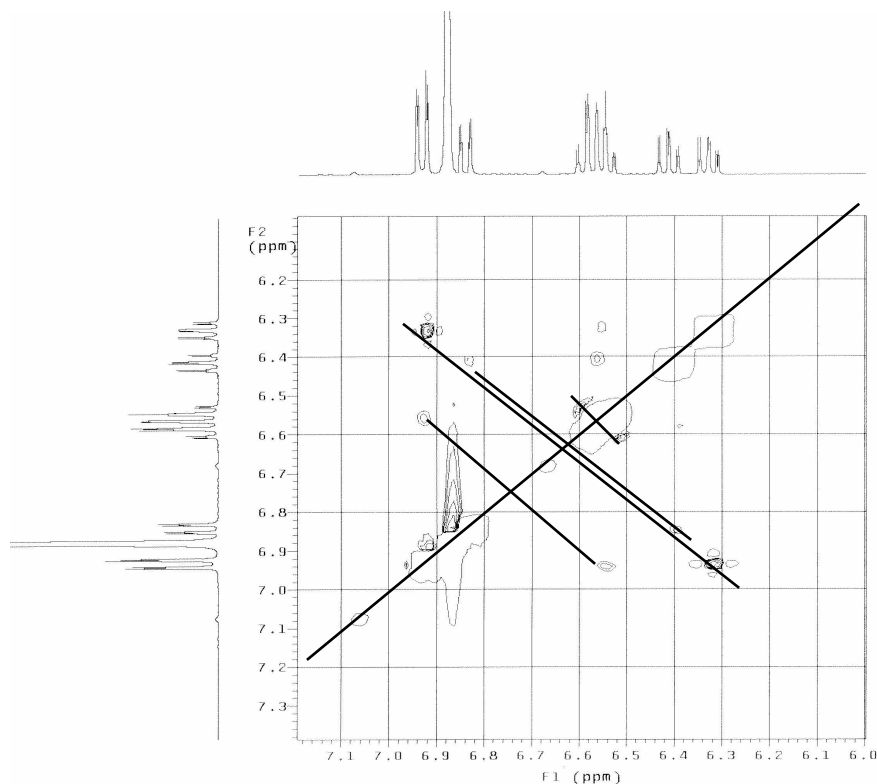


Figure 4.63. Aromatic region of the 2D-NOESY spectrum of 2-(*o*-chlorophenyl)imino-3-(*o*-chlorophenyl)-thiazolidine-4-one in benzene- d_6

4.4.4. Barrier to Rotation about N_3 -aryl bond of 2-(*o*-chlorophenyl)imino-3-(*o*-chlorophenyl)-thiazolidine-4-one

Barrier to rotation about N_3 -aryl bond of the compound was determined by thermal racemization method. Separation of isomers was done on Chiralcel OD-H column. The eluent used was 95:5 hexane:ethanol. The column temperature was 7°C and the flow rate 0.7 ml/min. The temperature at which thermal racemization took place was 70°C . The same procedure described in section 4.2.4 was followed for thermal racemization. The graph of obtained results (Figure 4.65) versus time is given in Figure 4.64. From the slope of the graph the rate constant, k was found to be 0.0001 s^{-1} . Energy barrier of the compound was found to be 110.7 kJ/mole.

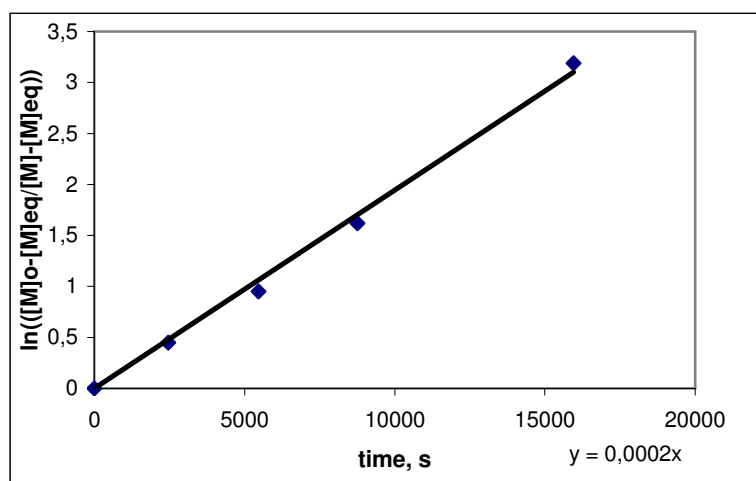


Figure 4.64. The plot of $\ln\left(\frac{[M]_0 - [M]_{eq}}{[M] - [M]_{eq}}\right)$ versus time at 343 K for 2-(*o*-chlorophenyl)imino-3-(*o*-chlorophenyl)-thiazolidine-4-one

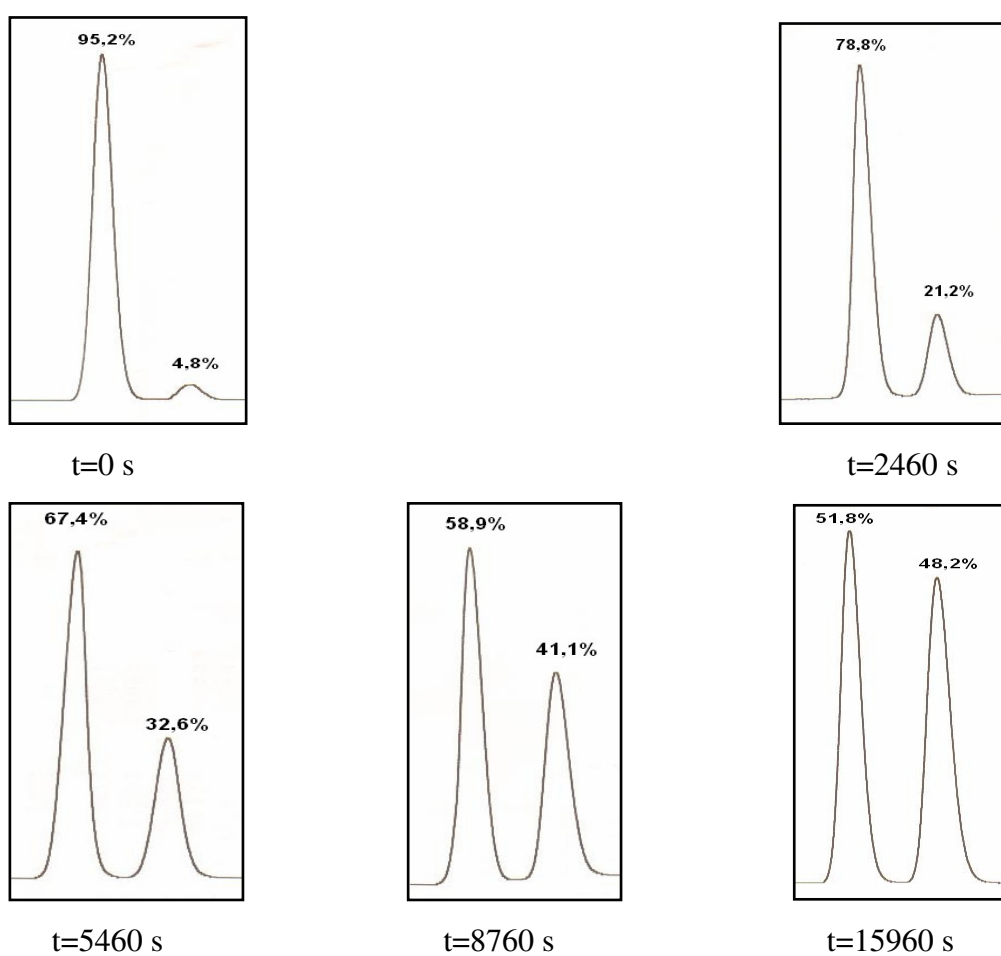


Figure 4.65. The chromatograms taken to follow thermal racemization process of 2-(*o*-chlorophenyl)imino-3-(*o*-chlorophenyl)-thiazolidine-4-one

4.5. 2-(*o*-Methoxyphenyl)imino-3-(*o*-methoxyphenyl)-thiazolidine-4-one

4.5.1. ¹H NMR Spectra of 2-(*o*-methoxyphenyl)imino-3-(*o*-methoxyphenyl)-thiazolidine-4-one

The ¹H NMR spectral assignments of 2-(*o*-methoxyphenyl)imino-3-(*o*-methoxyphenyl)-thiazolidine-4-one (Figure 4.66) in various solvents are given in Table 4.5 (Figure 4.69, 4.70, 4.71, 4.72, and 4.73)

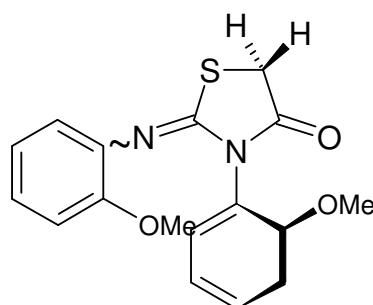


Figure 4.66. The general structure of 2-(*o*-methoxyphenyl)imino-3-(*o*-methoxyphenyl)-thiazolidine-4-one

In CDCl₃, toluene-d₈, and benzene-d₆ one AB splitting was observed for the diastereotopic methylene protons on C-5. In DMF-d₇ and methanol-d₄ the diastereotopic protons were not resolved (Figure 4.67). In toluene-d₈ one AB splitting for diastereotopic methylene protons on C-5 was observed in the 30°C to 90°C range (Figure 4.68).

Table 4.5. 400MHz spectral data for 2-(*o*-methoxyphenyl)imino-3-(*o*-methoxyphenyl)-thiazolidine-4-one in various solvents

Solvents	Protons on C-5 (ppm)	<i>o</i> -methoxy protons (ppm)	Aromatic protons (ppm)
DMF-d ₇	4.24	3.89 and 3.76	6.79-7.48
CDCl ₃	δ _A =4.01 δ _B =3.96	3,89 and 3,78	6.82-7.44
Methanol-d ₄	3.97 and 3.96	3,79 and 3,67	6.67-7.39
Toluene-d ₈	δ _A =3.12 δ _B =2.99	3,44 and 3,33	6.50-7.28
Benzene-d ₆	δ _A =2.82 δ _B =2.68	2.98 and 3.03	6.21-7.07

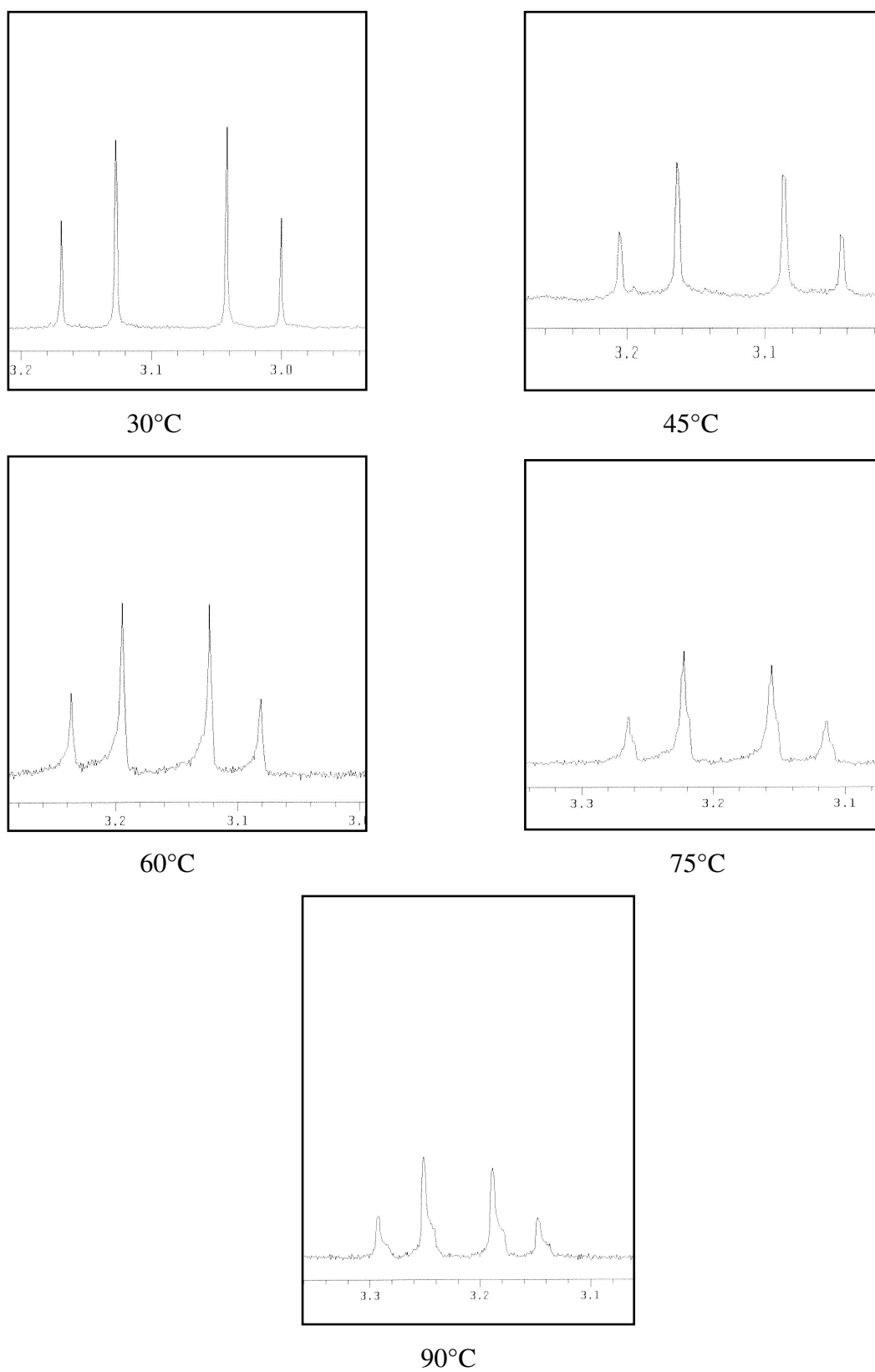


Figure 4.68. ^1H NMR signals diastereotopic methylene protons on the C-5 of 2-(*o*-methoxyphenyl)imino-3-(*o*-methoxyphenyl)-thiazolidine-4-one at various temperatures in toluene-d_8

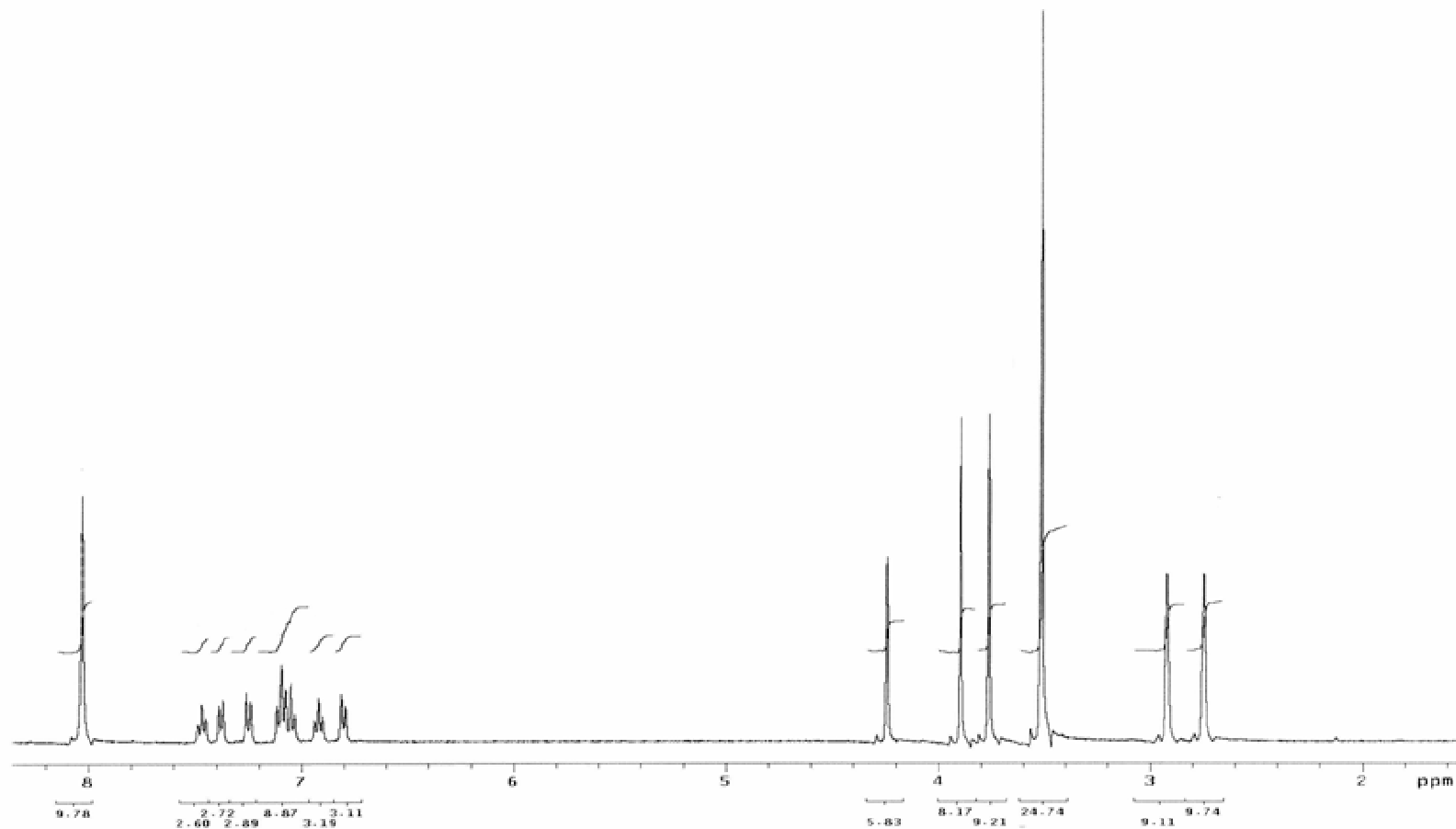


Figure 4.69. The 400 MHz ^1H NMR spectrum of 2-(*o*-methoxyphenyl)imino-3-(*o*-methoxyphenyl)-thiazolidine-4-one in DMF-d_7

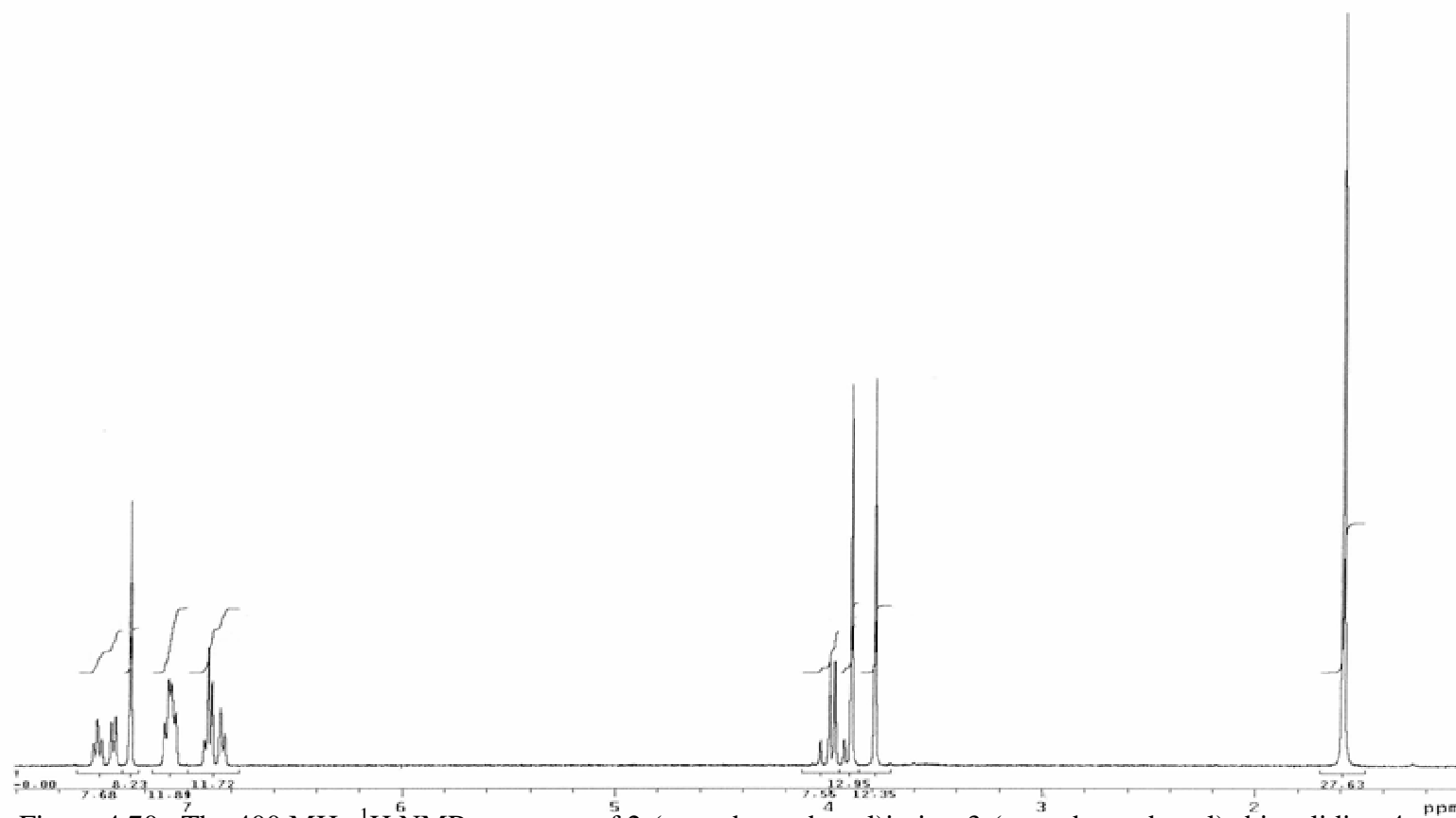


Figure 4.70. The 400 MHz ^1H NMR spectrum of 2-(*o*-methoxyphenyl)imino-3-(*o*-methoxyphenyl)-thiazolidine-4-one in CDCl_3

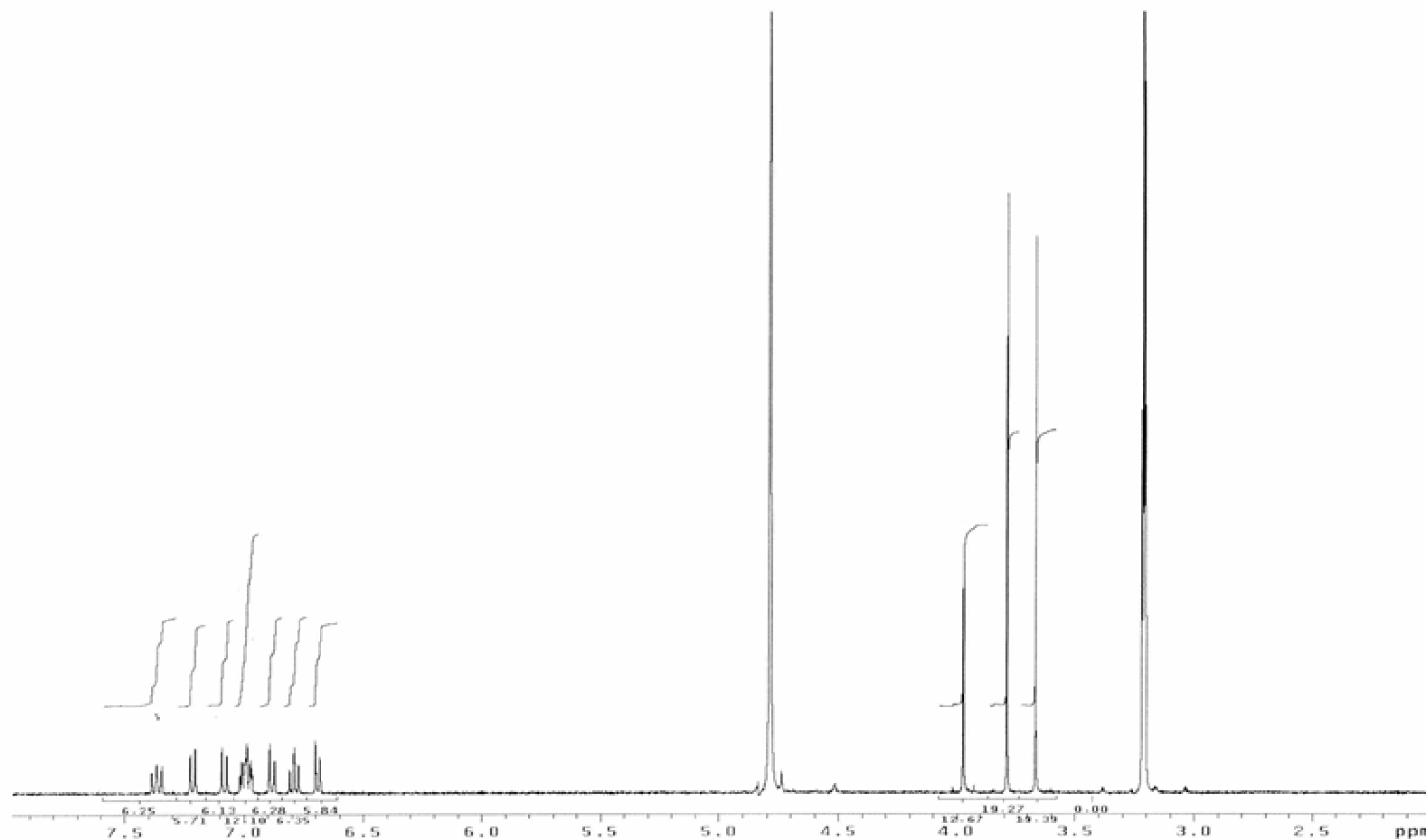


Figure 4.71. The 400 MHz ^1H NMR spectrum of 2-(*o*-methoxyphenyl)imino-3-(*o*-methoxyphenyl)-thiazolidine-4-one in methanol- d_4

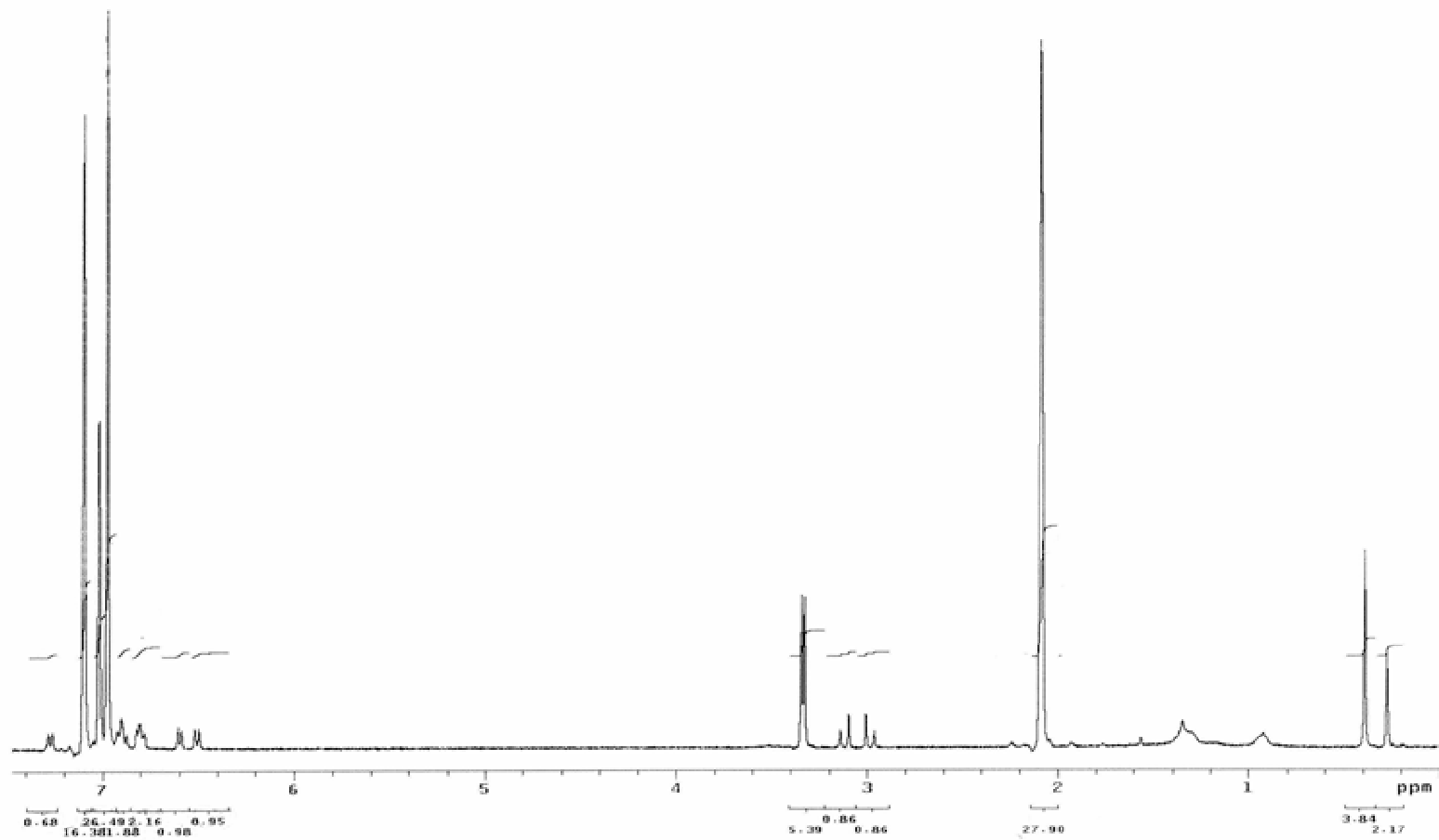


Figure 4.72. The 400 MHz ¹H NMR spectrum of 2-(*o*-methoxyphenyl)imino-3-(*o*-methoxyphenyl)-thiazolidine-4-one in toluene-d₈

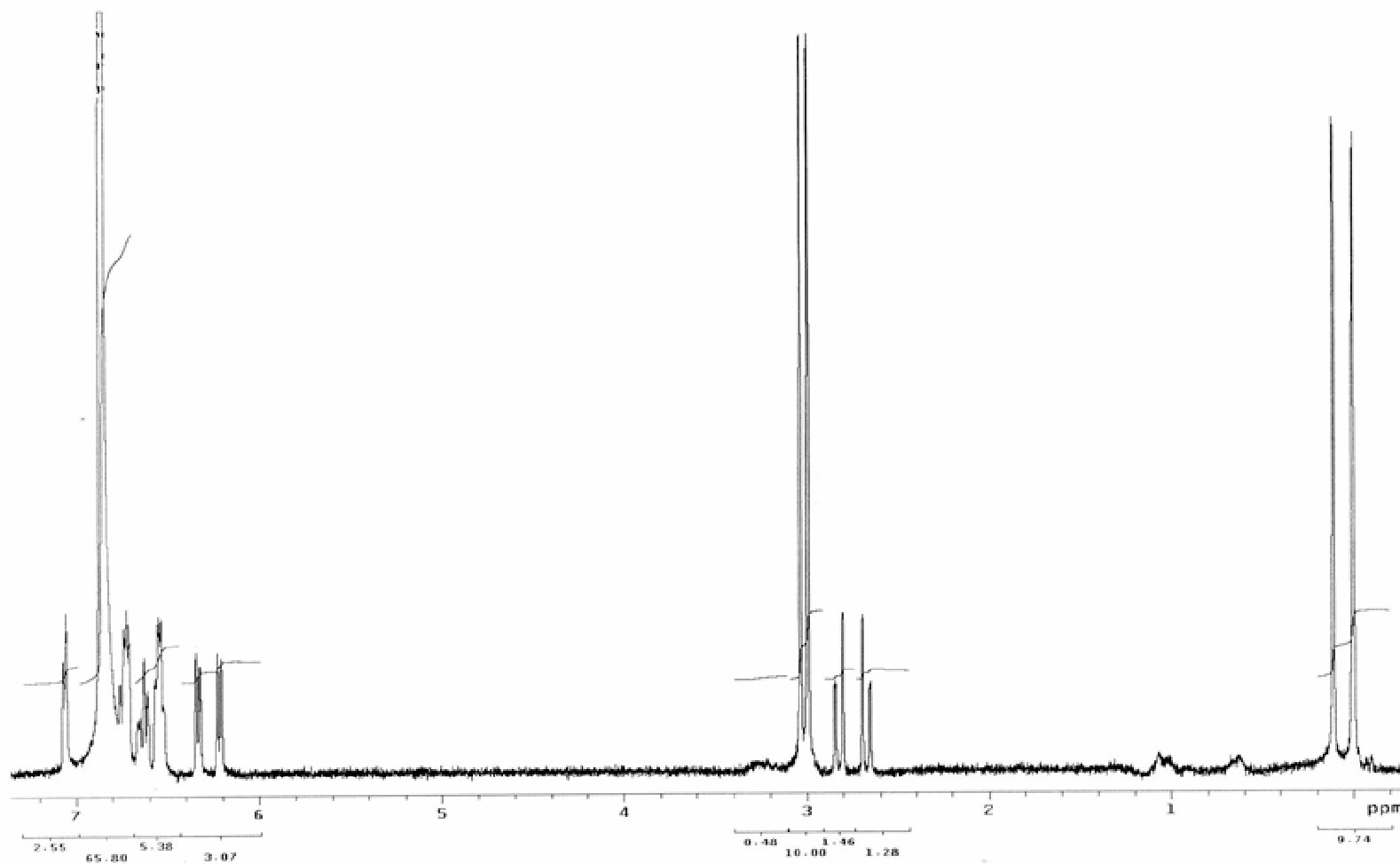


Figure 4.73. The 400 MHz ^1H NMR spectrum of 2-(*o*-methoxyphenyl)imino-3-(*o*-methoxyphenyl)-thiazolidine-4-one in benzene- d_6

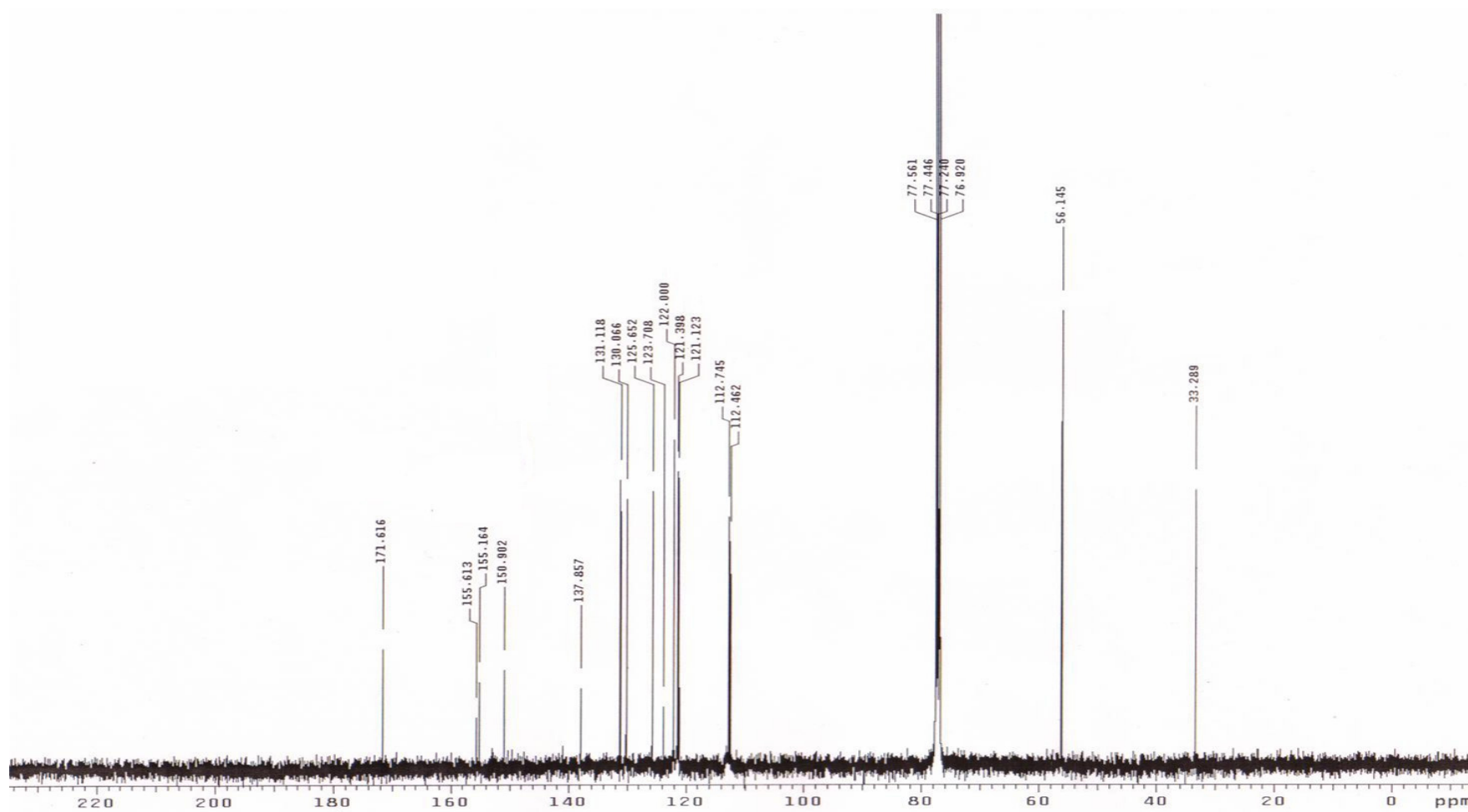


Figure 4.74. The ^{13}C NMR spectrum of 2-(*o*-methoxyphenyl)imino-3-(*o*-methoxyphenyl)-thiazolidine-4-one in CDCl_3

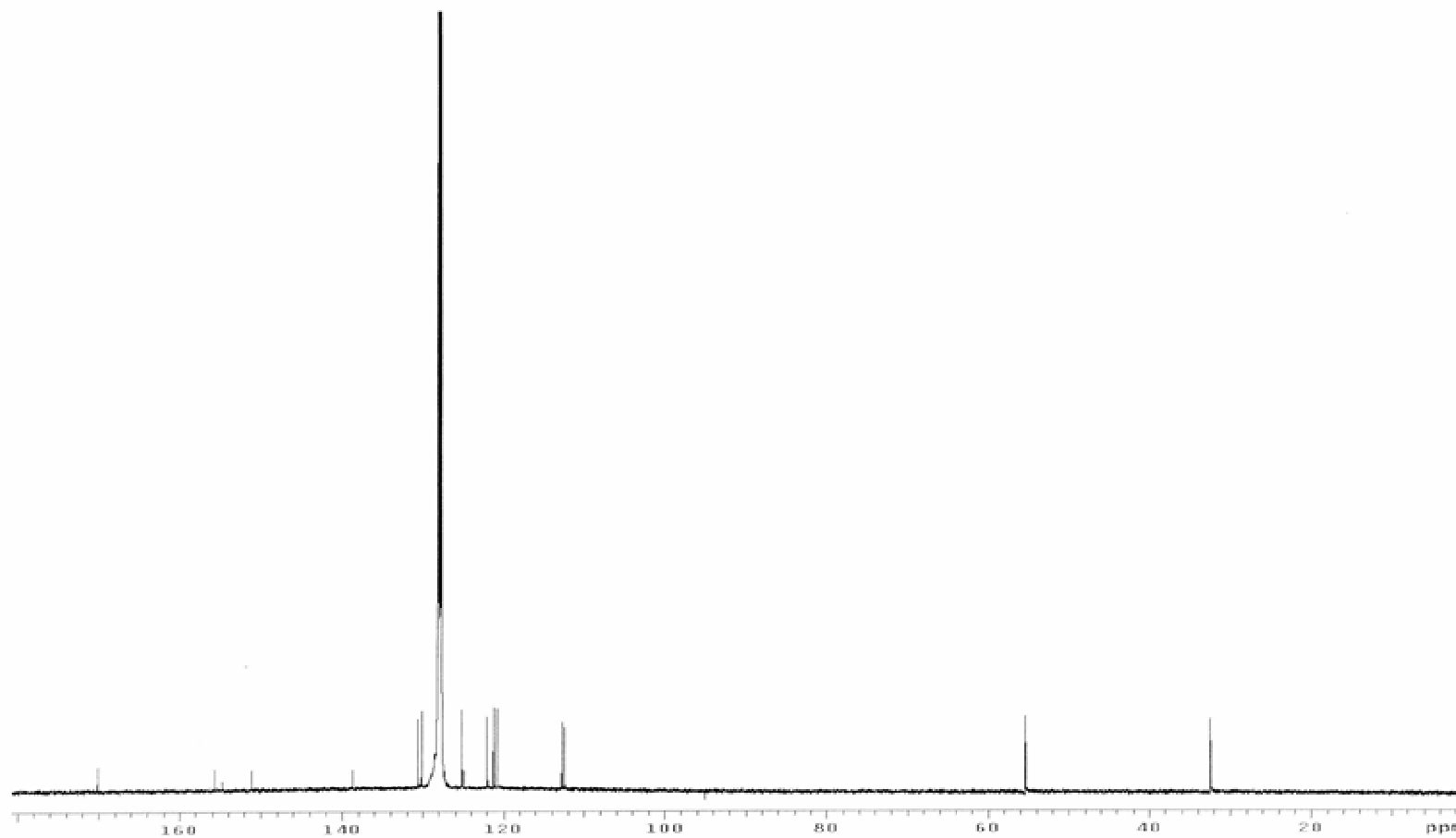


Figure 4.75. The ^{13}C NMR spectrum of 2-(*o*-methoxyphenyl)imino-3-(*o*-methoxyphenyl)-thiazolidine-4-one in benzene- d_6

4.5.3. 2D-COSY and 2D-NOESY Spectra of 2-(*o*-methoxyphenyl)imino-3-(*o*-methoxyphenyl)-thiazolidine-4-one

2D-NOESY spectrum of the 2-(*o*-methoxyphenyl)imino-3-(*o*-methoxyphenyl)-thiazolidine-4-one in benzene- d_6 (Figure 4.77) was compared to the 2D-COSY spectrum of the compound (Figure 4.76). Interactions between the protons observed in 2D-NOESY spectrum of the compound were the same as that found in 2D-COSY spectrum. As a result, through space interaction between two rings does not exist.

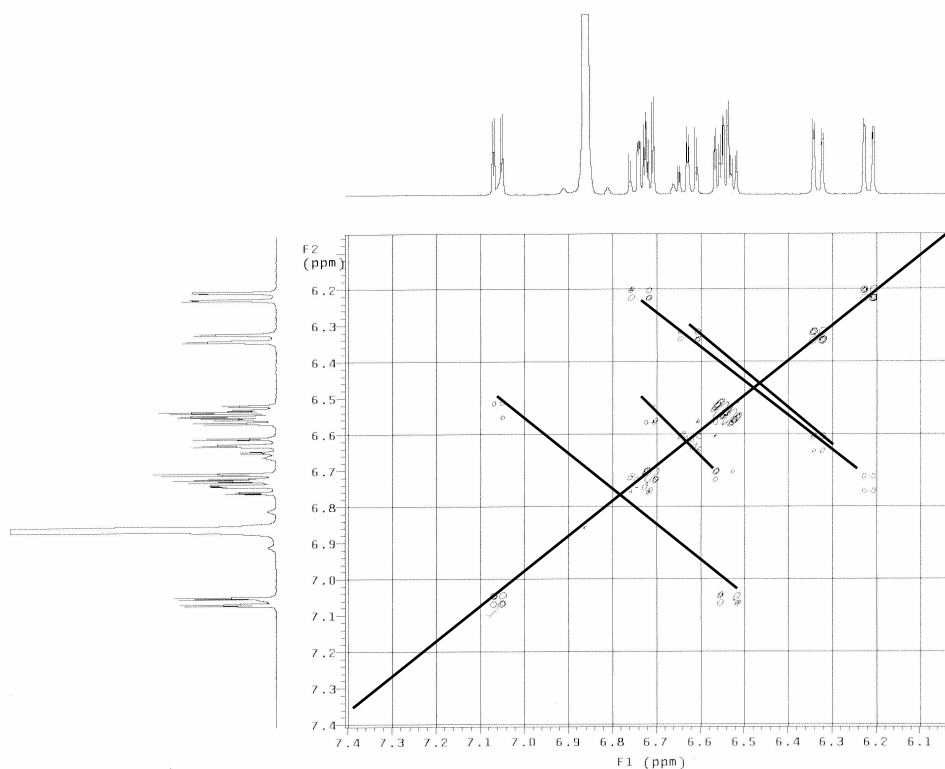


Figure 4.76. Aromatic region of the 2D-COSY spectrum of 2-(*o*-methoxyphenyl)imino-3-(*o*-methoxyphenyl)-thiazolidine-4-one in benzene- d_6

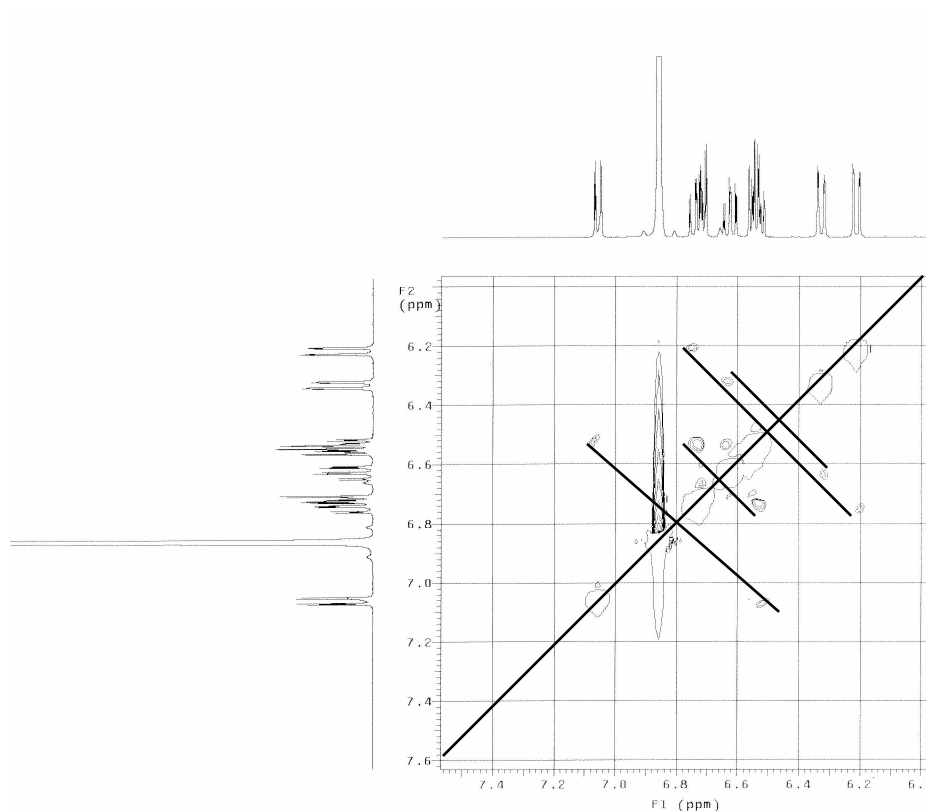


Figure 4.77. Aromatic region of the 2D-NOESY spectrum of 2-(*o*-methoxyphenyl)imino-3-(*o*-methoxyphenyl)-thiazolidine-4-one in benzene- d_6

4.5.4. Barrier to Rotation about N_3 -aryl bond of 2-(*o*-Methoxyphenyl)imino-3-(*o*-methoxyphenyl)-thiazolidine-4-one

Thermal racemization method was used to determine barrier to rotation about N_3 -aryl bond of the compound. Separation of the isomers was attempted on Chiralcel OD-H column. The eluent used was 95:5 hexane:ethanol and the column temperature was 7°C. the flow rate was 0.7 ml/min. The temperature at which thermal racemization took place 35°C. The same procedure explained in detail in section 4.2.4 was followed for thermal racemization. The graph of obtained results (Figure 4.79) versus time is given in Figure 4.78. From the slope of the graph the rate constant, k was calculated to be 0.00015 s^{-1} and the rotational barrier was found to be 98.1 kJ/mole.

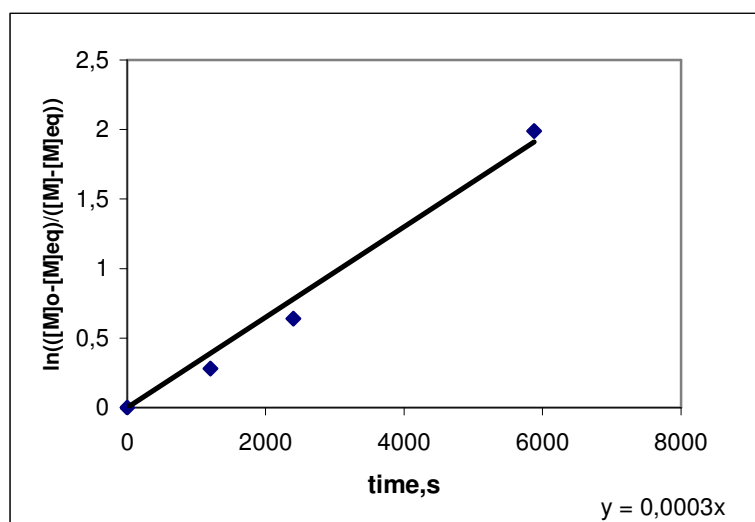


Figure 4.78. The plot of $\ln\left(\frac{[M]_0 - [M]_{eq}}{[M] - [M]_{eq}}\right)$ versus time at 308K for 2-(*o*-methoxyphenyl)imino-3-(*o*-methoxyphenyl)-thiazolidine-4-one

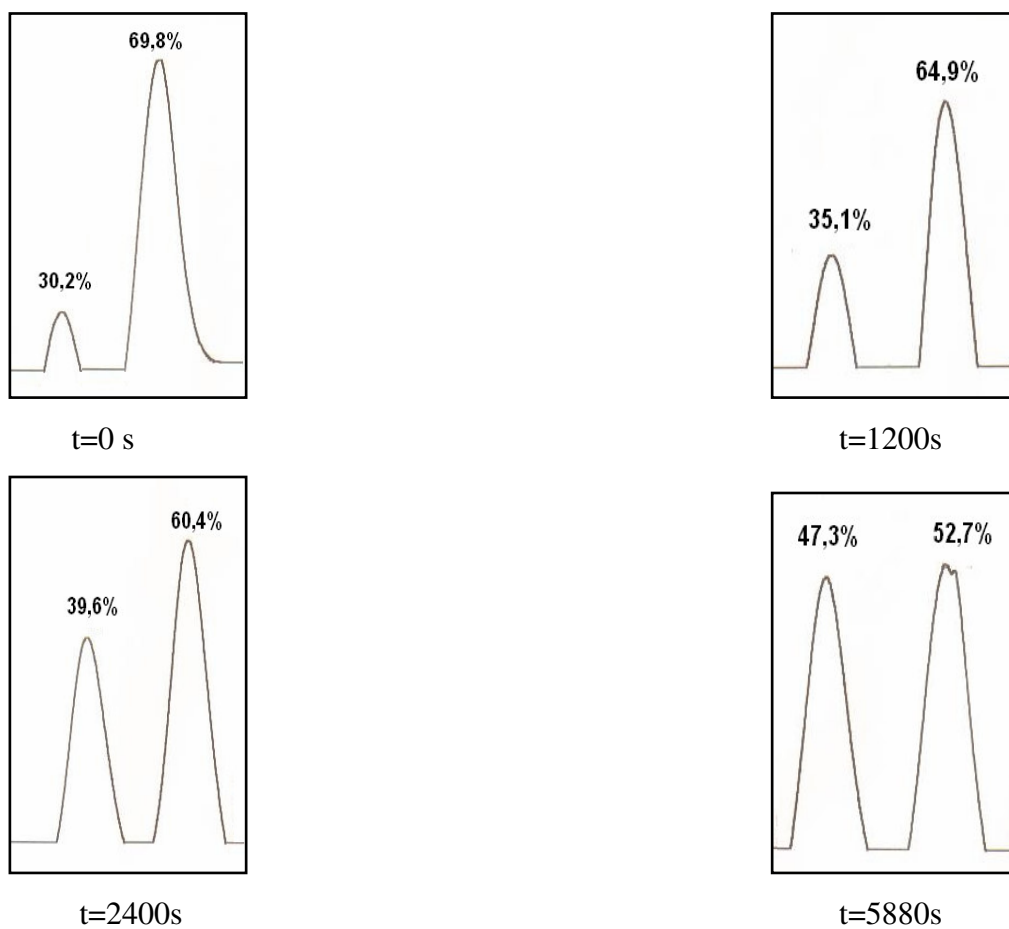


Figure 4.79. The chromatograms taken to follow thermal racemization process of 2-(*o*-methoxyphenyl)imino-3-(*o*-methoxyphenyl)-thiazolidine-4-one

4.6. Barriers to Rotations About N₃-Aryl Bond of the Compounds Studied

Energy barriers of the compounds studied were found as expected (Table 4.6). However, *o*-chlorophenyl derivative showed a barrier greater than *o*-tolyl derivative although the van der Waals radius of chlorine is smaller than that of methyl group. Electrostatic repulsion between lone pairs of carbonyl oxygen and chlorine atom can be expected to make the rotation around N₃-aryl bond more hindered and thus causing a larger barrier for this compound.

Table 4.6. The Rate Constants and Energy Barriers of the compounds studied

Compounds	T(K)	k(s ⁻¹)	ΔG [‡] (kJ/mole)
<i>o</i> -tolyl	333	1,5.10 ⁻⁴	106,2
<i>α</i> -naphthyl	333	2,5.10 ⁻⁵	111,2
<i>o</i> -chlorophenyl	343	1.10 ⁻⁴	110,7
<i>o</i> -methoxyphenyl	308	1,5.10 ⁻⁴	98,1

5. CONCLUSIONS

In this project, 2-arylimino-3-aryl-thiazolidine-4-one derivatives were synthesized by the reaction of the suitable *N,N'*-Diarylthioureas with α -bromoacetic acid. In these compounds N_3 -aryl bond rotation is hindered and except for the phenyl derivative the hindered rotation around this bond gives rise to **M** and **P** isomers. In addition, as far as the C=N bond is concerned, this bond may have **E** and **Z** configuration..

The ^1H NMR spectra of the compounds studied showed a strong solvent dependence. For 2-phenylimino-3-phenyl-thiazolidine-4-one, in aromatic solvents like toluene- d_8 and benzene- d_6 two chemical shifts were observed for the protons on C-5, which means that **E** and **Z** isomers coexist. But in the 2D-NOESY spectrum of the compound in benzene- d_6 any through space interactions due to the presence of **E** isomer were not observed. The reason why any through space interactions were not observed may be the fast rotation about the N_3 -aryl. Thus, in the NMR time scale the two phenyl rings may not spend enough time in close proximity to give a NOESY crosspeak. In addition, when the ^1H NMR spectrum of the compound were examined in toluene- d_8 , at temperatures below 15°C one chemical shift was observed for the C-5 protons, but at higher temperatures two chemical shifts were observed. This result can be explained by considering the **Z** to **E** isomerisation which is an equilibrium reaction where equilibrium constant is determined by relative population of the **E** and **Z** isomers. At temperatures below 15 °C, the equilibrium constant is too small give rise to an observable **E** isomers in the spectrum. As temperature increases the equilibrium constant increases for this endothermic process and thus **E** isomer becomes observable. In other solvents studied like DMF- d_7 , methanol- d_4 , CDCl_3 one chemical shift was observed for the C-5 protons, which means that only one isomer, probably **Z** isomer exists.

For 2-(*o*-tolyl)imino-3-(*o*-tolyl)-thiazolidine-4-one, N_3 -aryl bond rotation is a chiral axis, thus protons on the C-5 of the heterocyclic ring are diastereotopic and give AB type splitting in the ^1H NMR spectrum. The presence of further AB type splitting in toluene- d_8 indicated the presence of the **E** and **Z** isomers. In toluene- d_8 one AB splitting was observed for the diastereotopic protons on C-5 in the temperature range from -60 °C to 0 °C.

However at higher temperatures two AB splittings were observed up to 100 °C, which did not give rise to a coalescence, indicating the presence of the **E** and **Z** isomers. In DMF-d₇, methanol-d₄, CDCl₃ only one AB was observed for diastereotopic protons, so it was concluded that only one isomer exists in these solvents.

For 2-(α -naphthyl)imino-3-(α -naphthyl)-thiazolidine-4-one, 2-(*o*-chlorophenyl)imino-3-(*o*-chlorophenyl)-thiazolidine-4-one, 2-(*o*-methoxyphenyl)imino-3-(*o*-methoxyphenyl)-thiazolidine-4-one, one AB splitting was observed in all solvents studied, which means that N₃-aryl bond rotation is hindered and as far as the C=N bond is concerned, only one, probably the **Z** isomer exists.

The isomers were separated by using enantioselective HPLC and two peaks have been observed, 50 per cent each, which supports the presence of two enantiomers. The activation barriers of the compounds were determined by thermal racemization of the resolved enantiomers. When magnitudes of the obtained energy barriers were compared with the energy barriers of structurally related compounds, it has been found that the values obtained support the **Z** configuration of the C=N double bond.

REFERENCES

1. Christie, G. H. and J. Kenner, "The Molecular Configuration of Polynuclear Aromatic Compounds. Part I. The Resolution γ -6:6'-Dinitro-and 4:6:4':6'-Tetranitrodiphenic acids into Optically Active Components", *J. Chem. Soc.*, Vol. 121, pp. 614-620, 1922.
2. Bock, L. H. and R. Adams, "The preparation and Resolution of N-2-carboxyphenyl-2,5-dimethyl-3-carboxypyrrole", *J. Am. Chem. Soc.*, Vol. 53, pp. 374-376, 1931.
3. Chang, C. and R. Adams, "Stereochemistry of N,N'-dipyryls. Resolution of N,N',2,5,2',5'-tetramethyl-3,3'-dicarboxydipyrrol", *J. Am. Chem. Soc.*, Vol. 53, pp. 2353-2357, 1931.
4. Bock, L. H. and R. Adams, "Stereochemistry of Phenyl Pyrroles. XIX", *J. Am. Chem.*, Vol. 53, pp. 3519-3522, 1931.
5. Bentz, W. E., L. D. Colebrook, J. R. Fehlner and A. Rosowsky, "Hindered Rotation about C-N Bonds: Equilibrium of Diastereomeric Rotational Isomers", *Chem. Commun.*, pp. 974, 1970.
6. Colebrook, L. D., H. G. Giles and A. Rosowsky, "High Rotational Barriers about C-N Bonds in Aryl Substituted Heterocyclic Compounds Lacking Bulky *Ortho* Substituents", *Tetrahedron Letters*, No. 51, pp. 5239-5240, 1972.
7. Mintas, M., Z. Orhanović, K. Jakopić, H. Koller, G. Stühler and A. Mannschreck, "Enantiomers of Sterically Hindered N-aryl-4-pyridones: Chromatographic Enrichment and Thermal Interconversion", *Tetrahedron*, Vol. 41, No. 1, pp. 229-233, 1985.

8. Mintas, M., J. Vorkapic-Furac and A. Mannschreck, "Enantiomers and Barriers to Racemization of Hindered N-Aryl and N-Heteroarylpyrrolles", *J. Heterocyclic Chem.*, Vol. 29, pp. 327-333, 1992.
9. Doğan, İ., T. Burgemeister, S. İcli and A. Mannschreck, "Synthesis and NMR Studies of Chiral 4-Oxazolidinones and Rhodanines", *Tetrahedron*, Vol. 48, pp. 7157-7164, 1992.
10. Doğan, İ., N. Pustet and A. Mannschreck, "The Enantiomers of N-Aryl-2-thioxo-4-Oxazolidinones and N-Arylrhodanines. Investigation by Liquid Chromatography, Circular Dichroism and Thermal Racemization", *J. Chem. Soc. Perkin Trans.2*, pp. 1557-1560, 1993.
11. Oğuz, S. F. and İ. Doğan, "Determination of Energy Barriers and Racemization Mechanisms for Thermally Interconvertible Barbituric and Thiobarbituric acids enantiomers", *Tetrahedron:Asymmetry*, Vol. 14, pp. 1857-1864, 2003.
12. Demir Ordu, Ö. and İ. Doğan, "Determination of Energy Barriers and Racemization Mechanisms for Thermally Interconvertible 5,5-Dimethyl-3-(*o*-aryl)-2,4-oxazolidinedione enantiomers" *Tetrahedron:Asymmetry*, Vol. 15, pp. 925-933, 2004.
13. Doğan, İ. and S. İcli, "Conformational and Spectral Investigations of Thiazolidinone Derivatives by ^1H and ^{13}C NMR spectroscopy", *Spectroscopy Letters*, Vol. 16. pp. 499-511, 1983.
14. Boucekara, M., A. Djafri, N. Vanthuyne and C. Roussel, "Atropisomerism in some N,N'-diaryl-2-iminothiazoline Derivatives:Chiral Separation and Configurational Stability", *Arkivoc*, (X), pp. 72-79, 2002.
15. Kalinowski, H. O. and H. Kessler, "Fast Isomerization about Double Bonds", *Topics in Stereochemistry*, Vol. 7, pp. 295, 1973.

16. Oki, M., *Applications of Dynamic NMR Spectroscopy to Organic Chemistry*, Deerfield Beach, FL : VCH Publishers, 1985.
17. Cahn, R.S., C. Ingold and V. Prelog, “ Specification of Molecular Chirality”, *Angew. Chem. Internat. Edition*, Vol. 5, No. 4, pp. 385-415, 1966.
18. Demir Ordu, Ö., E. M. Yılmaz and İ. Doğan, “Determination of the Absolute Stereochemistry and the Activation Barriers of Thermally Interconvertible Heterocyclic Compounds Bearing A Naphthyl Substituent”, *Tetrahedron: Asymmetry*, Vol. 16, pp. 3752-3761, 2005.